

NASA CONTRACTOR REPORT



NASA CR-1

C.1

0061088



NASA CR-1828

LOAN COPY: RETURN TO
AFWL (DO 4L)
KIRTLAND AFB, N. M.

THE INITIAL DEVELOPMENT OF THE GENERAL NON-ISOENERGETIC COMPRESSIBLE FREE SHEAR LAYER

by P. Carpenter and W. Tabakoff

Prepared by
THE INSTITUTE OF SPACE SCIENCES
UNIVERSITY OF CINCINNATI
Cincinnati, Ohio 45221

for



0061088

1. Report No. NASA CR-1828		2. Government Accession No.		3. Recipient's Catalog No.	
4. Title and Subtitle THE INITIAL DEVELOPMENT OF THE GENERAL NON-ISOENERGETIC COMPRESSIBLE FREE SHEAR LAYER				5. Report Date October 1971	
				6. Performing Organization Code	
7. Author(s) P. Carpenter and W. Tabakoff				8. Performing Organization Report No.	
9. Performing Organization Name and Address The Institute of Space Sciences University of Cincinnati Cincinnati, Ohio 45221				10. Work Unit No.	
				11. Contract or Grant No. NGL-36-004-014	
12. Sponsoring Agency Name and Address National Aeronautics and Space Administration Washington, D. C. 20546				13. Type of Report and Period Covered Contractor Report	
				14. Sponsoring Agency Code	
15. Supplementary Notes					
16. Abstract The numerical integration of the equations governing the development of a free shear layer from arbitrary initial conditions, is carried out using a modification of Dorodnitsyn's Method of Integral Relations. The problem of the singularity at the origin is solved by splitting the domain of integration into two strips; and, also, transforming one of the dependent variables. The apparent indeterminateness of the third boundary condition is overcome by casting the equations in Crocco coordinates for the purposes of the numerical integration. The requirement, that continuity of normal stress be maintained for the higher order corrections to the solution of the boundary layer equations, is used to determine the location of the dividing streamline for the general case of a free shear layer growing about a curved axisymmetric free streamline. This procedure involves an asymptotic analysis of the complete Navier-Stokes equations. The effects of viscous heating ($Pr \neq 1$) are taken into consideration and Sutherland's law is used to determine coefficient of viscosity in the laminar case. A new eddy viscosity model is introduced for the turbulent free shear layer. Essentially it is an extension of Clauser's model. Results are presented showing the effects of compressibility (Mach numbers ranging from 0 to 10), and total enthalpy ratio (ranging from 0 to 5), on the development of such parameters as temperature and velocity along the dividing streamline, heat transfer and shear stress coefficients, and dividing streamline location; and on the position of the virtual origin. The effects of variation in initial velocity profile, and of a discontinuity in temperature at the origin, are also studied.					
17. Key Words (Suggested by Author(s)) Compressible free shear layer Wake velocity profiles Wake temperature profiles Wake dividing streamline Wake heat transfer Separation of flow				18. Distribution Statement Unclassified - unlimited	
19. Security Classif. (of this report) Unclassified		20. Security Classif. (of this page) Unclassified		21. No. of Pages 136	22. Price* \$3.00



ACKNOWLEDGEMENTS

The research presented in this report was supported by the NASA Multidisciplinary Research Grant NGL 36-004-014.

The interest and evaluations of the Progress Reports by Mr. B. H. Anderson of NASA Lewis Research Laboratory - Cleveland through the course of this work is gratefully acknowledged.

The assistance and encouragement of Dr. Paul Harrington, Director of the Institute of Space Sciences is also greatly appreciated.

TABLE OF CONTENTS

	<u>Page</u>
List of Figures	vii
Summary	ix
Symbols	xi
1. INTRODUCTION	1
1.1 Definition of Problem	1
1.2 A Brief Exposition of the Method of Integration	6
1.3 Survey of Theoretical Studies on Free Shear Layers	11
2. GENERAL ANALYSIS	16
2.1 Governing Equations	16
2.2 Asymptotic Behavior of Solutions	19
2.3 Derivation of the Integral Relations	24
2.4 Reduction of Integral Relations to a System of First Order Ordinary Differential Equations	26
2.5 The Location of the Dividing Streamline	34
2.6 The Inadmissability of Certain Orders of the Approximating Polynomials	53
3. THE EDDY VISCOSITY MODEL	55
4. WORKED EXAMPLE AND EXPLICIT FORMULAE FOR THE CASE $P_1 = 4, P_3 = 2$	59
4.1 Relationships Between Quantities Above and Below Dividing Streamline	59
4.2 Derivation of the System of Ordinary Differential Equations	62
4.3 Initial Conditions for the Integration	71
4.4 Determination of Velocity-Defect Thickness	72

TABLE OF CONTENTS (CONT'D)

	<u>Page</u>
4.5 Determination of Location of Dividing Streamline	73
4.6 Calculation of Velocity Profile	75
4.7 Calculation of Temperature Profile	77
4.8 Calculation of Properties on Dividing Streamline	78
4.9 Calculation of Position of Virtual Origin	79
5. DISCUSSION	81
5.1 Preliminary Remarks	81
5.2 Discussion of Results for Laminar Case	82
5.3 Discussion of Results for Turbulent Case	92
6. CONCLUSION	94
REFERENCES	95

LIST OF FIGURES

<u>Figure</u>		<u>Page</u>
1.1	A Free Shear Layer Developing From An Attached Boundary Layer	2
2.1	The Interaction Process at the Trailing Edge	17
2.2	Coordinate System for Free Streamline	35
5.1	Comparison of Various Approximations For the Coefficient of Viscosity	100
5.2	Variation of Dividing Streamline Velocity Development with Mach Number	101
5.3	Variation of Dividing Streamline Velocity Development with Free Stream Stagnation Temperature	106
5.4	Variation of Dividing Streamline Velocity Development with Total Enthalpy Ratio	108
5.5	The Effect of a Discontinuity in Total Enthalpy Ratio on the Development of Free Shear Layers	113
5.6	The Influence of the Initial Velocity Profile on the Development of Dividing Streamline Velocity	118
5.7	Development of the Dividing Streamline Velocity for the Turbulent Case	119
5.8	Comparison of Various Theoretical Predictions of the Asymptotic Value of Dividing Streamline Velocity with Mach Number	120

SUMMARY

The numerical integration of the equations governing the development of a free shear layer from arbitrary initial conditions, is carried out using a modification of Dorodnitsyn's Method of Integral Relations. With this method the solution of the equations is undertaken in two main steps. First, the system of partial differential equations is reduced to one of first-order ordinary differential equations. Second, this system is integrated by some standard technique.

The problem of the singularity at the origin is solved by splitting the domain of integration into two strips; and, also, transforming one of the dependent variables. The apparent indeterminateness of the third boundary condition is overcome by casting the equations in Crocco coordinates for the purposes of the numerical integration. The requirement, that continuity of normal stress be maintained for the higher order corrections to the solution of the boundary layer equations, is used to determine the location of the dividing streamline for the general case of a free shear layer growing about a curved axisymmetric free streamline. This procedure involves an asymptotic analysis of the complete Navier-Stokes equations.

The effects of viscous heating ($Pr \neq 1$) are taken into consideration and Sutherland's law is used to determine coefficient of viscosity in the laminar case. A new eddy viscosity

model is introduced for the turbulent free shear layer. Essentially it is an extension of Clauser's model.

Results are presented showing the effects of compressibility (Mach numbers ranging from 0 to 10), and total enthalpy ratio (ranging from 0 to 5), on the development of such parameters as temperature and velocity along the dividing streamline, heat transfer and shear stress coefficients, and dividing streamline location; and on the position of the virtual origin. The effects of variation in initial velocity profile, and of a discontinuity in temperature at the origin, are also studied.

The results display a strong dependence on Mach number, total enthalpy ratio, and temperature discontinuity at origin; but are only slightly affected by variation in the initial velocity profile. It was found that any attempt, to approximate the total heat transfer across the dividing streamline for values of $\frac{xv_1}{u_1 \delta_0^{**2}}$ less than 1000, would be highly inaccurate. Virtual origins downstream of the real ones were recorded for some total enthalpy ratios.

SYMBOLS

a	$\xi = a$ is a side of domain Δ .
$a_\ell(\xi)$	Coefficient of the polynomial approximating $\zeta^u(\xi, \bar{u})$. See Eqn. (2.4.13).
$a_{ik\ell}(\xi)$	Coefficient of polynomial approximating transformed independent variable v_i in k th strip.
A_{ij}	($i = 1, \dots, 6$; $j = 1, \dots, 6$). See Eqns. (4.2.3-10).
b	$\xi = b$ is a side of domain Δ . In section 1.2 only.
$b(x)$	Width of shear layer.
$b_\ell(\xi)$	Coefficient of polynomial approximating $\zeta^\ell(\xi, \bar{u})$. See Eqn. (2.4.13).
B_i	($i = 1, \dots, 6$). See Eqn. (4.2.2).
C	Chapman-Rubesin constant.
$c_\ell(\xi)$	Coefficient of polynomial approximating $\bar{H}^u(\xi, \bar{u})$. See Eqn. (2.4.14).
C_p	Specific heat at constant pressure.
$C_p^{(1)}$	Coefficient of pressure
C_i	($i = 1, \dots, 6$). See Eqn. (4.2.1).
C_{f_0}	Shear stress coefficient. See Eqn. (4.8.5).
D	Domain of general nonlinear system of partial differential equations.
$d_\ell(\xi)$	Coefficient of polynomial approximating $\bar{H}^\ell(\xi, \bar{u})$. See Eqn. (2.4.14).
$e(x)$	ε/ρ
$f_1(x)$	Unknown function arising from integration. Section 2.2 only.
$f_2(x)$	Unknown function arising from integration. Section 2.2 only.

$f_3(x)$	Unknown function arising from integration. Section 2.2 only.
$f_j(u)$	Set of weighting functions.
$f_j^u(\bar{u})$	Set of weighting functions for $\bar{u} > \bar{u}_0$.
$f_j^l(\bar{u})$	Set of weighting functions for $\bar{u} < \bar{u}_0$.
$f_{ik}(\eta)$	Function premultiplying approximating polynomial for transformed dependent variable v_i in k th strip.
$f_i(\epsilon)$	See Eqn. (2.5.7). Section 2.5 only.
F_i	Component of vector consisting of the zeroth order terms of the general nonlinear system of PDES.
f_{ij}	($i = 1, 2, 3; j = 1, \text{-----}, 4$). See Eqn. (4.1.4). ($i = 5, 6; j = 1, 5, 6$). See Eqn. (4.1.9).
$g(\eta)$	See Eqn. (1.3.1.24).
g_i	($i = 1, \text{-----}, 6$). See Eqn. (4.2.8).
g_{ij}	($i = 1, \text{-----}, 6; j = 5, 6$). See Eqn. (4.2.8).
$g_1(x)$	Unknown function arising from integration. Section 2.2 only.
$g_2(x)$	Unknown function arising from integration. Section 2.2 only.
$g_k(H)$	Set of weighting functions.
$g_k^u(\bar{H})$	Set of weighting functions for $\bar{u} > \bar{u}_0$.
$g_k^l(\bar{H})$	Set of weighting functions for $\bar{u} < \bar{u}_0$.
$g_{i\ell}(\eta)$	Set of weighting functions.
$g_i(\epsilon)$	See Eqn. (2.5.7). Section 2.5 only.
GG_i	($i = 1, 2, 3$). See Eqn. (4.2.9).
h	See Eqn. (1.3.1.27). Section 1.3 only.
H	Total enthalpy.
H_1	Total enthalpy in upper main stream.

H_2	Total enthalpy in lower secondary stream or quiescent region.
H_w	H at $x = 0, y = 0$.
\bar{H}	H/H_1
\bar{H}^u	\bar{H} for $\bar{u} > \bar{u}_0$.
\bar{H}^l	\bar{H} for $\bar{u} < \bar{u}_0$.
\bar{H}_0	\bar{H} at $\bar{u} = \bar{u}_0$.
$h_i(\epsilon)$	See Eqn. (2.5.7). Section 2.5 only.
h_i	($i = 1, \dots, 4$). Eqn. (4.2.11). ($i = 5, \dots, 8$). Eqn. (4.2.15).
h_{ij}	($i = 1, \dots, 4; j = 5, 6$). Eqn. (4.2.12). ($i = 5, \dots, 8; j = 5, 6$). Eqn. (4.2.15).
$H_i(y)$	Initial total enthalpy profile.
i_j	($i = 0, \dots, 5$). See Eqn. (4.2.12).
i_{ij}	($i = 0, \dots, 5; j = 5, 6$). See Eqn. (4.2.13).
IIIi	($i = 1, \dots, 6$). See Eqn. (4.2.18).
IYk	($k = 0, 1, \dots$). See Eqn. (4.6.6).
j_i	($i = 0, \dots, 5$). See Eqn. (4.2.16).
j_{ij}	($i = 0, \dots, 5; j = 1, 5, 6$). See Eqn. (4.2.17).
JJi	($i = 1, \dots, 6$). See Eqn. (4.2.19).
JYk	($k = 0, 1, 2, \dots$). See Eqn. (4.6.3).
k	Coefficient of thermal conductivity.
$k(x)$	Radius of curvature of free streamline.
K_1	Universal constant.
k_i	($i = 0, \dots, 7$). See Eqn. (4.4.5).
L	Reference length.
L_i	General nonlinear partial operator.
ℓ	Length of the free streamline.

l_i	$(i = 0, \text{-----}, 4)$. See Eqn. (4.5.3).
l_{ij}	$(i = 0, \text{-----}, 4); j = 2, \text{-----}, 6)$. See Eqn. (4.5.5).
m	$\frac{\gamma-1}{2} M_1^2$
M	Number of strips into which Δ is divided.
M_1	Mach number in upper main stream.
N	Number of weighting functions.
Nu_o	Local Nusselt Number. See Eqn. (4.8.3).
p	Pressure
P	$\sum_{k=1}^M P_k + Q$
Pr	Prandtl Number.
P_k	Order of approximating polynomial in kth strip.
$p^{(i)}(x,y)$	See Eqn. (2.5.7). Section 2.5 only.
$\tilde{p}^{(i)}(x,\tilde{y})$	See Eqn. (2.5.14). Section 2.5 only.
Q	See paragraph below Eqn. (1.2.7).
r	Radial coordinate
R	See Eqn. (2.5.52).
r_o	Displacement of free streamline from axis of symmetry.
$r_i(\epsilon)$	See Eqn. (2.5.14). Section 2.5 only.
$r^*(y)$	See Eqn. (2.5.52).
Re_l	$\frac{u_1 \rho_1 L}{\mu_1}$
$Re_{\delta_o}^{**}$	$\frac{u_1 \rho_1 \delta_o^{**}}{\mu_1}$
s	Metric. See Eqn. (2.5.1).
$s_i(\epsilon)$	See Eqn. (2.5.14). Section (2.5) only.

S	See Eqn. (2.5.31).
$t_i(\epsilon)$	See Eqn. (2.5.14). Section (2.5) only.
t_i	($i = 0, \dots, 11$). See Eqn. (4.4.4).
T	Temperature
T_1	Temperature in upper main stream.
T_2	Temperature in lower secondary stream or quiescent region.
\bar{T}	T/T_1
T_w	T at $x = 0, y = 0$
\bar{T}_0	Value of \bar{T} at $\bar{u} = \bar{u}_0$.
$\bar{\bar{T}}$	Stress tensor.
	Transformation mapping \underline{u} to \underline{v} , D to Δ .
u	Longitudinal velocity component.
u_1	Value of u in upper main stream.
u_2	Value of u in lower secondary stream.
\bar{u}	u_1/u_2
\bar{u}_0	Value of \bar{u} at $y = y_0$.
\underline{u}	Vector of dependent variables.
u_i	($i = 1, \dots, N$). Component of \underline{u} .
$u_i(y)$	Initial velocity profile at $x = 0$.
$u^{(i)}(x,y)$	See Eqn. (2.5.7). Section 2.5 only.
$\tilde{u}^{(i)}(x,\tilde{y})$	See Eqn. (2.5.14). Section 2.5 only.
v	Transverse velocity component.
\underline{v}	Transformed vector of dependent variables.
v_i	($i = 1, \dots, N$). Component of \underline{v} .
w	$v(1 + \frac{\rho' \underline{v} \underline{v}'}{\rho v})$: Turbulent case
	{ v : Laminar case

\bar{w}	w/u_1
$w^{(i)}(x,y)$	See Eqn. (2.5.7). Section 2.5 only.
$\tilde{w}^{(i)}(x,\tilde{y})$	See Eqn. (2.5.14). Section 2.5 only.
x	Longitudinal cartesian coordinate.
\bar{x}	x/L
x_v	Displacement of virtual origin behind real one.
y	Transverse cartesian coordinate.
\bar{y}	y/L
y_o	Position of dividing streamline.
\bar{y}_o	y_o/L
y_v	Displacement of virtual origin above real one.
\tilde{y}	Stretched coordinate. See Eqn. (2.5.13).
y^*	Stretched coordinate. See Eqn. (2.5.37).

Greek Alphabet:

α	See Eqn. (2.5.31).
β	Falkner-Skan parameter
γ	Ratio of specific heats.
$\delta(\epsilon)$	See Eqn. (2.5.13).
δ_1	See Eqn. (2.5.29).
δ_o	Boundary layer thickness at $x = 0$.
δ_o^*	Displacement thickness at $x = 0$.
δ_o^{**}	Momentum thickness at $x = 0$.
Δ	Transformed domain of general nonlinear system of PDEs.
Δ'	General symbol for a shear layer thickness parameter.
$\Delta^*(x)$	Velocity defect thickness. Eqn. (3.4).

ϵ	Eddy viscosity in turbulent case. in laminar case.
ϵ	See Eqn. (2.5.6). Section 2.5 only.
ϵ_1	Value of ϵ in upper main stream.
ϵ_2	Value of ϵ in lower secondary stream or quiescent region.
ϵ_T	Turbulent coefficient of thermal conductivity.
$\bar{\epsilon}$	ϵ/ϵ_1 .
$\zeta(\xi, \bar{u})$	$\partial\eta/\partial\bar{u}$
η	Transformation maps y to η . Section 1.2 only.
η	See Eqn. (2.4.3).
η_k	Upper edge of k th strip in .
θ	See Eqn. (2.5.2).
λ	$\frac{H_2}{H_1}$
λ_T	$\frac{T_2}{T_1}$
Λ_i	Transformed general nonlinear partial operator.
μ	Coefficient of viscosity
μ_1	Value of μ in upper main stream.
μ_2	Value of μ in lower secondary stream or quiescent region.
$\bar{\mu}$	μ/μ_1
ν	Kinematic coefficient of viscosity.
ν_1	Value of ν in upper main stream.
ν_2	Value of ν in lower secondary stream or quiescent region.
$\bar{\nu}$	ν/ν_1
ξ	Transformation maps x to ξ . Section 1.2 only.

ξ	See Eqn. (2.4.3).
ρ	Density.
ρ_1	Value of ρ in upper main stream.
ρ_2	Value of ρ in lower secondary stream or quiescent region.
$\bar{\rho}$	ρ/ρ_1
$\bar{\rho}_0$	Value of $\bar{\rho}$ at $\bar{u} = \bar{u}_0$.
σ	Jet spreading or similarity parameter.
τ	Longitudinal shear stress component.
ϕ	Third cartesian coordinate or aximuthal angle.
Φ	Velocity potential.
ψ	Stream function.
ω	Chapman viscosity index.

Subscripts:

1	Upper main stream.
2	Lower secondary stream or quiescent region.
0	Dividing streamline.

Superscripts:

-	$() / ()_1$
u	Quantity above dividing streamline.
l	Quantity below dividing streamline.
v	= 0; plane case. =1; axisymmetric case.

1. INTRODUCTION

1.1 Definition of Problem

The objective of this investigation is to develop a method for numerically integrating the differential equations which govern the growth of a free shear layer starting from an arbitrary initial velocity profile. Figure 1 is a diagrammatic sketch of this situation. The shear layer is assumed to develop under constant pressure, and the interaction effects, that would occur at the origin in a physically realistic case, are overlooked. The integration scheme will encompass the effects of compressibility and heat transfer at arbitrary Prandtl number. It will apply to both turbulent and laminar, and to both axisymmetric and plane free shear layers.

The study of free shear layers is partly motivated by their widespread application in the Chapman-Korst type theories for separated supersonic flows. This group of theories originated with Chapman^{1,2} and Korst's^{3,4,5} treatment of the problem of supersonic flow over a rearward facing step. There are a large number of theories which treat the rearward-facing step and the related problem of the supersonic near-wake using the Chapman-Korst model, and these have been extensively reviewed by the author in Reference 6.

In the past, investigators using the Chapman-Korst model have taken the initial boundary layer into account by simply replacing the real shear layer by an equivalent asymptotic free shear layer. That is to say, they approximated the be-

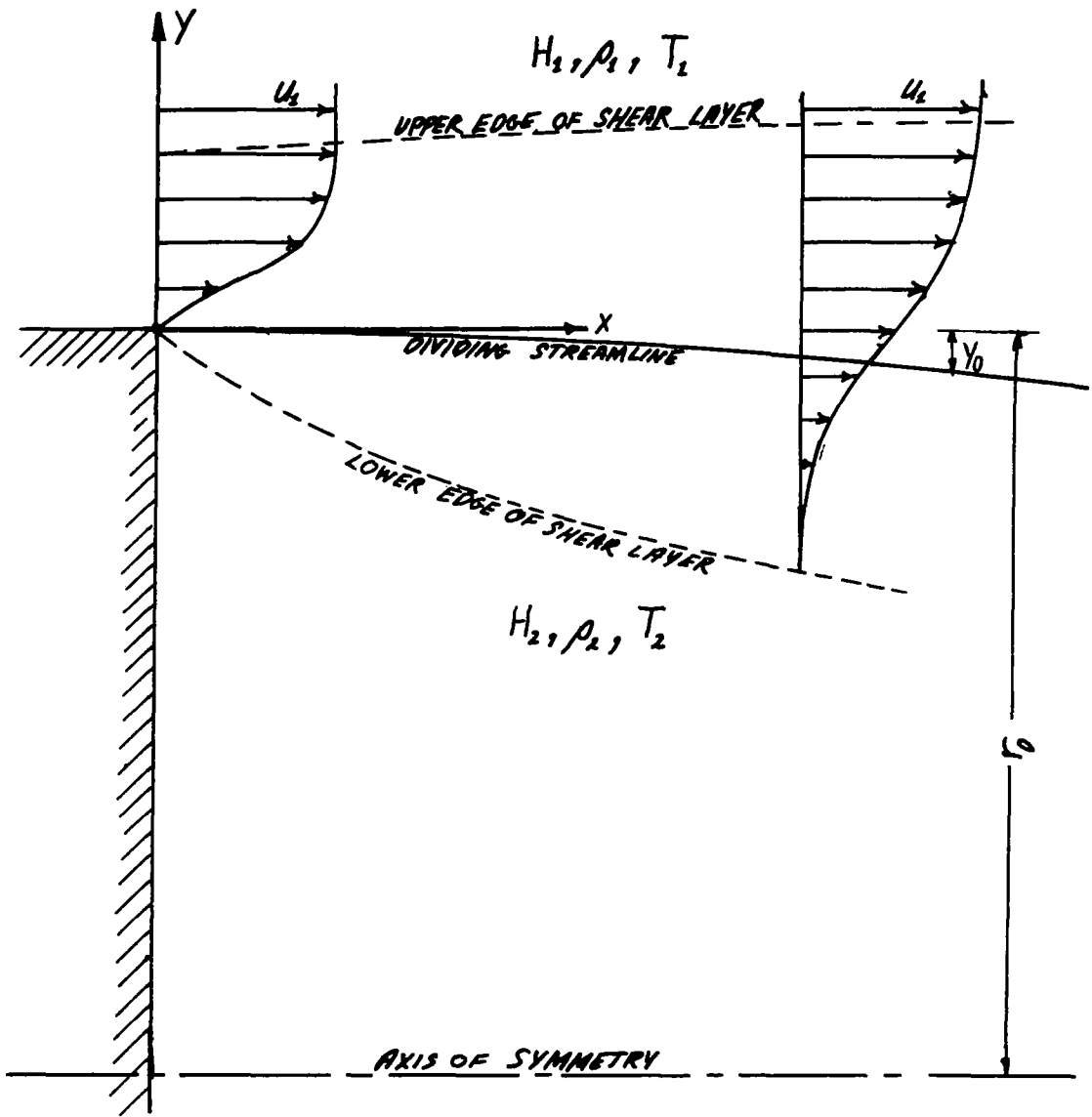


FIG. 1.1 A FREE SHEAR LAYER DEVELOPING FROM AN ATTACHED BOUNDARY LAYER

havior of the real shear layer, by that of a longer shear layer originating from a boundary layer of zero thickness. It is partly the purpose of this investigation to evaluate this type of approximation, particularly with regard to its estimates for the heat transfer across and velocity along the dividing streamline, i.e., the streamline which lies on the interface between the air previously quiescent and that previously part of the attached boundary layer.

The mathematical difficulties that arise in a study of free shear layers make it a more interesting problem in many ways than that of the boundary layer. This is most vividly illustrated by the apparent non-uniqueness of the solution to the boundary layer equations in the case of the free shear layer.

To appreciate this situation a comparison of the boundary conditions for the two cases must be made.

$$\begin{array}{ll} u \rightarrow u_1 ; & y \uparrow \infty \\ u = v = 0 ; & y = 0 \end{array} \quad \text{Attached boundary layer}$$

$$\begin{array}{ll} u \rightarrow u_1 ; & y \uparrow \infty \\ u \rightarrow 0 & ; y \uparrow -\infty \\ v = 0 \text{ at } & y = y_0(x) \end{array} \quad \text{Free shear layer}$$

Note that the position of the dividing streamline, $y_0(x)$, is unknown a priori; although the equations can be solved in the $x - u$ plane, leaving the orientation in space arbitrary.

It will be shown that in order to fix $y_0(x)$, it is necessary to investigate the higher order corrections to the boundary layer solutions. This is in sharp contrast to the attached boundary layer where the zeroth order solution can be determined uniquely, independently of the higher order corrections.

The other main mathematical difficulties peculiar to the problem of the development of free shear layers are connected with the singularity at the origin. This singularity has two aspects.

(i) The algebraic singularity.

Goldstein⁷ was the first to point out that if one specifies an initial velocity profile arbitrarily, without regard for the pressure distribution downstream, then the existence of an algebraic singularity at the origin seriously hampers any attempt to continue an integration of the boundary layer equations downstream. This occurs even with an attached boundary layer.

In the case in question, this singularity is easily demonstrated. Consider the incompressible boundary layer equation, viz.

$$u \frac{\partial u}{\partial x} + v \frac{\partial u}{\partial y} = \frac{\partial \tau}{\partial y}$$

Now at the origin $(0,0)$ it is clear that in general $\frac{\partial \tau}{\partial y} \neq 0$ and $\frac{\partial u}{\partial y} \neq 0$. But $u = v = 0$, therefore, in order for the above equation to be satisfied $\frac{\partial u}{\partial x} = 0\left(\frac{1}{u}\right)$ at $(0,0)$.

(ii) Discontinuity in boundary conditions at origin.

This singularity is compounded here by the fact that at the origin the initial conditions are such that $u = 0$ and $T = T_w$ at $y = 0$, but at the limit $x \rightarrow 0$, $u \rightarrow 0$ and $T \rightarrow T_2$ as $y \rightarrow -\infty$. However, this also implies an infinite $\frac{\partial u}{\partial x}$, as well as an infinite $\frac{\partial T}{\partial x}$.

In addition, the infinite domain and behavior of the solution at $y \rightarrow \pm\infty$ make this a more difficult problem in numerical integration than the corresponding attached boundary layer.

The case of the turbulent free shear layer also presents the difficulty of finding a suitable eddy viscosity model. The most common approach in the case of the asymptotic free shear layer, is to follow Görtler's⁸ version of the Prandtl-Reichardt^{9,10} constant exchange coefficient theory. That is to use

$$\epsilon = \frac{1}{4\sigma^2} u_1 x$$

where σ is a constant, known as the jet spreading or similarity parameter, which depends on the free stream Mach number.

However, in the case of the developing free shear layer, this is not a particularly useful approach, since σ also depends on x and on the shape of the initial profile. In addition, there seems to be considerable confusion as regards the variation of σ with M_1 . Therefore, because of

these difficulties a new approach was tried. Essentially it is an extension of Clauser's¹¹ model for the eddy viscosity in the outer part of a turbulent boundary layer.

1.2 A Brief Exposition on the Method of Integration.

The method used for the numerical solution of the partial differential equations, which govern the development of a free shear layer, is based on Dorodnitsyn's^{12,13} extension of Galerkin's method for nonlinear ordinary differential equation. This method was chosen mainly because it is thought to have several advantages for application to the problem at hand. Its application to an extremely varied group of problems, including those governed by elliptic, parabolic, hyperbolic and mixed equations is thoroughly discussed in Reference 14.

In the Russian literature the method is invariably referred to as the method of integral relations, but some American authors have called it the GKD (Galerkin-Kantorovich-Dorodynitsyn) method, and, occasionally, the method of weighted residuals. Despite its increasing popularity, the technique is still subject to widespread misunderstanding, and therefore, it might prove useful to present below a brief explanation of the general method of attack.

The numerical solution of a system of partial differential equations using this technique takes place in two main steps. First, the system of partial differential equations is reduced to a system of ordinary differential equations.

Second, the system of ordinary differential equations is integrated numerically; in general, this is a much easier task.

This reduction is achieved in the following way, although it should be pointed out that the steps are not necessarily carried out in the same order for every problem.

Consider a set of general nonlinear partial operators L_i , which involve derivatives with respect to x and y , to arbitrary order and degree. Consider a system of partial differential equations

$$L_i \underline{u} = F_i(x, y, u_1, \dots, u_N) \tag{1.2.1}$$

$$\underline{u} = (u_1, \dots, u_N) ; i = 1, \dots, N$$

with the appropriate boundary conditions, which is to be integrated over a domain D . Now suppose it is possible to find a transformation \mathcal{J} that maps (x, y, u_1, \dots, u_N) to a $(\xi, \eta, v_1, \dots, v_N)$ space and D to Δ , such that the system (1.2.1) becomes

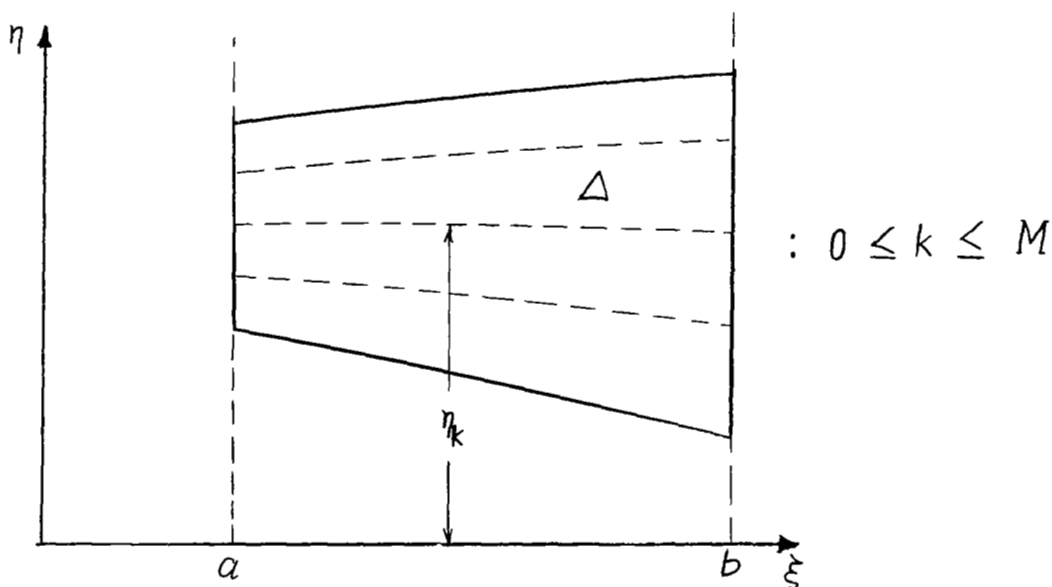
$$L_i \underline{v} = \phi_i(\xi, \eta, v_1, \dots, v_N) \tag{1.2.2}$$

$$\underline{v} = (v_1, \dots, v_N) ; i = 1, \dots, N$$

to be integrated over Δ . And such that $(\eta^2 + v_1^2 + \dots + v_N^2)^{1/2}$ be bounded. Of course, \mathcal{J} may be an identity trans-

formation if $(y^2 + u_1^2 + \dots + u_N^2)^{1/2}$ is already bounded. The requirement of boundedness is necessary to ensure the convergence of certain approximating polynomials. For convenience, one more restriction is placed on \mathcal{J} ; namely that the transformed domain Δ , have two of its sides be lines $\xi = a$ and $\xi = b$, where b may be $+\infty$.

Now Δ is divided into M strips, as shown below,



Suppose there exists a function $f_{ik}(\eta)$, $2 \leq i \leq N$, $1 \leq k \leq M$ in each strip for each of $N-1$ dependent variable v_2, \dots, v_N , such that it satisfies the boundary conditions and/or interfacial conditions to be imposed on the appropriate v_i . Then the dependent variables are approximated by the expressions

$$v_i = f_{ik}(\eta) \sum_{\ell=1}^{P_k} a_{ik\ell}(\xi) \eta^{\ell-1}; \quad \begin{array}{l} 2 \leq i \leq N \\ 1 \leq k \leq M \end{array} \quad (1.2.3)$$

in each of the M strips. Where P_k is the order of the approximating polynomial in the kth strip.

It should be noted that in many applications, e.g. attached boundary layer problems, only one strip is necessary, i.e. $M = 1$, and that it is seldom necessary to have more than three strips.

It is now assumed that a set of weighting functions

$$g_{i\ell}(\eta) : \begin{matrix} 2 \leq i \leq N \\ 1 \leq \ell \leq P \end{matrix} ; P = \sum_{k=1}^M P_k + Q \quad (1.2.4)$$

exist, such that they are linearly independent and piecewise continuous across the strips.* A further restriction on the class of weighting functions will be introduced below. Also the meaning of the symbol Q will be explained.

Next, the following set of $(N-1)P$ equations is constructed.

$$\bar{\Lambda}_{i\ell} \underline{v} = \bar{\Phi}_{i\ell}(\xi, \eta, v_1, \dots, v_N) \quad (1.2.5)$$

where

$$\begin{aligned} \bar{\Lambda}_{i\ell} &= g_{i\ell}(\eta) \Lambda_1 + \frac{dg_{i\ell}(\eta)}{d\eta} \Lambda_i \\ \bar{\Phi}_{i\ell} &= g_{i\ell}(\eta) \Phi_1 + \frac{dg_{i\ell}(\eta)}{d\eta} \Phi_i \end{aligned} \quad \begin{matrix} : 2 \leq i \leq N \\ : 1 \leq \ell \leq P \end{matrix} \quad (1.2.6)$$

*Actually it is probable that the class of weighting functions could be extended to include generalized functions, such as the Dirac delta function.

Each equation in the system (1.2.5) is now integrated with respect to η from $\eta = \eta_0$ to $\eta = \eta_M$, i.e.

$$\sum_{k=1}^M \int_{\eta_{k-1}}^{\eta_k} \{ \int (\bar{\Lambda}_{i\ell} \underline{v} - \bar{\Phi}_{i\ell}) d\eta \} = 0 \quad (1.2.7)$$

$$: 2 \leq i \leq N$$

$$: 1 \leq \ell \leq P$$

The additional requirement on the set of weighting functions is now introduced. They are to be picked in such a way that the dependent variable v_1 be eliminated from the equations (1.2.7).

The approximating expressions (1.2.3) are now substituted into the system (1.2.7). The integrations in (1.2.7) are carried out and the result is a set of $(N-1)P$ ordinary differential equations. The dependent variables of this system of $(N-1)P$ ordinary differential equations are the coefficients of (1.2.3) i.e. $a_{ik\ell}(\xi)$ of which there are $(P-Q)(N-1)$. The remaining $Q(N-1)$ variables are partly made up of those of the $\eta_k(\xi)$ which are undetermined in advance. However, often some of the $a_{ik\ell}(\xi)$ can be eliminated by means of interfacial conditions, so it is possible for the number Q to end up negative.

The resulting approximating system of ordinary differential equations are now integrated by an appropriate numerical method on an electronic digital computer.

The procedure outlined above can be generalized to higher dimensions.

The advantages of this technique are:

(a) It makes use of the well-developed area of numerical integration of systems of ordinary differential equations.

(b) In effect, in this method it is an integral which is being approximated. The accuracy of approximation in this is increased to some extent as a result of a decrease in the coefficient of the remainder term. In addition, an integral represents a smoother function than the integrand function. Finally, the integral has continuous representation even when the integrand function has a finite discontinuity.

(c) The numerical instability, often encountered when finite difference techniques are employed, can be avoided.

1.3 A Short Survey of Theoretical Studies on Free Shear Layers

From a mathematical viewpoint free shear layers may be divided into two main classes; namely, plane shear layers with step-type initial conditions, vis-a-vis those that fall outside this category. The distinction the former group enjoys is that of self-similarity, that is to say there exists a transformation of the independent variables such that the velocity and temperature profiles are invariant with longitudinal displacement. Mathematically this implies that the governing equations can be reduced to a system of ordinary differential equations; indeed, if the Prandtl Number is taken as one, a single equation will result. Because of this essential simplification and because free shear layers developing from arbitrary initial conditions

tend toward the self-similar state as the distance downstream approaches infinity, the plane free shear layer with step-type initial conditions, usually referred to as the asymptotic half-jet, has been a widely studied problem.

If in the turbulent case the eddy viscosity is approximated by Prandtl's mixing length model, the governing equations reduce to a linear ordinary differential equation, which was first derived and solved by Tollmien¹⁵ in 1926. However, it was later realized that the mixing length formulation is unsatisfactory for free mixing problems and a new eddy viscosity model, based on the idea of constant exchange coefficients, was proposed by Reichardt⁹ and Prandtl¹⁰. Using this new model Görtler⁸ solved the asymptotic half-jet problem: first deriving a non-linear ordinary differential equation, and then integrating it analytically, by expanding the solution in terms of the small parameter $\frac{u_1 - u_2}{u_1 u_2}$.

Owing to its instability the homogeneous incompressible laminar free shear layer does not occur in nature; consequently it did not, at first, receive the attention accorded its turbulent counterpart. On the other hand, the inhomogeneous case is of practical interest in meteorology, oceanography, and to certain processes in chemical engineering; and for this reason was tackled by Keulegan¹⁶ and Lock¹⁷. In addition the homogeneous problem was considered by Lessen¹⁸ in the course of a stability study. In contrast, at supersonic speeds the laminar free shear layer becomes stable, and its occurrence in many

separated flow phenomena led to the numerical study of Chapman¹⁹. More recently, Crane²⁰ has extended Görtler's⁸ series solution into the compressible regime; and Mills²¹, as well as Jacques and Gailly²², have presented accurate numerical solutions for the general compressible laminar and turbulent free shear layer.

The theoretical methods for solving the problem of free shear layers developing from non-step-type initial conditions may be further subdivided into five classes.

1. Methods based on local coordinates at the origin:

Inspired by Goldstein's⁷ treatment of the problem of the wake behind a flat plate, Denison and Baum²³ dealt with the singularity at the origin by transforming the independent variables in order to begin their numerical integration, which was continued by means of finite differences. Their paper presents the only accurate solution to date for the developing free shear layer; albeit using only the Blasius profile as initial condition, with Prandtl Number set as one, and determining the coefficient of viscosity by the crude assumption $\mu = T$. Later Baum²⁴ showed how their analysis could be extended to the case of the self-similar blowing profile as initial condition.

2. Momentum-Integral Methods:

The sole contribution to this category is due to Kubota and Dewey²⁵, Their method employs two free parameters, using as the two governing equations momentum-integral relations valid above and below the dividing streamline respectively. Their results compare rather poorly to those of Denison and Baum.

3. Methods based on linearization of equations of motion:

Taking note of the success of Görtler⁸ and Pai's²⁶ application of small perturbation techniques to the asymptotic half-jet problem, Chapman and Korst²⁷ advanced the following linearization of the momentum equation

$$u_1 \frac{\partial u}{\partial x} = \nu \frac{\partial^2 u}{\partial y^2}$$

This can be transformed into a form of the heat equation and integrated analytically. The basic method was extended to compressible turbulent iso-energetic shear layers by Korst et al.²⁸; then to the non-isoenergetic case by Page²⁹; and finally to two-stream mixing by Korst and Chow³⁰.

4. The Virtual Origin Approximation:

The basic idea, which was first introduced by Kirk³¹, is to replace the real shear layer by an asymptotic half-jet growing from a virtual origin upstream of the real one. Subsequently Nash³² and Hill^{33,34} have refined and improved on the original Kirk method.

5. Equivalent Bleed Approximation:

This concept was first used by Carriere and Sirieix³⁵. The idea is to replace the real shear layer by an equivalent asymptotic half-jet starting from the same origin, but having a small amount of mass flux, with an attendant momentum flux, somehow interposed between the air in the upper stream and that entrained from the quiescent region. Golik³⁶, and Korst and Chow³⁰, have also given this type of approximation some attention.

From this brief and inadequate survey it could perhaps be inferred that the problem of the general developing free shear layer has not as yet been treated satisfactorily.* It is the purpose of the investigation herein presented to go some of the way toward correcting this state of affairs by providing a reasonably accurate numerical study of the development of the general compressible free shear layer.

*A complete survey and critique of the theory of free shear layers is presented by the author in reference 37.

2. GENERAL ANALYSIS

2.1 Governing equations

In the case of the laminar asymptotic free shear layer, i.e. one with no initial boundary layer velocity profile, it can be shown rigorously by means of asymptotic analysis that, in the limit of $Re_1 \rightarrow \infty$, the solution of the equations shown below (viz. the regular compressible boundary layer equations) furnishes the zeroth order terms in an asymptotic expansion of the solution of the full Navier-Stokes equations. For a turbulent free shear layer it is generally assumed that the terms in the averaged Navier-Stokes equations involving the mean quantities are of the same order as their counterparts in the laminar free shear layer.

However, the case of the free shear layer developing from a given boundary layer velocity profile is somewhat different. The existence of the singularity at the origin means that in a small region around the origin, $\frac{\partial u}{\partial x} = 0 \left(\frac{\partial u}{\partial y} \right)$. This fact invalidates the use of the regular boundary layer equations in this region. In actuality, the boundary layer equations would cease to be valid at a distance $O\left(\frac{1}{\sqrt{Re_1}}\right)$ upstream from the origin. In this region the boundary layer would no longer behave parabolically and would start to adjust itself to the presence of the trailing edge. In addition, a complicated interaction with the boundary layer on the rearward facing base wall, involving the formation of a separation shock wave, would occur in most real instances of supersonic flow over rearward facing steps

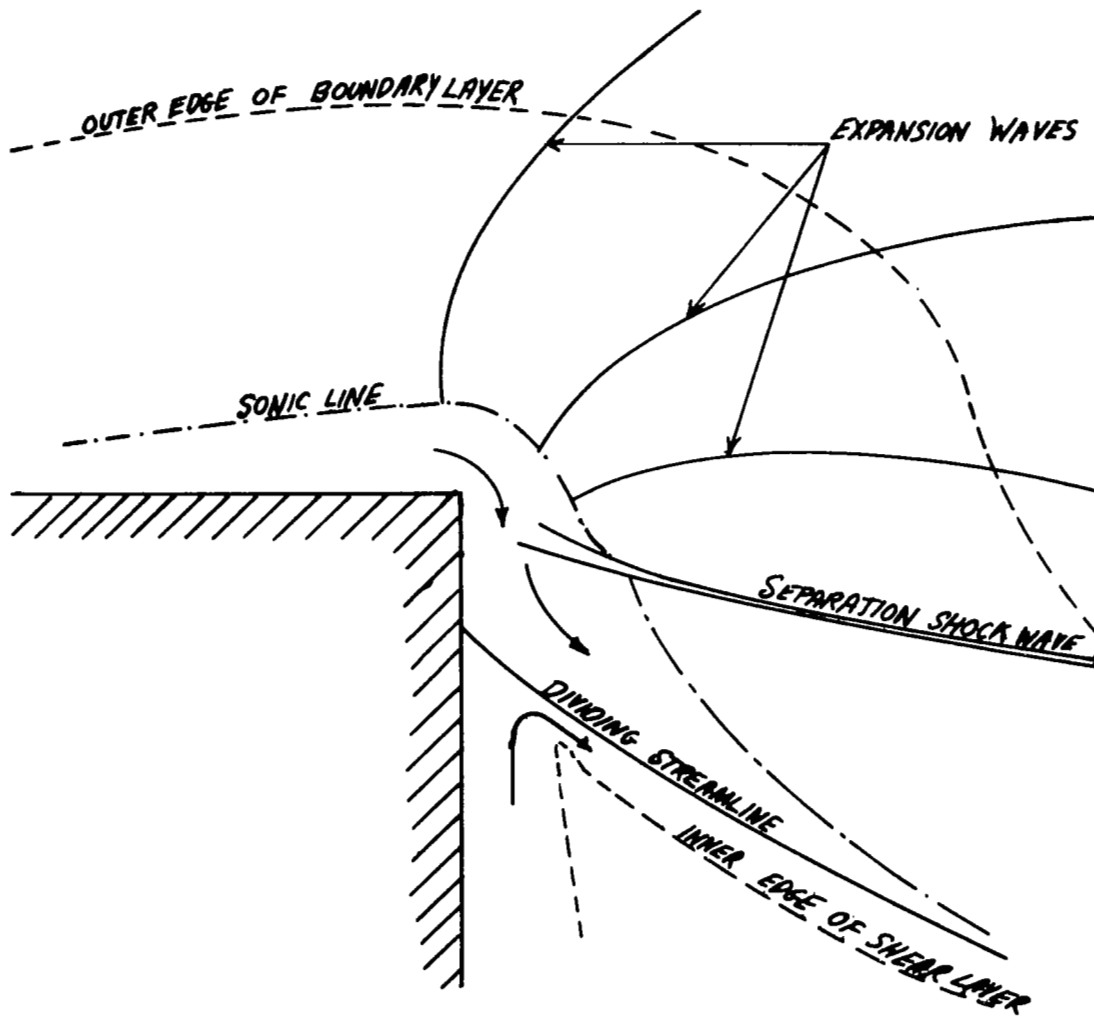


FIG. 2.1 THE INTERACTION PROCESS AT THE TRAILING EDGE

and related configurations.^{38, 39, 40} See Fig. 2.1. In what follows these interactions are ignored, and the regular boundary layer equations are assumed to be valid throughout the region of interest. This attitude can be justified by noting the small extent of the interaction region in most cases.

The boundary layer equations for compressible shear layers developing under constant pressure can be written in the following form.

$$\frac{\partial}{\partial x} (\rho u r_0^v) + \frac{\partial}{\partial y} (\rho w r_0^v) = 0 \quad (2.1.1)$$

$$\rho \left(u \frac{\partial u}{\partial x} + w \frac{\partial u}{\partial y} \right) = \frac{\partial}{\partial y} \left(\epsilon \frac{\partial u}{\partial y} \right) \quad (2.1.2)$$

$$\rho \left(u \frac{\partial H}{\partial x} + w \frac{\partial H}{\partial y} \right) = \frac{\partial}{\partial y} \left[\frac{\epsilon}{Pr} \frac{\partial}{\partial y} \left(H + (Pr-1) \frac{u^2}{2} \right) \right] \quad (2.1.3)*$$

where

$v =$
 0 : plane
 1 : axisymmetric

$w =$
 v : laminar
 $v \left(1 + \frac{\overline{\rho'v'}}{\rho v} \right)$: turbulent

$\epsilon =$
 μ , molecular viscosity : laminar
 eddy viscosity : turbulent**

$Pr =$
 laminar Prandtl number = $\frac{C_p \mu}{k}$
 turbulent Prandtl number = $\frac{C_p \epsilon}{\lambda_t}$

*Eqn. (1.3.3) is derived by multiplying the energy equation written in terms of temperature by C_p and adding it to Eqn. (1.3.2) times u .

**Strictly the molecular viscosity should also be included, however it only becomes comparable to the eddy viscosity at the edges of the shear-layer where both are negligibly small.

λ_t = eddy conductivity coefficient

$h = C_p T$ = specific enthalpy

$H = C_p T_0 = C_p T + \frac{u^2}{2}$ = specific total enthalpy

and r_0 is the displacement of x-axis from axis of symmetry.

See Fig. 1.1.

The appropriate boundary conditions are given by:

$$\begin{aligned} u &\rightarrow u_1 & : & & y &\rightarrow +\infty \\ H &\rightarrow H_1 & & & & \end{aligned} \quad (2.1.4)$$

$$\begin{aligned} u &\rightarrow 0 & : & & y &\rightarrow -\infty \\ H &\rightarrow H_2 & & & & \end{aligned}$$

Plus arbitrary initial conditions.

$$\begin{aligned} u &= u_i(y) & : & & & \\ & & & & \text{at } x = 0 & \\ H &= H_i(y) & : & & & \end{aligned} \quad (2.1.5)$$

2.2 Asymptotic behavior of solutions

It is necessary in the main body of the analysis to have a knowledge of the asymptotic behavior of $\frac{\partial u}{\partial y}$ and H as $y \rightarrow +\infty$.

Introduce a stream function ψ , such that

$$u = \frac{1}{\rho r_0} v \frac{\partial \psi}{\partial y} \quad ; \quad w = - \frac{1}{\rho r_0} v \frac{\partial \psi}{\partial x} \quad (2.2.1)$$

whence the continuity equation is automatically satisfied,

and equation (2.1.2) becomes

$$\rho \left\{ \frac{1}{\rho r_0} v \frac{\partial \psi}{\partial y} \frac{\partial}{\partial x} \left(\frac{1}{\rho r_0} v \frac{\partial \psi}{\partial y} \right) - \frac{1}{\rho r_0} v \frac{\partial \psi}{\partial x} \frac{\partial}{\partial y} \left(\frac{1}{\rho r_0} v \frac{\partial \psi}{\partial y} \right) \right\} = \frac{\partial}{\partial y} \left\{ \epsilon \frac{\partial}{\partial y} \left(\frac{1}{\rho r_0} v \frac{\partial \psi}{\partial y} \right) \right\} \quad (2.2.2)$$

Now

$$u \rightarrow u_1 \quad \text{as} \quad y \rightarrow +\infty$$

i.e.

$$\frac{1}{\rho r_0^v} \frac{\partial \psi}{\partial y} \rightarrow u_1 \quad \text{as} \quad y \rightarrow +\infty \quad (2.2.3)$$

Integration yields

$$\psi \sim \rho_1 r_0^v u_1 y + f_1(x) \quad : \quad y \rightarrow +\infty \quad (2.2.4)$$

where $f_1(x)$ is some unknown function of x .

Hence in the limit $y \rightarrow +\infty$, eq. (2.2.2) becomes

$$\begin{aligned} \rho_1 \left\{ u_1 \frac{\partial}{\partial x} (u_1) - \frac{1}{\rho_1 r_0^v} \left[\rho_1 u_1 y \frac{dr_0^v}{dx} + \frac{df_1}{dx} \right] \cdot \left[\frac{\partial}{\partial y} \left(\frac{1}{\rho_0 r_0^v} \frac{\partial \psi}{\partial y} \right) \right] \right\} \\ = \frac{\partial}{\partial y} \left\{ \epsilon \frac{\partial}{\partial y} \left(\frac{1}{\rho r_0^v} \frac{\partial \psi}{\partial y} \right) \right\} \end{aligned} \quad (2.2.5)$$

The first term is zero, since u_1 is constant, and there are two possibilities, viz.

$$(i) \quad r_0^v = \text{const.} \quad \text{i.e.} \quad \frac{dr_0^v}{dx} = 0 \quad (2.2.6)$$

$$(ii) \quad \frac{dr_0^v}{dx} \neq 0 \quad (2.2.7)$$

Taking the first possibility, equation (2.2.5) reduces to

$$- \frac{1}{r_0^v} \frac{df_1}{dx} \frac{\partial}{\partial y} \left(\frac{1}{\rho_0 r_0^v} \frac{\partial \psi}{\partial y} \right) = \frac{\partial}{\partial y} \left\{ \epsilon \frac{\partial}{\partial y} \left(\frac{1}{\rho r_0^v} \frac{\partial \psi}{\partial y} \right) \right\} \quad (2.2.8)$$

integrating once yields

$$\frac{\partial}{\partial y} \left(\frac{1}{\rho r_0^v} \frac{\partial \psi}{\partial y} \right) = - \frac{1}{r_0^v \epsilon_1} \frac{df_1}{dx} \left(\frac{1}{\rho r_0^v} \frac{\partial \psi}{\partial y} \right) + \text{const.} \quad : \quad y \rightarrow +\infty$$

or

$$\frac{\partial u}{\partial y} \sim + \frac{1}{r_0^v \epsilon_1} \frac{df_1}{dx} (u_1 - u) \quad : \quad y \rightarrow \infty \quad (2.2.9)$$

Turning to the second case, (2.2.7), eq. (2.2.5) reduces to

$$- \rho_1 u_1 \nu \frac{d}{dx} (\log r_0) y \frac{\partial}{\partial y} \left(\frac{1}{\rho r_0 \nu} \frac{\partial \psi}{\partial y} \right) = \frac{\partial}{\partial y} \left\{ \varepsilon \frac{\partial}{\partial y} \left(\frac{1}{\rho r_0 \nu} \frac{\partial \psi}{\partial y} \right) \right\}$$

or

$$- \rho_1 u_1 \nu \frac{d}{dx} (\log r_0) y \frac{\partial u}{\partial y} = \frac{\partial}{\partial y} \left\{ \varepsilon \frac{\partial u}{\partial y} \right\} \quad (2.2.10)$$

integrating once gives

$$- \frac{1}{\varepsilon_1} \rho_1 u_1 \nu \frac{d}{dx} (\log r_0) \{ y u - \int u_1 dy \} = \frac{\partial u}{\partial y} + \text{const.}$$

i.e.

$$\frac{\partial u}{\partial y} = \frac{\rho_1 u_1}{\varepsilon_1} \nu \frac{d}{dx} (\log r_0) \{ y(u_1 - u) \} \quad (2.2.11)$$

Now consider the asymptotic behavior when $y \rightarrow -\infty$

$$u = \frac{1}{\rho r_0 \nu} \frac{\partial \psi}{\partial y} \rightarrow 0 \quad \text{as } y \rightarrow -\infty \quad (2.2.12)$$

whence

$$\psi \sim -g_1(x) \quad \text{as } y \rightarrow -\infty \quad (2.2.13)$$

where $g(x)$ is some unknown function.

In which case, equation (2.2.2) reduces to

$$+ \frac{1}{r_0 \nu} \frac{dg_1}{dx} \frac{\partial u}{\partial y} = \frac{\partial}{\partial y} \left(\varepsilon \frac{\partial u}{\partial y} \right) \quad (2.2.14)$$

integrating once obtains

$$\frac{\partial u}{\partial y} \sim \frac{1}{\varepsilon_2 r_0 \nu} \frac{dg_1}{dx} u \quad ; \quad y \rightarrow -\infty \quad (2.2.15)$$

The asymptotic behavior of H can be established by observing that if $Pr = 1$, then equation (2.1.3) becomes

$$\rho \left(u \frac{\partial H}{\partial x} + w \frac{\partial H}{\partial y} \right) = \frac{\partial}{\partial y} \left(\epsilon \frac{\partial H}{\partial y} \right) \quad (2.2.16)$$

Whence on comparison with equation (2.1.2) it can be seen that the solution to equation (2.2.16) is

$$H = A + B u \quad (2.2.17)$$

where

$$A = H_2 \quad (2.2.18)$$

$$B = \frac{H_1 - H_2}{u_1} \quad (2.2.19)$$

in view of the boundary conditions (2.1.4).

The Prandtl number for air is close to 1, and moreover the neglected term of equation (2.1.3) involves $\frac{\partial u}{\partial y}$ which is zero in the limits $y \rightarrow \pm\infty$. Therefore equation (2.2.17) should represent the asymptotic behavior of H.

It is also necessary to have some knowledge of the asymptotic behavior of w as $y \rightarrow \pm\infty$ in order to fix the position of the dividing streamline. See section 2.5.

First consider the case of $\frac{dr_0}{dx} = 0$.

From eqn. (2.2.4 and 1) is obtained the result

$$w = - \frac{1}{\rho_1 r_0} \frac{df_1}{dx} + o(1) \quad : \quad y \rightarrow \infty \quad (2.2.20)$$

similarly from eqns. (2.2.13 and 1)

$$w = \frac{1}{\rho_2 r_0} \frac{dg_1}{dx} + o(1) \quad : \quad y \rightarrow -\infty \quad (2.2.21)$$

In order to obtain additional terms in asymptotic expansions for w as $y \rightarrow \pm\infty$, the expressions for $\frac{\partial u}{\partial y}$ must be integrated. For instance, consider eqn. (2.2.9), integrating once gives

$$u = u_1 - \exp(-f_2(x)y) + o(e^{-y}) : y \rightarrow \infty \quad (2.2.22)$$

where

$$f_2 = \frac{1}{r_0^v \epsilon_1} \frac{df_1}{dx}$$

integrating again with respect to y leads to

$$\psi = \rho_1 u_1 r_0^v y + f_1(x) + \frac{\rho_1 r_0^v}{f_2} e^{-f_2 y} + o(e^{-y}) \quad : y \rightarrow \infty \quad (2.2.23)$$

Thus from eqn. (2.2.1)

$$w = \frac{-1}{\rho_1 r_0^v} f_1'(x) + \frac{f_2'}{f_2} y e^{-f_2 y} + \frac{f_2'}{f_2} e^{-f_2 y} + o(e^{-y}) : y \rightarrow \infty \quad (2.2.24)$$

Similar treatment yields the following result for the lower limit.

$$w = \frac{1}{\rho_2 r_0} \frac{dg_1}{dx} + \frac{g_2'}{g_2} e^{g_2 y} + o(e^y) \quad : y \rightarrow \infty \quad (2.2.25)$$

where

$$g_2 = \frac{1}{\epsilon r_0} \frac{dg_1}{dx}$$

Turning to the case where $\frac{dr_0}{dx} \neq 0$. Integrating eqn.

(2.2.11) once yields the following result.

$$u = u_1 - e^{-f_3(x)} \frac{y^2}{2} + o(e^{-y^2}) \quad : y \rightarrow \infty \quad (2.2.26)$$

where

$$f_3(x) = \frac{\rho_1 u_1}{\epsilon_1} \frac{d}{dx} (\log r_0)$$

integrating again with respect to y leads to

$$\psi = \rho_1 u_1 r_0 y + f_1(x) - \frac{\sqrt{\pi}}{2} \operatorname{erf}\left(y \left\{ \frac{f_3}{2} \right\}^{1/2}\right) : y \rightarrow \infty \quad (2.2.27)$$

But

$$\operatorname{erf}(x) \sim 1 - \frac{e^{-x^2}}{\sqrt{\pi} x} \left[1 - \frac{1}{2x^2} + \dots \right] \quad : x \rightarrow \infty \quad (2.2.28)$$

substituting this asymptotic expansion into eqn. (2.2.27)

results in the following expansions for ψ

$$\psi = \rho_1 u_1 r_0 y + f_1(x) - \frac{\sqrt{\pi}}{2} + \frac{1}{\sqrt{2f_3}} \frac{e^{-y^2}}{y} \frac{f_3}{2} \left[1 - \frac{1}{f_3 y^2} + \dots \right] \quad : y \rightarrow \infty \quad (2.2.29)$$

Therefore from eqn. (2.2.1)

$$w = -u_1 \frac{d}{dx} (\log r_0) y + \frac{1}{\rho_1 r_0} f_1'(x) - \frac{1}{\rho_1 r_0} \frac{f_3'}{2(2f_3)^{1/2}} y e^{-\frac{f_2}{2} y^2} + o(y e^{-y^2}) \quad : y \rightarrow \infty \quad (2.2.30)$$

The behavior of w at the lower limit is similar to eqn. (2.2.25).

2.3 Derivation of the integral relations

This step is roughly equivalent to obtaining the system of equations (1.2.7), except that the application of transformation \mathcal{J} and the division into strips is left to the next section.

Suppose there exists a set of weighting functions $f_j(u)$ which are linearly independent and piecewise continuous in u . An additional requirement will be imposed later. Now multiply equation (2.1.1) by $f_j(u)$, and equation (2.1.2) by $r_0^v \frac{df_j}{du}$ and integrate their sum with respect to y from $-\infty$ to $+\infty$. Thus the following system of equations are obtained.

$$\frac{d}{dx} \int_{-\infty}^{\infty} \rho u r_0^v f_j(u) dy + \rho w r_0^v f_j(u) \Big|_{-\infty}^{\infty} = \int_{-\infty}^{\infty} \frac{\partial}{\partial y} (\epsilon r_0^v \frac{\partial u}{\partial y}) f_j''(u) dy \quad (2.3.1)$$

Now it is required that $f_j(u)$ be such that

$$f_j(u_1) = f_j(0) = 0 \quad (2.3.2)$$

whence integrating the right-hand side by parts equation

(2.3.1) becomes

$$\frac{d}{dx} \int_{-\infty}^{\infty} \rho u r_0^v f_j(u) dy = - \int_{-\infty}^{\infty} \epsilon r_0^v \left(\frac{\partial u}{\partial y}\right)^2 \frac{d^2 f_j}{du^2} dy \quad , j = 0, 1, 2, \dots \quad (2.3.3)$$

Consider a second set of weighting functions $g_k(u)$, or equivalently $g_k(H)$, with the same requirements. Multiply equation (2.1.1) by $g_k(H)$ and equation (2.1.3) by $r_0^v \frac{d}{dH} g_k(H)$, add and integrate with respect to y from $-\infty$ to $+\infty$. Thus a second system of equations are obtained, viz.

$$\frac{d}{dx} \int_{-\infty}^{\infty} \rho u r_0^v g_k(H) dy + \rho w r_0^v g_k(H) \Big|_{-\infty}^{\infty} = \int_{-\infty}^{\infty} r_0^v \frac{\partial}{\partial y} \left\{ \frac{\epsilon}{Pr} \frac{\partial}{\partial y} \left[H + (Pr-1) \frac{u^2}{2} \right] \right\} \frac{dg_k}{dH} dy \quad (2.3.4)$$

Require that the weighting functions $g_k(H)$ be such that

$$g_k(H_1) = g_k(H_2) = 0 \quad (2.3.5)$$

Thus integrating the right hand side by parts leads to the following system of equations

$$\frac{d}{dx} \int_{-\infty}^{\infty} \rho u r_0^v g_k(H) dy = - \int_{-\infty}^{\infty} \frac{\epsilon}{Pr} r_0^v \frac{\partial}{\partial y} \left[H + (Pr-1) \frac{u^2}{2} \right] \frac{d^2 g_k}{dH^2} \frac{\partial H}{\partial y} dy \quad (2.3.6)$$

Note that one of the three dependent variables, namely w , has been eliminated, and two sets of integral relations, equation (2.3.3) and equation (2.3.6) replace the original partial differential equations.

2.4 Reduction of integral relations to a system of first order ordinary differential equations.

1. As a first step, it is necessary to cast equations (2.3.5) and (2.3.6) into non-dimensional form. In this way the following systems of equations are obtained.

$$\frac{d}{d\bar{x}} \int_{-\infty}^{\infty} \bar{\rho} \bar{u} f_j(\bar{u}) \bar{r}_0^v d\bar{y} = - \frac{\varepsilon_1}{L u_1 \rho_1} \int_{-\infty}^{\infty} \bar{\varepsilon} \left(\frac{\partial \bar{u}}{\partial \bar{y}} \right)^2 f_j''(\bar{u}) \bar{r}_0^v d\bar{y} \quad (2.4.1)$$

$j = 0, 1, 2, \dots$

$$\begin{aligned} \frac{d}{d\bar{x}} \int_{-\infty}^{\infty} \bar{\rho} \bar{u} g_k(\bar{H}) \bar{r}_0^v d\bar{y} &= \frac{-\varepsilon_1}{L \rho_1 u_1} \frac{1}{Pr} \left\{ \int_{-\infty}^{\infty} \bar{\varepsilon} \left(\frac{\partial \bar{H}}{\partial \bar{y}} \right)^2 g_k''(\bar{H}) \bar{r}_0^v d\bar{y} \right. \\ &+ \left. \frac{2(\gamma-1)M_1^2}{2+(\gamma-1)M_1^2} (Pr-1) \int_{-\infty}^{\infty} \bar{\varepsilon} \bar{u} \frac{\partial \bar{u}}{\partial \bar{y}} \frac{\partial \bar{H}}{\partial \bar{y}} g_k''(\bar{H}) \bar{r}_0^v d\bar{y} \right\} \\ &k = 0, 1, 2, \dots \end{aligned} \quad (2.4.2)$$

where $\bar{x} = \frac{x}{L}$, $\bar{y} = \frac{y}{L}$, $\bar{u} = \frac{u}{u_1}$, $\bar{H} = \frac{H}{H_1}$, $\bar{\rho} = \frac{\rho}{\rho_1}$, $\bar{\varepsilon} = \frac{\varepsilon}{\varepsilon_1}$ and L is some characteristic length scale.

The integration of the left hand sides of equations (2.4.1) and (2.4.2) will be greatly facilitated if the integrand contains only known functions of \bar{u} . Therefore the following transformation is made.

$$\xi = \int \bar{r}_0^{2v} d\bar{x}, \quad \eta = \int \bar{\rho} \bar{r}_0^v d\bar{y} \quad (2.4.3)$$

whence equations (2.4.1) and (2.4.2) become

$$\frac{d}{d\xi} \int_{-\infty}^{\infty} \bar{u} f_j(\bar{u}) d\eta = - \frac{\varepsilon_1}{L u_1 \rho_1} \int_{-\infty}^{\infty} \bar{\varepsilon} \bar{\rho} \left(\frac{\partial \bar{u}}{\partial \eta} \right)^2 f_j''(\bar{u}) d\eta \quad (2.4.4)$$

$j = 0, 1, 2, \dots$

and

$$\begin{aligned} \frac{d}{d\xi} \int_{-\infty}^{\infty} \bar{u} g_k(\bar{H}) d\eta = & - \frac{\epsilon_1}{L\rho_1 u_1} \frac{1}{Pr} \left\{ \int_{-\infty}^{\infty} \bar{\epsilon} \left(\frac{\partial \bar{H}}{\partial \eta} \right)^2 g_k''(\bar{H}) d\eta \right. \\ & \left. + \frac{2(\gamma-1)M_1^2}{2+(\gamma-1)M_1^2} (Pr-1) \int_{-\infty}^{\infty} \bar{\epsilon} \bar{u} \frac{\partial \bar{u}}{\partial \eta} \frac{\partial \bar{H}}{\partial \eta} g_k''(\bar{H}) d\eta \right\} \end{aligned} \quad (2.4.5)$$

$k = 0, 1, 2, \dots$

It also is necessary to ensure boundedness of the domain. This is achieved by carrying out the following transformation.

$$(\xi, \eta) \rightarrow (\xi, \bar{u}) \quad (2.4.6)$$

resulting in the systems of equations given below.

$$\frac{d}{d\xi} \int_0^1 \bar{u} f_j(\bar{u}) \zeta(\xi, \bar{u}) d\bar{u} = - \frac{\epsilon_1}{Lu_1 \rho_1} \int_0^1 \bar{\epsilon} f_j''(\bar{u}) \frac{1}{\zeta(\xi, \bar{u})} d\bar{u} \quad (2.4.7)$$

$j = 0, 1, 2, \dots$

and

$$\begin{aligned} \frac{d}{d\xi} \int_0^1 \bar{u} g_k(\bar{H}) \zeta(\xi, \bar{u}) d\bar{u} = & - \frac{\epsilon_1}{Lu_1 \rho_1} \frac{1}{Pr} \left\{ \int_0^1 \bar{\epsilon} \left(\frac{\partial \bar{H}}{\partial \bar{u}} \right)^2 g_k''(\bar{H}) \frac{1}{\zeta(\xi, \bar{u})} d\bar{u} \right. \\ & \left. + \frac{2(Pr-1)(\gamma-1)}{2+(\gamma-1)M_1^2} M_1^2 \int_0^1 \bar{\epsilon} \bar{u} \frac{\partial \bar{H}}{\partial \bar{u}} g_k''(\bar{H}) \frac{1}{\zeta(\xi, \bar{u})} d\bar{u} \right\} \end{aligned} \quad (2.4.8)$$

$k = 0, 1, 2, \dots$

where

$$\zeta(\xi, \bar{u}) = \frac{\partial \eta}{\partial \bar{u}} \quad (2.4.9)$$

The above transformation also has the advantage that the solution is unique in (ξ, \bar{u}) coordinates, and is independent of the position of the dividing streamline

2. Partly because of the difficulty with the boundary condition discontinuity at the origin, and in part owing to the asymptotic behavior of $\zeta(\xi, \bar{u})$ and $\bar{H}(\xi, \bar{u})$, it is virtually a necessity to divide the domain into two strips. The dividing streamline $y_0(x)$ provides a logical choice for the interface.

Designating quantities in the upper and lower strips by superscripts u and ℓ respectively, the following choices for weighting functions are made.

$$\begin{aligned} f_j^u(\bar{u}) &= (\bar{u}^{j+1} - 1) & : \bar{u} > \bar{u}_0 \\ f_j^\ell(\bar{u}) &= \bar{u}^{j+1} & : \bar{u} < \bar{u}_0 \end{aligned} \quad (2.4.10)$$

$j = 0, 1, 2, 3, \dots$

$$\begin{aligned} g_k^u(\bar{H}) &= \bar{H}^{k+1} - 1 & : \bar{H} > \bar{H}_0 \\ g_k^\ell(\bar{H}) &= \bar{H}^{k+1} - \lambda^{k+1} & : \bar{H} < \bar{H}_0 \end{aligned} \quad (2.4.11)$$

$k = 0, 1, 2, \dots$

where

$$\lambda = \frac{H_2}{H_1} \quad (2.4.12)$$

Leaving to one side the case of $\frac{dr_0^v}{dx} \neq 0$, the dependent variables $\zeta(\xi, \bar{u})$ and $\bar{H}(\xi, \bar{u})$ are approximated by the following expressions

$$\begin{aligned} \text{(a)} \quad \zeta^u(\xi, \bar{u}) &= \frac{1}{(1-\bar{u})} \sum_{\ell=1}^{P_1} a_\ell(\xi) \bar{u}^{\ell-1} & : \bar{u} > \bar{u}_0 \\ \text{(b)} \quad \zeta^\ell(\xi, \bar{u}) &= \frac{1}{\bar{u}} \sum_{\ell=1}^{P_2} b_\ell(\xi) \bar{u}^{\ell-1} & : \bar{u} < \bar{u}_0 \end{aligned} \quad (2.4.13)$$

$$\begin{aligned}
(a) \quad \bar{H}^u(\xi, \bar{u}) &= \{\lambda + (1 - \lambda)\bar{u}\} \sum_{\ell=1}^{P_3} c_{\ell}(\xi) \bar{u}^{\ell-1} : \bar{u} > \bar{u}_0 \\
(b) \quad \bar{H}^k(\xi, \bar{u}) &= \{\lambda + (1 - \lambda)\bar{u}\} \sum_{\ell=1}^{P_4} d_{\ell}(\xi) \bar{u}^{\ell-1} : \bar{u} < \bar{u}_0
\end{aligned}
\tag{2.4.14}$$

The functions of \bar{u} that premultiply the polynomials in equations (2.4.13, 14) are determined from the analysis in section 2.1, specifically equations (2.2.9 and 15). Strictly speaking, the expansion in (2.4.13a and 14a) should be in terms of powers of $(1 - \bar{u})$, but this makes no practical difference.

The coefficients $b_{\ell}(\xi)$ can be obtained as functions of the $a_{\ell}(\xi)$ and $\bar{u}_0(\xi)$, by requiring continuity of \bar{u} and its derivatives with respect to \bar{y} at the interface, or equivalently

$$\begin{aligned}
\frac{\partial^n \bar{u}}{\partial \bar{u}^n}(\xi, \bar{u}_0) &= \frac{\partial^n \bar{u}^{\ell}}{\partial \bar{u}^n}(\xi, \bar{u}_0) \\
n &= 0, 1, \dots, P_2 - 1
\end{aligned}
\tag{2.4.15}$$

Similarly, $d_{\ell}(\xi)$ are found in terms of $c_{\ell}(\xi)$, by requiring continuity of \bar{H} and its derivatives.

It is possible to reduce all the quantities in equations (2.4.7, 8) to functions of ξ and \bar{u} . For instance,

$$\bar{T} = (1 + m) \bar{H} - m \bar{u}^2
\tag{2.4.16}$$

where

$$m = \frac{\gamma-1}{2} M_1^2$$

$$\bar{\rho} = \frac{1}{\bar{T}} \quad (2.4.17)$$

and

$$\varepsilon = \begin{cases} \bar{T}^\omega, & \text{or Sutherland's law is used : laminar} \\ \bar{\rho} e(\xi) & : \text{turbulent} \end{cases} \quad (2.4.18)$$

$e(\xi)$ is known as the kinematic eddy viscosity, and is generally assumed to be constant across turbulent free shear layers.

Equations (2.4.10 to 18) are now substituted into equations (2.4.7 and 8). The result is a system of first order nonlinear ordinary differential equations, with $\bar{u}_0, a_1, a_2, \dots, a_{P_1}; c_1, \dots, c_{P_3}$ as dependent variables. $P_1 + 1$ of these equations are furnished by equations (2.4.7), the remaining P_3 come from equations (2.4.8). The system can be represented succinctly by using a matrix formulation, i.e.

$$A_{ij} B_j = C_i \quad 1 \leq i, j \leq 1 + P_1 + P_3 \quad (2.4.19)$$

summing repeated indices

where A_{ij} and C_i depend on ξ and the dependent variables, and B_j are the first derivatives of the dependent variables with respect to ξ .

As things stand, the matrix A_{ij} is singular at $\xi = 0$. This is because of the singularity at the origin, which re-

sults in $\frac{d\bar{u}_0}{d\xi} \rightarrow \infty$ as $\xi \rightarrow 0$.

This difficulty can be overcome by replacing B_1 by $\bar{u}_0^{N_s} \frac{d\bar{u}_0}{d\xi}$ or equivalently making a change of dependent variable from \bar{u}_0 to $\frac{1}{N_s+1} \bar{u}_0^{N_s+1}$ in the system (2.4.19). $N_s = 1$ when $a_0(0) \neq 0$, i.e. a regular profile; and $N_s = \Gamma+2$ when $a_\Gamma(0) = 0$, i.e. a power-law profile. This procedure can be seen to be equivalent to the local coordinates used by Baum²³, but has the advantage of simplicity and flexibility. The discontinuity in the boundary conditions on \bar{H} , is handled by setting $c_1(0) = \lambda_w$, where $\lambda_w = H_w/H_2$.

3. The case of $\frac{dr}{dx} = 0$ is more complicated. The trouble is that equation (2.2.11) shows

$$\zeta^u(\xi, \bar{u}) \sim \frac{1}{\eta(1-\bar{u})} a_1(\xi) : \bar{u} \uparrow 1 \quad (2.4.20)$$

but the fact that $\frac{1}{\eta(1-\bar{u})}$ is singular at the x-axis prohibits the use of an approximation like

$$\zeta^u(\xi, \bar{u}) = \frac{1}{\eta(1-\bar{u})} \sum_{\ell=1}^{P_1} a_\ell(\xi) \bar{u}^{\ell-1} \quad (2.4.21)$$

near $y = 0$, or $\bar{u} = \bar{u}_0$.

Because of this difficulty, two alternatives are proposed.

(i) Use the approximation (2.4.13a), since $\bar{u} \uparrow 1$ much faster than $\bar{y} \uparrow +\infty$, and since eqns. (2.4.7 and 8) are

the same in the two cases. However, this approach is really not completely satisfactory.

(ii) Divide the domain into three strips, in which the following approximations are made:

$$0 \leq \bar{u} \leq \bar{u}_0 : \zeta^\ell(\xi, \bar{u}) = \frac{1}{\bar{u}} \sum_{\ell=1}^{P_1} b_\ell(\xi) \bar{u}^{\ell-1} \quad (2.4.22)$$

$$\bar{u}_0 \leq \bar{u} \leq \bar{u}_r : \zeta^u(\xi, \bar{u}) = \sum_{\ell=1}^{P_2} a_\ell(\xi) \bar{u}^{\ell-1} \quad (2.4.23)$$

$$\bar{u}_r \leq \bar{u} \leq 1 : \zeta^{u'}(\xi', \bar{u}) = \frac{1}{\eta(1-\bar{u})} \sum_{\ell=1}^{P'_2} a'_\ell(\xi) \bar{u}^{\ell-1} \quad (2.4.24)$$

where \bar{u}_r is some arbitrary convenient constant number, say 0.7.

It will also be necessary to modify the transformation (2.4.3) in the third strip (2.4.24). Thus (2.4.3) is replaced by

$$\xi' = \xi, \quad \eta' = \int_0^{\bar{y}} \bar{\rho}_r \bar{v} \bar{y} d\bar{y} \quad (2.4.25)$$

The above procedure does not necessarily involve any additional dependent variables, because providing $P_2 \geq P_2'$ and P_ℓ , the $b_\ell(\xi)$ and at least some of the $a_\ell'(\xi)$ can be found in terms of the $a_\ell(\xi)$ by requiring continuity of

$\frac{\partial^{(n)} \bar{u}}{\partial \bar{y}^{(n)}}$ for $n = 0, 1, \dots, N$, $N \leq P_2'$ or P_1 , at two inter-

faces. However, there is one difficulty, namely, it is now necessary to know the value of \bar{y}_0 , i.e. the displace-

ment of the dividing streamline from the x-axis, to relate the a_ℓ' to the a_ℓ .

In section 2.5 it is shown that \bar{y}_0 may be determined by the step-by-step numerical integration of a first-order ordinary differential equation. Thus, this second procedure is feasible. However, no numerical results have yet been obtained by following it.

2.5 The Location of the Dividing Streamline

1. It may be recalled that Lock¹⁷ used the requirement that the normal stress be continuous to fix the position of the dividing streamline for the case of incompressible inhomogeneous mixing. In the homogeneous case he found that the continuity condition was automatically satisfied, and concluded that the position of the interface was indeterminate. However, this automatic satisfaction ceases to occur when the higher order correction terms to the boundary layer solution are considered. This fact allows Lock's principle to be extended to compressible homogeneous mixing.

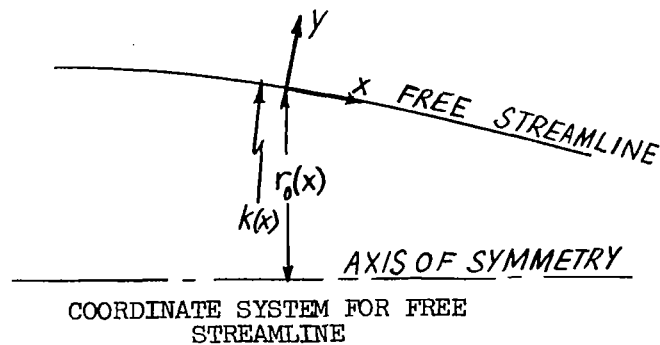
The extended principle may be stated as follows:

The dividing streamline must be so oriented that the displacement effects of the shear layer on the main and secondary streams lead to a higher order correction to the predicted flow field maintaining a continuous normal stress at the interface.

In order to apply and understand this principle, it is necessary to go through the motions of an asymptotic analysis of the Navier-Stokes equations. This will be done for the case of interest, namely that of a shear layer developing between a quiescent fluid and a stream parallel to a free streamline. The following exposition is an extension of ideas first presented by Ting⁴¹.

Consider the complete governing equations written in terms of the coordinates shown in Fig. 2.2.

Fig. 2.2



for which, the metric s is defined

$$ds^2 = (1 + ky)^2 dx^2 + dy^2 + (r_0 + y \cos \theta)^2 d\phi^2 \quad (2.5.1)$$

where ϕ is the azimuthal angle for axisymmetric flow and the third cartesian coordinate for plane flow, and where

$$\theta = \sin^{-1} (r_0'); \quad \cos \theta = -k r_0'' \quad (2.5.2)$$

The equations of motion in terms of these coordinates can be written as follows:

$$\frac{\partial}{\partial x} \{ (r_0 + y \cos \theta)^v \rho u \} + \frac{\partial}{\partial y} \{ (1 + ky) (r_0 + y \cos \theta)^v \rho w \} = 0 \quad (2.5.3)$$

$$\frac{\rho u}{(1+ky)} \cdot \frac{\partial u}{\partial x} + \rho w \frac{\partial u}{\partial y} + \frac{\rho u w}{(1+ky)} k = - \frac{1}{(1+ky)} \cdot \frac{\partial p}{\partial x} + \epsilon^2 (\nabla \cdot \bar{T})_x \quad (2.5.4)$$

$$\frac{\rho u}{(1+ky)} \cdot \frac{\partial w}{\partial x} + \rho w \frac{\partial w}{\partial y} - \frac{\rho u^2}{(1+ky)} k = - \frac{\partial p}{\partial y} + \epsilon^2 (\nabla \cdot \bar{T})_y \quad (2.5.5)$$

where

$$\epsilon^2 = \frac{\mu_1}{\rho_1 L u_1} \quad (2.5.6)$$

$$\begin{aligned}
 w^{(0)}(x, y) &= 0 \\
 &\text{if } \frac{dr_0}{dx} = 0 \\
 p^{(0)}(x, y) &= \text{const} = p_1 \qquad (2.5.9) \\
 \text{-----}
 \end{aligned}$$

If $\frac{dr_0}{dx} \neq 0$, the solutions are more complicated, but it is still true that

$$\begin{aligned}
 u^{(0)}(x, 0^+) &= 1 \\
 u^{(0)}(x, 0^-) &= 0 \qquad (2.5.10)
 \end{aligned}$$

$$w^{(0)}(x, 0^+) = 0 \qquad (2.5.11)$$

$$p^{(0)}(x, 0^+) = \text{const.} \qquad (2.5.12)$$

It can be seen that this procedure has led to the prediction of an infinite velocity gradient at $y = 0$. However, the complete equations of motion do not permit the existence of a discontinuity, therefore it is inferred that at $y = 0$ the gradient is finite but very steep. But if this is the case, $\frac{\partial u}{\partial y}$ will no longer be $O(1)$ and the procedure leading to the reduced equations will no longer be valid.

To correct this situation a stretched coordinate is introduced, having the definition

$$\tilde{y} = \frac{y}{\delta(\epsilon)} \qquad (2.5.13)$$

δ must be of such an order that $\frac{\partial u}{\partial \tilde{y}} = O(1)$. An additional set of asymptotic expansions, valid near $y = 0$, are also introduced, viz.

$$\begin{aligned}
u &= \sum_{i=0}^{\infty} r_i(\epsilon) \tilde{u}^{(i)}(x, \tilde{y}) \\
w &= \sum_{i=0}^{\infty} s_i(\epsilon) \tilde{w}^{(i)}(x, \tilde{y}) && \text{for the limit} \\
&&& \epsilon \rightarrow 0, x, \tilde{y} \text{ fixed} \\
p &= \sum_{i=0}^{\infty} t_i(\epsilon) \tilde{p}^{(i)}(x, \tilde{y}) && (2.5.14)
\end{aligned}$$

- - - - - where $r_i = o(r_{i-1})$ etc.

δ is determined to be $O(\epsilon)$ by requiring the viscous dissipation term in the energy equation to remain finite in the limit $\epsilon \rightarrow 0$; x, \tilde{y} fixed. r_0 and t_0 are evidently $O(1)$, and it follows from the continuity equation (2.5.3) that $s_0 = O(\epsilon)$.

If the asymptotic expansions (2.5.14) are substituted into the equations of motion (2.5.3-5) and the appropriate limit process applied, the result will be the regular boundary layer equations (eqns. 2.1.1.-3) rewritten in non-dimensional form in x, \tilde{y} coordinates), and the condition

$$\frac{\partial \tilde{p}^{(0)}}{\partial \tilde{y}} = 0 \tag{2.5.15}$$

This is assuming $k(x), r_0'(x)$ are $O(1)$. Thus the continuity of normal stress is ensured for the zeroth order approximation.

The boundary conditions are supplied by requiring

$$\begin{aligned}
\tilde{u}^{(0)}(x, \infty) &= u^{(0)}(x, 0^+) = 1 \\
\tilde{u}^{(0)}(x, -\infty) &= u^{(0)}(x, 0^-) = 0 \\
\tilde{w}^{(0)}(x, \tilde{y}_0) &= 0 && (2.5.16)
\end{aligned}$$

where \tilde{y}_0 is the position of the dividing streamline.

In order to continue to the next highest order correction terms, it is assumed that

$$f_1 = \epsilon f_0, \text{ etc.} \quad (2.5.17)$$

If it transpires that this choice is incorrect an incompatibility will arise.

The asymptotic expansions (2.5.7) are again substituted into the governing equations (2.5.3-5) and the limit $\epsilon \rightarrow 0, x, y$ fixed, is applied for a second time. It is immediately apparent that the sum of the zeroth order solution and first order correction still satisfies the flow equations for inviscid irrotational flow, because the viscous terms are $O(\epsilon^2)$.

In addition, the equations

$$\frac{\partial p^{(1)}}{\partial x} = \frac{\partial p^{(1)}}{\partial y} = 0 \quad (2.5.18)$$

are seen to hold for the lower stream i.e. for $y < 0$. This implies

$$u^{(1)} = 0, \quad w^{(1)} = \text{const.} : y < 0 \quad (2.5.19)$$

Turning to the case of the first order correction to the boundary layer solution; the asymptotic expansions (2.5.14) are again substituted into the equations of motion (2.5.3-3) and the limit $\epsilon \rightarrow 0, x, \tilde{y}$ fixed, is applied once more. One of the results is that the transverse momentum equation becomes

$$\frac{\partial \tilde{p}^{(1)}}{\partial \tilde{y}} = \tilde{\rho}^{(0)} \tilde{u}^{(0)2} k(x) \quad (2.5.20)$$

or applying the principle of stress continuity

$$\tilde{p}^{(1)}(x, \tilde{y}) = p^{(1)}(x, 0^-) + k \int_{-\infty}^{\tilde{y}} \tilde{\rho}^{(0)} \tilde{u}^{(0)2} d\tilde{y}, \quad (2.5.21)$$

This means that the value of \tilde{y}_0 must be such that the first order pressure correction terms allow the condition (2.5.21) to be satisfied as $y \uparrow \infty$.

The pressure correction terms, namely $p^{(1)}(x, 0^+)$ and $p^{(1)}(x, 0^-)$ are found by applying Bernoulli's theorem to the solutions of the irrotational inviscid flow equations. However, before this can be done it is necessary to formulate the boundary conditions for these equations, and for this purpose it is convenient to consider the cases $\frac{dr_0}{dx} = 0$ and $\frac{dr_0}{dx} \neq 0$ separately.

2. $\frac{dr_0}{dx} = 0$

In this case the condition (2.5.21) becomes

$$p^{(1)}(x, 0^+) = p^{(1)}(x, 0^-) \quad (2.5.22)$$

and the boundary conditions for the sum of the zeroth order solution and the first order correction are simply given by

$$\begin{aligned} w^{(1)}(x, 0^+) &= \tilde{w}^{(0)}(x, \infty) \\ w^{(1)}(x, 0^-) &= \tilde{w}^{(0)}(x, -\infty) \end{aligned} \quad (2.5.23)$$

Now given the results of eqn. (2.5.19) it is apparent from Bernoulli's equation that

$$p^{(1)}(x, 0^-) = 0(\epsilon^2)$$

or more correctly

$$p^{(1)}(x, 0^-) = 0 \quad (2.5.24)$$

At this juncture the analysis is further divided into subcases.

a) Supersonic Main Stream: ($M_1 > 1$) Plane Flow

Using the linearized theory⁴³, it can be shown that

$$c_p^{(1)} = \frac{-2}{(M_1^2 - 1)^{1/2}} \cdot \tilde{w}^{(0)}(x, \infty) + O(\epsilon^2) \quad (2.5.25)$$

Therefore $\tilde{y}_0(x)$ must be chosen so that

$$\tilde{w}^{(0)}(x, \infty) = 0 \quad (2.5.26)$$

This condition can be rewritten in the following more convenient form

$$\frac{d}{d\bar{x}} \int_{\bar{y}_0}^{\infty} (1 - \bar{\rho}\bar{u}) d\bar{y} + (1 - \bar{\rho}_0\bar{u}_0) \frac{d\bar{y}_0}{d\bar{x}} = 0 \quad (2.5.27)$$

Where use has been made of the continuity equation (2.1.1).

Note that eqn. (2.5.27) is written in terms of the notation of Section 2.4., and is a first order ordinary differential equation for \bar{y}_0 , which can be written as

$$\frac{d\bar{y}_0}{d\bar{x}} + \frac{1}{(1 - \bar{\rho}_0\bar{u}_0)} \frac{d\delta_1}{d\bar{x}} = 0 \quad (2.5.28)$$

where

$$\delta_1 = \int_{\bar{u}_0}^1 (\bar{T} - \bar{u}) \zeta(\xi, \bar{u}) d\bar{u} \quad (2.5.29)$$

is independent of the value of \bar{y}_0 .

b) Supersonic Main Stream: Axisymmetric flow $r_0 = \text{const.}$

The coefficient of pressure on a slender body is given by

the formula⁴⁴, (with modification to the case in point) written below

$$\begin{aligned}
 C_p(x, R) &= -2 \left. \frac{\partial \Phi}{\partial x} \right|_{r=R} - \left. \left(\frac{\partial \Phi}{\partial r} \right)^2 \right|_{r=R} \\
 &= \frac{1}{\pi} \int_0^{x-\alpha R} \frac{s''(y)}{[(x-y)^2 - \alpha^2 R^2]^{1/2}} dy - [R'(x)]^2 + O(t^4 \log \frac{1}{t})
 \end{aligned}
 \tag{2.5.30}$$

where t is the thickness

$$\alpha = (M_1^2 - 1)^{1/2}$$

$$S = RR'$$

$$\text{and } R = r_0 + \epsilon \int_0^x w^{(1)}(x, 0^+) dx = r_0 + \epsilon r^* \tag{2.5.31}$$

It can be shown in a straight forward way that eqn. (2.5.30) leads to equation

$$C_p^{(1)}(x, 0^+) = \frac{r_0}{\pi} \int_0^{x-\alpha r_0} \frac{dw^{(1)}(y, 0^+)}{dy} \frac{dy}{[(x-y)^2 - \alpha^2 r_0^2(x)]^{1/2}} = 0
 \tag{2.5.32}$$

Now the question becomes, What form of $\frac{dw^{(1)}}{dy}(y, 0^+)$ will satisfy this integral equation, if $C_p^{(1)}(x, 0^+)$ is zero?

Assuming that (2.5.32) has a unique solution, then the solution must be

$$\frac{dw^{(1)}}{dy}(y, 0^+) = 0 \tag{2.5.33}$$

or from eqn. (2.5.27)

$$(1 - \bar{\rho}_0 \bar{u}_0) \cdot \frac{d^2 \bar{y}_0}{d\bar{x}^2} - \frac{d}{d\bar{x}} (\bar{\rho}_0 \bar{u}_0) \frac{d\bar{y}_0}{d\bar{x}} + \frac{d^2 \delta_1}{d\bar{x}^2} = 0 \tag{2.5.34}$$

Integration leads once more to eqn. (2.5.28)

c) Subsonic Main Stream, ($M_1 < 1$): Plane Case

Use of the small perturbation theory of Munk⁴⁵ and Glauert⁴⁶, adapted to the case in hand, leads to the following result.

$$(1 - M_1^2)^{1/2} C_p^{(1)}(\bar{x}, 0^+) = - \frac{2}{\pi} \int_0^{\infty} w^{(1)}(y, 0^+) \frac{dy}{x - y} : 0 \leq x < \infty \quad (2.5.35)$$

This equation does not have a unique solution, since it is satisfied by any distribution of the form

$$w^{(1)}(y, 0^+) \sim \frac{1}{y^{n/2}} \quad \text{where } n = 1, 3, 5, \dots \dots (a)$$

$$\text{or } = 0 \quad (b)$$

However, all solutions of form (a) can be eliminated since they are singular at the origin. Hence eqn. (2.5.28) applies to this case also.

d) Subsonic Main Stream, ($M_1 < 1$): Axisymmetric Case $\frac{dr_0}{dx} = 0$

In this case small perturbation theory^{45,46} yields the following formula for coefficient of pressure.

$$(1 - M_1^2)^{1/2} C_p^{(1)}(x, 0^+) = \frac{r_0}{\pi} \int_0^{\infty} \frac{dw^{(1)}(y, 0^+)}{dy} \frac{dy}{[(x-y)^2 - r_0^2]^{1/2}} \quad (2.5.36)$$

Again, assuming that the only admissible distribution which satisfies this equation is one that is identically zero, one is

led to the conclusion that eqn. (2.5.28) applies to this case as well.

$$3. \quad \underline{\frac{dr_0}{dx} \neq 0}$$

This case is quite complicated in comparison.

In the first place it will be noted from eqn. (2.2.30) that the $\lim_{\tilde{y} \rightarrow \infty} \tilde{w}^{(0)}(x, \tilde{y})$ does not exist. Because of this fact the simple matching procedure used in eqn. (2.5.23) is no longer applicable. In order to obtain the upper boundary condition in this instance, the technique of intermediate expansions is employed. This technique was introduced by Kaplun⁴⁷ in a study of the flow around a circular cylinder at low Reynolds number. Its intuitive basis is the assumption that there exists an overlap region, between the shear layer and the main stream, where both sets of asymptotic expansions are valid. Certain theorems have been proven, thereby setting the technique on a fairly firm foundation.

To apply the technique an intermediate limit process is introduced, i.e.

$$\epsilon \downarrow 0, \quad x, \quad y^* = \frac{y}{\eta} \text{ fixed.} \quad (2.5.37)$$

where $\epsilon < \eta < 1$

or more correctly $\epsilon = o(\eta) = o(1)$

If the asymptotic expansion (2.2.30) is written in terms of the coordinates in (2.5.37) it becomes

$$\begin{aligned} \epsilon \tilde{w}^{(0)} = & -\frac{1}{r_0} \frac{dr_0}{dx} \cdot y^* \eta + \frac{1}{r_0} f_1'(x) \epsilon \\ & - \frac{1}{r_0} \cdot \frac{f_3'}{2(2f_3)^{\frac{1}{2}}} y^* \eta \exp\left(-\frac{f_3}{2} y^* \frac{2\eta^2}{\epsilon^2}\right) + o(\eta e^{\eta^2/\epsilon^2}) : \epsilon \downarrow 0 \end{aligned} \quad (2.5.38)$$

since $\rho_1 = u_1 = 1$

While the velocity in the main stream can be expanded in a Taylor's series

$$w = w(x,0) + \frac{\partial w}{\partial y}(x,0)y + \dots \quad (2.5.39)$$

or in terms of the asymptotic expansion (2.5.7)

$$w = \frac{\partial}{\partial y} w^{(0)}(x,0)y + \varepsilon [w^{(1)}(x,0) + \frac{\partial w^{(1)}}{\partial y} y] + \dots \quad (2.5.40)$$

When this is expressed in terms of the intermediate variables the result is

$$w = \eta y^* \frac{\partial w^{(0)}}{\partial y}(x,0) + \varepsilon w^{(1)}(x,0) + \varepsilon \eta \frac{\partial w^{(1)}}{\partial y} y^* + O(\varepsilon \eta) : \varepsilon \rightarrow 0 \quad (2.5.41)$$

Now the postulation of the existence of an overlap domain means that eqns (2.5.41) and $w = \varepsilon \tilde{w}^{(0)} + \varepsilon^2 \tilde{w}^{(1)} + \dots$ should match when written in terms of the intermediate variable.

Thus a comparison of eqns (2.5.41) and (2.5.38) shows that

$$y^* \frac{\partial}{\partial y} w^{(0)}(x,0) = -y^* \frac{1}{r_0} \frac{dr_0}{dx} \quad (2.5.42)$$

and

$$w^{(1)}(x,0) = \frac{1}{r_0} f_1'(x) \quad (2.5.43)$$

The first statement contains no new information since it follows directly from the continuity equation. The second one yields the required boundary condition which can be rewritten in a more usable form, viz.

$$w^{(1)}(x, 0) = \lim_{\tilde{y} \rightarrow \infty} \left(\tilde{w}^{(0)} - \tilde{y} \frac{\partial \tilde{w}^{(0)}}{\partial \tilde{y}} \right) \quad (2.5.44)$$

By using the continuity equation and after some manipulation, this equation becomes

$$w^{(1)}(x, 0^+) = \frac{1}{\bar{r}_0} \frac{d}{d\bar{x}} \int_{\bar{y}_0}^{\infty} \bar{r}_0 (1 - \bar{\rho} \bar{u}) d\bar{y} + (1 - \bar{\rho}_0 \bar{u}_0) \frac{d\bar{y}_0}{d\bar{x}} \quad (2.5.45)$$

Note that eqn. (2.5.45) is written in terms of the notation of section 2.4.

A similar difficulty is encountered when an attempt is made to apply (2.5.21), because the integral is unbounded as $\tilde{y} \rightarrow \infty$. Again, intermediate expansions can be used to overcome this problem.

Eqn. (2.2.26) substituted into eqn. (2.5.17) leads to the following asymptotic expansion for $\tilde{p}^{(1)}(x, \tilde{y})$.

$$\tilde{p}^{(1)}(x, \tilde{y}) = k\rho_1 u_1^2 \tilde{y} - 2 \left(\frac{\pi}{2}\right)^{1/2} k\rho_1 u_1 + \tilde{p}^{(1)}(x, -\infty) + o(1) : \tilde{y} \rightarrow \infty \quad (2.5.46)$$

$$\text{where } \rho_1 = \rho^{(0)}(x, 0^+) = 1$$

$$u_1 = u^{(0)}(x, 0^+) = 1 \quad (2.5.47)$$

$$\text{and as before } \tilde{p}^{(1)}(x, -\infty) = p^{(1)}(x, 0^-) = 0$$

In addition, application of a Taylor's series to the free stream pressure produces the following result.

$$p(x, y) = p^{(0)}(x, 0) + \frac{\partial p}{\partial y}^{(0)}(x, 0)y + \dots + \epsilon p^{(1)}(x, 0) + \dots \quad (2.5.48)$$

If both of these, i.e. (2.5.46 and 48) are written in terms of the intermediate variable (2.5.37) the following two asymptotic expansions will be obtained.

$$\begin{aligned}
 p &= \tilde{p}^{(0)}(x, y^*) + k\rho_1 u_1^2 y^{*\eta} + 2k\rho_1 u_1^2 \left(\frac{\pi}{2}\right)^{\frac{1}{2}} \varepsilon + o(\varepsilon) \\
 p &= p^{(0)}(x, y^*) + \frac{\partial p^{(0)}}{\partial y}(x, 0) y^{*\eta} + p^{(1)}(x, 0) \varepsilon + o(\varepsilon)
 \end{aligned}
 \tag{2.5.49}$$

A matching of the two expansions provides the conditions given below

$$\begin{aligned}
 \tilde{p}^{(0)}(x, \tilde{y}) &= p^{(0)}(x, y) = p_1 \\
 k\rho_1 u_1^2 &= \frac{\partial p^{(0)}}{\partial y}(x, 0^+) \\
 2k\rho_1 u_1^2 \left(\frac{\pi}{2}\right)^{\frac{1}{2}} &= p^{(1)}(x, 0^+)
 \end{aligned}
 \tag{2.5.50}$$

The first of these has already been used, the second merely states that the centrifugal force per unit volume must be balanced by the transverse pressure gradient, but the third provides the requisite condition on $p^{(1)}(x, 0)$.

At this juncture it is convenient to consider the supersonic and subsonic cases separately.

e) Supersonic Main Stream; ($M_1 > 1$): Plane case $\frac{dr_0}{dx} \neq 0$

This corresponds to the situation encountered when applying the Chapman-Korst model to separated flows. In plane supersonic flows, the free streamline is always straight so

$\frac{dr_0}{dx} = \text{const.}$, and therefore this case can be treated the same

way as a), providing the complicated interactions at the origin are overlooked.

f) Supersonic Main Stream; ($M > 1$): Axisymmetric case

$$\frac{dr_0}{dx} \neq 0$$

If small perturbation theory⁴⁴ is applied to this case, the coefficient of pressure will be given by eqn. (2.5.32).

Whence it can be shown that

$$\begin{aligned} C_p^{(1)}(x, 0^+) &= \frac{1}{\pi} \int_0^{x-\alpha r_0} \frac{[3r_0''(y)r^{*'}(y) + 3r_0'(y)r^{*''}(y) + r_0(y)r^{*'''}(y)]}{[(x-y)^2 - \alpha^2 r_0^2(x)]^{\frac{1}{2}}} dy \\ &+ \frac{1}{\pi} \int_0^{x-r_0} \frac{r_0'''(y)r^*(y) dy}{[(x-y)^2 - r_0^2(x)]^{\frac{1}{2}}} \\ &- 2 r_0'(x)r^{*'}(x) \end{aligned} \quad (2.5.51)$$

where

$$r^*(y) = \int_0^x w^{(1)}(y, 0^+) dy = \int_0^x \frac{\delta_1'(y)}{r_0'(y)} dy + \int_0^x [1 - \rho_0 u_0] y_0' dy \quad (2.5.52)$$

using eqn. (2.5.45), and where

$$\delta_1(x) = \int_{\bar{u}_0}^1 (\bar{T} - \bar{u}) \zeta(\xi, \bar{u}) d\bar{u}$$

For supersonic free streamlines r_0''' , $r_0'' \ll r_0'$, therefore

unless $r_0'(y)$ or $r_0^*(y)$ become large compared to $r_0^{*''}$ and $r_0^{*''''}$, the terms involving $r_0^{*''}$ and $r_0^{*''}$ in the integral of eqn. (2.5.51) can be neglected. Making this approximation and using eqn. (2.5.50), eqn. (2.5.51) becomes

$$\frac{2(2\pi)^{\frac{1}{2}}}{\gamma M_1^2} k = \frac{1}{\pi} \int_0^{x-\alpha r_0} \frac{[3r_0'(y)r_0^{*''}(y) + r_0(y)r_0^{*''''}(y)]}{[(x-y)^2 - \alpha^2 r_0^2(x)]^{\frac{1}{2}}} dy - 2r_0'(x)r_0^{*'}(x) \quad (2.5.53)$$

If eqn. (2.5.52) is substituted into eqn. (2.5.53) the result is the following integral equation for $\frac{dy_0}{dx}$.

$$2(1-\rho_0 u_0)r_0' \frac{dy_0}{dx} = F_1(x, M_1) + \frac{1}{\pi} \int_0^{x-\alpha r_0} \frac{[F_2(y, M_1)Y_0'(y) + F_3(y, M_1)Y_0''(y)]}{[(x-y)^2 - \alpha^2 r_0^2(x)]^{\frac{1}{2}}} dy + \frac{1}{\pi} \int_0^{x-r_0} \frac{F_4(y, M_1)Y_0^{*''}(y) dy}{[(x-y)^2 - \alpha^2 r_0^2(x)]^{\frac{1}{2}}} \quad (2.5.54)$$

where

$$F_1(x, M_1) = \frac{1}{\pi} \int_0^{x-\alpha r_0} \left[\delta_1^{*''''}(y) + \delta_1''(y) \frac{r_0'(y)}{r_0(y)} - \delta_1'(y) \frac{r_0'(y)^2}{r_0(y)^2} \right] \cdot \frac{dy}{[(x-y)^2 - \alpha^2 r_0^2(x)]^{\frac{1}{2}}}$$

$$- \frac{2r_0'}{r_0} \delta_1' - \frac{2(2\pi)^{\frac{1}{2}}}{\gamma M_1^2} k \quad (a)$$

$$F_2(x, M_1) = -3r_0'(\rho_0 u_0)' - r_0(\rho_0 u_0)'' \quad (b)$$

$$F_3(x, M_1) = 3r_0' (1 - \rho_0 u_0) - 2r_0 (\rho_0 u_0)' \quad (c)$$

$$F_4(x, M_1) = -r_0 (1 - \rho_0 u_0) \quad (d)$$

(2.5.55)

Since this integral equation is very complicated, a further approximation is almost a necessity. This can be achieved by observing that if k is set equal to zero, eqn. (2.5.30) would lead to the following equation.

$$\frac{1}{\pi} \int_0^{x-\alpha R} \frac{S''(y)}{[(x-y)^2 - \alpha^2 R^2]^{\frac{1}{2}}} dy - [R'(x)]^2 = 0 \quad (2.5.56)$$

where $R = r_0 + \epsilon r^*$.

But only two solutions for R would generate a zero coefficient of pressure, namely

$$R = r_0 \text{ implying } r^* = 0 \quad (2.5.57)$$

$$\text{or } R = \text{const.} = r_0(0) \text{ implying } r^* = \frac{r_0(0) - r_0}{\epsilon}$$

The second possibility violates the order assumption on r^* , i.e. $r^* = O(1)$, since at some point sufficiently far from the origin $\frac{r_0(0) - r_0(x)}{\epsilon} = O(\epsilon^{-1})$. Therefore, it is rejected.

Hence, if $r^* = 0$ is taken as the solution it will lead once again to the equation

$$w^{(1)}(x, 0+) = 0 \quad (2.5.58)$$

or using eqn. (2.5.45) with the notation of section 2.4 the following first order differential equation for \bar{Y}_0 is obtained

$$\frac{d\bar{y}_0}{d\xi} + \frac{1}{r_0(1-\bar{\rho}_0\bar{u}_0)} \cdot \frac{d\delta_1}{d\xi} = 0 \quad (2.5.59)$$

Unfortunately, the assumptions of slender body theory are often poorly met by free streamlines, in which case, the displacement flow would have to be treated as a perturbation on the undisturbed flow field containing the free streamline.

g) Subsonic Main Stream; ($M_1 < 1$): 2-D case $\frac{dr_0}{dx} \neq 0$

This could correspond to the application of a Chapman-Korst type model to subsonic near wake flow behind a blunt trailing edge.

Small perturbation theory will give

$$\frac{2(1-M_1^2)^{\frac{1}{2}}}{\gamma M_1^2} (2\pi)^{\frac{1}{2}} k = - \frac{2}{\pi} \int_0^{\ell} w^{(1)}(y, 0^+) \frac{1}{x-y} dy \quad (2.5.60)$$

where ℓ is the value of x at the 'end' of the streamline.

If the curvature, $k(x)$, is ignored as before, eqn. (2.5.28) will be obtained. Otherwise the integral equation (2.5.60) will have to be solved for $w^{(1)}(y, 0^+)$ which will lead to a first order ordinary differential equation for $\bar{y}_0(x)$ of the form

$$\frac{d\bar{y}_0}{d\xi} + \frac{1}{(1-\bar{\rho}_0\bar{u}_0)} \frac{d\delta_1}{d\xi} = f(\xi) \quad (2.5.61)$$

h) Subsonic Main Stream; ($M_1 < 1$): Axisymmetric case $\frac{dr_0}{dx} \neq 0$

This could also correspond to the application of the Chapman-Korst model to subsonic base flow.

The treatment of this case is fairly similar to that of (f), except that (2.5.53) becomes

$$\frac{(1-M_1^2)^{\frac{1}{2}} (2\pi)^{\frac{1}{2}}}{\gamma M_1^2} = \frac{1}{\pi} \int_0^{\ell} \frac{[3r_0'(y)r_0''(y) + r_0(y)r_0'''(y)] dy}{[(x-y)^2 - r_0^2(x)]^{\frac{1}{2}}} \quad (2.5.62)$$

which again leads to an involved integral equation for $\frac{d\bar{y}_0}{dx}$.

If the same arguments are followed for this case, eqn. (2.5.59) will apply as an approximation.

4. The methods outlined above cannot be automatically applied to turbulent free shear layers with any degree of confidence. The reason is that the Reynolds stresses have an unknown order of magnitude, and also contribute to a transverse pressure gradient which is non-zero to zeroth order. See, for example, Rotta⁴⁸.

However, Mills²¹ has shown that experimental data for two stream homogeneous incompressible asymptotic mixing layers agree quite well with solutions using Ting's⁴¹ criterion at least for $\frac{u_2}{u_1}$ ranging from 0 to 0.4. For ratios above 0.4 the discrepancy between the theoretical predictions of \bar{y}_0 and the experimental curve becomes increasingly large. A comparison between available experimental data for a compressible developing turbulent free shear layer and theoretical predictions will also be made when suitable experimental data become available.

Finally, it might be pointed out that similar uniqueness problems would probably arise whenever interior layers are

introduced in an asymptotic analysis of systems of partial differential equations which are third order or higher. Presumably it would be possible to generalize the technique presented above to cover these problems.

2.6 The Inadmissability of Certain Orders of the Approximating Polynomials

P_2 cannot be an even number in equation (2.4.13b). This restriction is necessary because in the course of determining the $b_\ell(\xi)$ from equations (2.4.15) an incompatibility arises between $\frac{\partial^{P_2-1} \zeta^u}{\partial u^{P_2-1}}$ and $\frac{\partial^{P_2-1} \zeta^\ell}{\partial u^{P_2-1}}$ which results in the lower part of the profile being forced to ultimately turn up as $\bar{u} \rightarrow 0$ such that $\bar{y} \rightarrow +\infty$. This situation can best be understood in terms of an example.

Consider the case of $P_2 = 2$.

Equations (2.4.15) yields

$$\frac{1}{(1-\bar{u}_0)} [a_1 + a_2 \bar{u}_0] = \frac{1}{\bar{u}_0} [b_1 + b_2 \bar{u}_0] \quad (2.6.1)$$

$$\frac{1}{(1-\bar{u}_0)^2} [a_0 + a_1] = -\frac{b_0}{\bar{u}_0^2} \quad (2.6.2)$$

Note that the left hand side of equation (2.6.2) must be positive, because $\zeta^u(\xi, \bar{u})$ must be positive as $\bar{u} \rightarrow 1$. On the other hand, b_0 must be positive, because $\zeta^\ell(\xi, \bar{u})$ has to be positive as $\bar{u} \rightarrow 0$. Therefore, there is an incompatibility in the approximations for the slope of ζ . This incompatibility carries over to higher order derivatives of ζ when the degree

of the approximating polynomial is increased by $2n$ ($n=1,2,3,\dots$).

It is also worth mentioning at this juncture that when $P_3 = 1$ in equation (2.4.14), the first equation of the system (2.4.8) cannot be used. This is owing to the Prandtl number not appearing on the right hand side of system (2.4.8) until $k = 1$. Thus for $P_3 = 1$, the equation from (2.4.8) corresponding to $k = 1$ must be used. This restriction is lifted for $P_3 > 1$.

3. THE EDDY VISCOSITY MODEL

As noted in Section 1.1, a difficulty with the choice of eddy viscosity model is encountered in developing turbulent free shear layers. It was pointed out that the common formulation for the eddy viscosity of an asymptotic half-jet, viz.

$$\varepsilon = \frac{1}{4\sigma^2} \rho u, x \quad (3.1)$$

is not satisfactory because it ignores the nonlinear initial development. However, to allow for the initial development, x could be replaced by the function $F(x/L)$. Some investigators have attempted to determine F ; most notably, Korst et al.²⁸ by empirical means; and more recently Lamb^{49,50,51} analytically, in the form of an implicit relationship. See the review by Carpenter³⁷ for a detailed survey and critique.

It may also be recalled from Section 1.1 that there is the additional difficulty of determining the variation of the jet spreading parameter, σ , with Mach Number and total enthalpy ratio. For this reason it would appear preferable to follow Nash⁵², and replace $\frac{1}{4\sigma^2} F(x/L)$ by $K_1 \Delta^*(x)$, i.e. write

$$e(x) = K_1 u_1 \Delta^*(x) \quad (3.2)$$

where $\Delta^*(x)$ is some, as yet unknown, thickness parameter; and K_1 is a universal constant. In any case this conforms with Prandtl⁹ and Reichardt's¹⁰ original idea of a constant exchange

coefficient proportional to the characteristic size of the large energy-carrying eddies.

In order for $\Delta^*(x)$ to be satisfactory it must meet three requirements, viz.

a) $\Delta^*(x) \sim x$ as $x \uparrow \infty$.

b) It must be a real measure of the total width of the free shear layer.

c) It must be such that the correlation $\overline{u'v'} = \frac{\tau}{\rho}$ should be very nearly invariant under a streamwise Galilean transformation.

The first requirement is necessary so that the shear layer develops toward the correct, experimentally verified, asymptotic state.

The second because the characteristic size of the large energy-carrying eddies is supposed to be comparable to the actual width of the shear layer.

The third requirement comes about because it is desired to follow Morkovin's⁵³ hypothesis on the effect of compressibility on the Reynolds shear stress. He suggested that since the velocity fluctuations are an order of magnitude smaller than the average components, it followed that at moderate Mach Numbers $\overline{u'v'}$ would be unaffected by compressibility. This proposal has received support from other investigators^{54,55,56,57}.

It has been shown by Herring and Mellor⁵⁶ that for the outer part of a compressible boundary layer, the formulation

$$\Delta^*(x) = \int_0^{\infty} (1 - \bar{u}) dy \quad (3.3)$$

i.e. velocity-defect thickness, leads to Galilean invariance. This is, in fact, the eddy viscosity model proposed by Clauser¹¹. It was discovered, or at least explained, by drawing an analogy between the turbulent boundary layer and a laminar one having a thin sublayer of a different fluid with much lower viscosity near the wall. Maise and McDonald⁵⁷ have confirmed that the use of the velocity-defect thickness, rather than displacement thickness*, leads to a more satisfactory correlation with experimental data.

There appears to be no reason why this formulation of $\Delta^*(x)$ would not be suitable for free shear layers, providing it be appropriately generalized. To this end, $\Delta^*(x)$ is defined as

$$\Delta^*(x) = \int_{-\infty}^{y_0(x)} \bar{u} dy + \int_{y_0(x)}^{\infty} (1 - \bar{u}) dy \quad (3.4)$$

Moreover, in this form $\Delta^*(x)$ also satisfies the three requirements.

In the absence of any better information, Mellor and Herring's⁵⁶ value of 0.016 for the universal constant is retained.

*In the case of an incompressible boundary layer such as studied by Clauser the velocity-defect and displacement thicknesses are indistinguishable.

Thus the eddy viscosity is given by the expression below.

$$\varepsilon(x) = 0.016 \rho u_1 \left\{ \int_0^{y_0} \bar{u} \, dy + \int_{y_0}^{\infty} (1 - \bar{u}) \, dy \right\} \quad (3.5)$$

4. WORKED EXAMPLE AND EXPLICIT FORMULAE FOR THE CASE $P_1 = 4$, $P_3 = 2$.

In this section the formulae and actual ordinary differential equations for the case where the velocity profile is characterized by four free parameters ($P_1 = 4$), and the total enthalpy profile by two ($P_3 = 2$), are presented.

4.1 Relationships Between Quantities Above and Below Dividing Streamline

1. Relationship between velocity profiles.

Eqns. (2.4.13a and b) become

$$\zeta^u(\xi, \bar{u}) = \frac{1}{(1-\bar{u})} [a_0(\xi) + a_1(\xi)\bar{u} + a_2(\xi)\bar{u}^2] \quad : \bar{u} > \bar{u}_0 \quad (a)$$

$$\zeta^l(\xi, \bar{u}) = \frac{1}{\bar{u}} [b_0(\xi) + b_1(\xi)\bar{u} + b_2(\xi)\bar{u}^2] \quad : \bar{u} < \bar{u}_0 \quad (b)$$

(4.1.1)

Continuity of ζ , $\frac{\partial \zeta}{\partial \xi}$ and $\frac{\partial^2 \zeta}{\partial \xi^2}$ is required at $\bar{u} = \bar{u}_0$. This leads to the following expressions for b_0 , b_1 , b_2 in terms of a_0 , a_1 , a_2 .

$$b_0 = \frac{\bar{u}_0^3}{(1-\bar{u}_0)^3} [a_0 + a_1 + a_2] \quad (a)$$

$$b_2 = \frac{1}{(1-\bar{u}_0)^2} [a_0 + a_1 + 2a_2\bar{u}_0 - a_2\bar{u}_0^2] + \frac{b_0}{\bar{u}_0^2} \quad (b)$$

$$b_1 = \frac{1}{(1-\bar{u}_0)} [a_0 + a_1\bar{u}_0 + a_2\bar{u}_0^2] - \frac{b_0}{\bar{u}_0} - b_2\bar{u}_0 \quad (c)$$

(4.1.2)

Differentiation of eqns. (4.1.2a,b,c) results in the following formulae.

$$\frac{db}{d\xi} i-1 = f_{i1} \frac{d\bar{u}_0}{d\xi} + f_{i2} \frac{da_0}{d\xi} + f_{i3} \frac{da_1}{d\xi} + f_{i4} \frac{da_2}{d\xi} \quad (4.1.3)$$

$$i = 1, 2, 3$$

where

$$f_{11} = \frac{3\bar{u}_0^2}{(1-\bar{u}_0)^4} (a_0 + a_1 + a_2); \quad f_{12} = f_{13} = f_{14} = \frac{\bar{u}_0^3}{(1-\bar{u}_0)^3}$$

$$f_{31} = \frac{2}{(1-\bar{u}_0)^3} (a_0 + a_1 + 2a_2\bar{u}_0 - a_2\bar{u}_0^2) + \frac{2a_2}{(1-\bar{u}_0)} - \frac{2b_0}{\bar{u}_0^3} + \frac{f_{11}}{\bar{u}_0^2}$$

$$f_{32} = f_{33} = \frac{1}{(1-\bar{u}_0)^2} + \frac{f_{12}}{\bar{u}_0^2}; \quad f_{34} = \frac{\bar{u}_0}{(1-\bar{u}_0)^2} (2 - \bar{u}_0) + \frac{f_{14}}{\bar{u}_0^2}$$

$$f_{21} = \frac{1}{(1-\bar{u}_0)^2} (a_0 + a_1\bar{u}_0 + a_2\bar{u}_0^2) + \frac{1}{(1-\bar{u}_0)} (a_1 + 2a_2\bar{u}_0)$$

$$+ \frac{b_0}{\bar{u}_0^2} - b_2 - \frac{f_{11}}{\bar{u}_0} - f_{31} \bar{u}_0$$

$$f_{22} = \frac{1}{(1-\bar{u}_0)} - \frac{f_{12}}{\bar{u}_0} - f_{32}\bar{u}_0; \quad f_{23} = \frac{\bar{u}_0}{(1-\bar{u}_0)} - \frac{f_{13}}{\bar{u}_0} - f_{33}\bar{u}_0$$

$$f_{24} = \frac{\bar{u}_0^2}{(1-\bar{u}_0)} - \frac{f_{14}}{\bar{u}_0} - f_{34}\bar{u}_0$$

$$(4.1.4)$$

a_0, a_1, a_2 and \bar{u}_0 are the four free parameters that characterize the velocity profile.

2. Relationship between the stagnation enthalpy profiles.

Eqns. (2.4.14a and b) become

$$\bar{H}^u(\xi, \bar{u}) = [\lambda + (1 - \lambda)\bar{u}] \cdot [c_0 + c_1\bar{u} + c_2\bar{u}^2] : \quad \bar{u} > \bar{u}_0 \quad (a)$$

$$\bar{H}^l(\xi, \bar{u}) = [\lambda + (1 - \lambda)\bar{u}] \cdot [d_0 + d_1\bar{u} + d_2\bar{u}^2] : \quad \bar{u} < \bar{u}_0 \quad (b)$$

$$(4.1.5)$$

Now since $\bar{H}^u = \lambda + (1 - \lambda)\bar{u}$ at $\bar{u} = 1$ and $\bar{H}^l = \lambda + (1 - \lambda)\bar{u}$ at $\bar{u} = 0$, it can be seen that

$$c_0 + c_1 + c_2 = 1 \quad ; \quad d_0 = 1$$

Therefore, eqns. (4.1.5a and b) become

$$\bar{H}^u = [\lambda + (1 - \lambda)\bar{u}] [c_0(\xi) + c_1(\xi)\bar{u} + (1 - c_1(\xi) - c_0(\xi))\bar{u}^2] \quad (a)$$

$$\bar{H}^l = [\lambda + (1 - \lambda)\bar{u}] [1 + d_1(\xi)\bar{u} + d_2(\xi)\bar{u}^2] \quad (b)$$

$$(4.1.6)$$

The d's can be found in terms of the c's by requiring continuity of \bar{H} and $\frac{\partial \bar{H}}{\partial \bar{u}}$ at $\bar{u} = \bar{u}_0$. Whence

$$d_2 = \frac{1 - c_0}{\bar{u}_0^2} + (1 - c_1 - c_0) \quad (a)$$

$$d_1 = c_1 + 2(1 - c_1 - c_0)\bar{u}_0 - 2d_2\bar{u}_0 \quad (b)$$

$$(4.1.7)$$

Differentiation of eqns. (4.1.1a and b) results in the following formulae.

$$\frac{dd_i}{d\xi} = f_{(i+4)1} \frac{d\bar{u}_0}{d\xi} + f_{(i+4)5} \frac{dc_0}{d\xi} + f_{(i+4)6} \frac{dc_1}{d\xi} \quad (4.1.8)$$

where

$$f_{61} = - \frac{2(1 - c_0)}{\bar{u}_0^3} ; f_{65} = - 1 - \frac{1}{\bar{u}_0^2} ; f_{66} = - 1$$

$$f_{51} = 2(1 - c_1 - c_0) - 2d_2 - 2\bar{u}_0 f_{61} ; f_{55} = - 2\bar{u}_0(1 + f_{65})$$

$$f_{56} = 1 - 2\bar{u}_0(1 + f_{66})$$

$$(4.1.9)$$

c_0 and c_1 are the two free parameters that characterize the stagnation enthalpy profile.

4.2 Derivation of the System of Ordinary Differential Equations

The left-hand sides of the system of equations (2.4.7 and 8) are the same in both the laminar and turbulent cases. If the four equations corresponding to $j = 0, 1, 2, 3$ from (2.4.7) and the two corresponding to $k = 0, 1$ from (2.4.8) are considered, the integrals on the left hand side may be carried out analytically. This leads to a set of first order ordinary differential equations which may be written in matrix formulation as

$$A_{ij} B_j = C_i \quad i = 1, \dots, 6; j = 1, \dots, 6 \quad (4.2.1)$$

where

$$\begin{aligned} B_1 &= \frac{da_0}{d\xi}; B_2 = \frac{da_1}{d\xi}; B_3 = \frac{da_2}{d\xi} \\ B_4 &= \bar{u}_0^{N_s} \frac{d\bar{u}_0}{d\xi} = \frac{d}{d\xi} \left(\frac{u_0^{N_s+1}}{N_s+1} \right); B_5 = \frac{dc_0}{d\xi}; B_6 = \frac{dc_1}{d\xi} \end{aligned} \quad (4.2.2)$$

$$A_{11} = -\frac{1}{2}(1 - \bar{u}_0^2) + \frac{\bar{u}_0^2}{2} f_{12} + \frac{\bar{u}_0^3}{3} f_{22} + \frac{\bar{u}_0^4}{4} f_{32} \quad (a)$$

$$A_{12} = -\frac{1}{3}(1 - \bar{u}_0^3) + \frac{\bar{u}_0^2}{2} f_{13} + \frac{\bar{u}_0^3}{3} f_{23} + \frac{\bar{u}_0^4}{4} f_{33} \quad (b)$$

$$A_{13} = -\frac{1}{4}(1 - \bar{u}_0^4) + \frac{\bar{u}_0^2}{2} f_{14} + \frac{\bar{u}_0^3}{3} f_{24} + \frac{\bar{u}_0^4}{4} f_{34} \quad (c)$$

$$A_{14} = \begin{array}{ll} a_0 & : N_s = 1 \\ & : \xi = 0 \\ a_1 & : N_s = 2 \end{array}$$

$$A_{14} = [(a_0 + b_0)\bar{u}_0 + (a_1 + b_1)\bar{u}_0^2 + (a_2 + b_2)\bar{u}_0^3 + \frac{u_0^2}{2} f_{11} + \frac{\bar{u}_0^3}{3} f_{21} + \frac{\bar{u}_0^4}{4} f_{31}] \frac{1}{\bar{u}_0^{N_s}} \quad : \quad \xi > 0 \quad (d)$$

where $N_s = 1$: ordinary initial velocity profile.

$N_s = 2$: parabola-type velocity profile (i.e. $\bar{y} = \bar{u}^2$)

$$A_{15} = A_{16} = 0 \quad (e)$$

$$A_{21} = -\frac{1}{2}(1 - \bar{u}_0^2) - \frac{1}{3}(1 - \bar{u}_0^3) + f_{12} \frac{\bar{u}_0^3}{3} + f_{22} \frac{\bar{u}_0^4}{4} + f_{32} \frac{\bar{u}_0^5}{5} \quad (4.2.3) \quad (a)$$

$$A_{22} = -\frac{1}{3}(1 - \bar{u}_0^3) - \frac{1}{4}(1 - \bar{u}_0^4) + f_{13} \frac{\bar{u}_0^3}{3} + f_{23} \frac{\bar{u}_0^4}{4} + f_{33} \frac{\bar{u}_0^5}{5} \quad (b)$$

$$A_{23} = -\frac{1}{4}(1 - \bar{u}_0^4) - \frac{1}{5}(1 - \bar{u}_0^5) + f_{14} \frac{\bar{u}_0^3}{3} + f_{24} \frac{\bar{u}_0^4}{4} + f_{34} \frac{\bar{u}_0^5}{5} \quad (c)$$

$$A_{24} = \begin{matrix} a_0 & : & N_s = 1 \\ & & : & \xi = 0 \\ a_1 & : & N_s = 2 \end{matrix}$$

$$A_{24} = [a_1 \bar{u}_0 + (a_1 + b_0 + a_0)\bar{u}_0^2 + (a_1 + a_2 + b_1)\bar{u}_0^3 + (a_2 + b_2)\bar{u}_0^4 + \frac{\bar{u}_0^3}{3} f_{11} + \frac{\bar{u}_0^4}{4} f_{21} + \frac{\bar{u}_0^5}{5} f_{31}] \cdot \frac{1}{\bar{u}_0^{N_s}} \quad : \quad \xi > 0 \quad (d)$$

$$A_{25} = A_{26} = 0 \quad (e)$$

(4.2.4)

$$A_{31} = -\frac{1}{2}(1 - \bar{u}_0^2) - \frac{1}{3}(1 - \bar{u}_0^3) - \frac{1}{4}(1 - \bar{u}_0^4) + f_{22}\frac{\bar{u}_0^5}{5} + f_{32}\frac{\bar{u}_0^6}{6} + f_{12}\frac{\bar{u}_0^4}{4} \quad (\text{a})$$

$$A_{32} = -\frac{1}{3}(1 - \bar{u}_0^3) - \frac{1}{4}(1 - \bar{u}_0^4) - \frac{1}{5}(1 - \bar{u}_0^5) + f_{13}\frac{\bar{u}_0^4}{4} + f_{23}\frac{\bar{u}_0^5}{5} + f_{33}\frac{\bar{u}_0^6}{6} \quad (\text{b})$$

$$A_{33} = -\frac{1}{4}(1 - \bar{u}_0^4) - \frac{1}{5}(1 - \bar{u}_0^5) - \frac{1}{6}(1 - \bar{u}_0^6) + f_{14}\frac{\bar{u}_0^4}{4} + f_{24}\frac{\bar{u}_0^5}{5} + f_{34}\frac{\bar{u}_0^6}{6} \quad (\text{c})$$

$$A_{34} = \begin{array}{l} a_0 \quad : \quad N_s = 1 \\ \quad \quad : \quad \xi = 0 \\ a_1 \quad : \quad N_s = 2 \end{array}$$

$$A_{34} = [a_0\bar{u}_0 + (a_0 + a_1)\bar{u}_0^2 + (b_0 + a_0 + a_1 + a_2)\bar{u}_0^3 + (a_1 + a_2 + b_1)\bar{u}_0^4 + (a_2 + b_2)\bar{u}_0^5 + \frac{\bar{u}_0^4}{4} f_{11} + \frac{\bar{u}_0^5}{5} f_{21} + \frac{\bar{u}_0^6}{6} f_{31}] \frac{1}{\bar{u}_0^{N_s}} \quad : \quad \xi > 0 \quad (\text{d})$$

$$A_{35} = A_{36} = 0 \quad (\text{e})$$

(4.2.5)

$$A_{41} = -\frac{1}{2}(1 - \bar{u}_0^2) - \frac{1}{3}(1 - \bar{u}_0^3) - \frac{1}{4}(1 - \bar{u}_0^4) - \frac{1}{5}(1 - \bar{u}_0^5) + \frac{\bar{u}_0^5}{5} f_{12} + \frac{\bar{u}_0^6}{6} f_{22} + \frac{\bar{u}_0^7}{7} f_{32} \quad (\text{a})$$

$$A_{42} = -\frac{1}{3}(1 - \bar{u}_0^3) - \frac{1}{4}(1 - \bar{u}_0^4) - \frac{1}{5}(1 - \bar{u}_0^5) - \frac{1}{6}(1 - \bar{u}_0^6) + \frac{\bar{u}_0^5}{5} f_{13} + \frac{\bar{u}_0^6}{6} f_{23} + \frac{\bar{u}_0^7}{7} f_{33} \quad (\text{b})$$

$$A_{43} = -\frac{1}{4}(1 - \bar{u}_0^4) - \frac{1}{5}(1 - \bar{u}_0^5) - \frac{1}{6}(1 - \bar{u}_0^6) - \frac{1}{7}(1 - \bar{u}_0^7) \\ + \frac{\bar{u}_0^5}{5} f_{14} + \frac{\bar{u}_0^6}{6} f_{24} + \frac{\bar{u}_0^7}{7} f_{34} \quad (c)$$

$$A_{44} = \begin{array}{l} a_0 \quad : \quad N_s = 1 \\ a_1 \quad : \quad N_s = 2 \end{array} \quad : \quad \xi = 0$$

$$A_{44} = [a_0 \bar{u}_0 + (a_0 + a_1) \bar{u}_0^2 + (a_0 + a_1 + a_2) \bar{u}_0^3 \\ + (b_0 + a_0 + a_1 + a_2) \bar{u}_0^4 + (b_1 + a_1 + a_2) \bar{u}_0^5 \\ + (b_2 + a_2) \bar{u}_0^6 + \frac{\bar{u}_0^5}{5} f_{11} + \frac{\bar{u}_0^6}{6} f_{21} + \frac{\bar{u}_0^7}{7} f_{31}] \frac{1}{\bar{u}_0 N_s} \\ : \quad \xi = 0 \quad (d)$$

$$A_{45} = A_{46} = 0 \quad (e)$$

(4.2.6)

$$A_{51} = \frac{g_1}{2}(1 - \bar{u}_0^2) + \frac{g_2}{3}(1 - \bar{u}_0^3) + \frac{g_3}{4}(1 - \bar{u}_0^4) \\ + GG1 \cdot f_{12} + GG2 \cdot f_{22} + GG3 \cdot f_{32} \quad (a)$$

$$A_{52} = \frac{g_1}{3}(1 - \bar{u}_0^3) + \frac{g_2}{4}(1 - \bar{u}_0^4) + \frac{g_3}{5}(1 - \bar{u}_0^5) \\ + GG1 \cdot f_{13} + GG2 \cdot f_{23} + GG3 \cdot f_{33} \quad (b)$$

$$A_{53} = \frac{g_1}{4}(1 - \bar{u}_0^4) + \frac{g_2}{5}(1 - \bar{u}_0^5) + \frac{g_3}{6}(1 - \bar{u}_0^6) \\ + GG1 \cdot f_{14} + GG2 \cdot f_{24} + GG3 \cdot f_{34} \quad (c)$$

$$A_{54} = \begin{array}{l} -g_1 a_0 \quad : \quad N_s = 1 \\ -g_1 a_1 \quad : \quad N_s = 2 \end{array} \quad : \quad \xi = 0$$

$$g_4 = (1 - \lambda) + \lambda d_1; g_5 = (1 - \lambda)d_1 + \lambda d_2; g_6 = (1 - \lambda)d_2$$

$$g_{15} = \lambda; g_{16} = 0; g_{25} = 1; g_{26} = \lambda; g_{35} = (1 - \lambda)$$

$$g_{36} = g_{35}; g_{41} = \lambda f_{51}; g_{45} = \lambda f_{55}; g_{46} = \lambda f_{56}$$

$$g_{51} = (1 - \lambda)f_{51} + \lambda f_{61}; g_{55} = (1 - \lambda)f_{55} + \lambda f_{65}$$

$$g_{56} = (1 - \lambda)f_{56} + \lambda f_{66}; g_{61} = (1 - \lambda)f_{61}; g_{65} = (1 - \lambda)f_{65}$$

$$g_{66} = (1 - \lambda)f_{66} \quad (4.2.8)$$

$$GG1 = g_4 \frac{\bar{u}_0^{-2}}{2} + g_5 \frac{\bar{u}_0^{-3}}{3} + g_6 \frac{\bar{u}_0^{-4}}{4}$$

$$GG2 = g_4 \frac{\bar{u}_0^{-3}}{3} + g_5 \frac{\bar{u}_0^{-4}}{4} + g_6 \frac{\bar{u}_0^{-5}}{5}$$

$$GG3 = g_4 \frac{\bar{u}_0^{-4}}{4} + g_5 \frac{\bar{u}_0^{-5}}{5} + g_6 \frac{\bar{u}_0^{-6}}{6} \quad (4.2.9)$$

$$\begin{aligned} A_{61} &= \frac{i_0}{2}(1 - \bar{u}_0^{-2}) + \frac{i_1}{3}(1 - \bar{u}_0^{-3}) + \frac{i_2}{4}(1 - \bar{u}_0^{-4}) + \frac{i_3}{5}(1 - \bar{u}_0^{-5}) \\ &\quad + \frac{i_4}{6}(1 - \bar{u}_0^{-6}) + \frac{i_5}{7}(1 - \bar{u}_0^{-7}) + GG4 \cdot f_{12} + GG5 \cdot f_{22} + GG6 \cdot f_{32} \end{aligned} \quad (a)$$

$$\begin{aligned} A_{62} &= \frac{i_0}{3}(1 - \bar{u}_0^{-3}) + \frac{i_1}{4}(1 - \bar{u}_0^{-4}) + \frac{i_2}{5}(1 - \bar{u}_0^{-5}) + \frac{i_3}{6}(1 - \bar{u}_0^{-6}) \\ &\quad + \frac{i_4}{7}(1 - \bar{u}_0^{-7}) + \frac{i_5}{8}(1 - \bar{u}_0^{-8}) + GG4 \cdot f_{13} + GG5 \cdot f_{23} + GG6 \cdot f_{33} \end{aligned} \quad (b)$$

$$\begin{aligned}
A_{63} = & \frac{i_0}{4}(1-\bar{u}_0^4) + \frac{i_1}{5}(1-\bar{u}_0^5) + \frac{i_2}{6}(1-\bar{u}_0^6) + \frac{i_3}{7}(1-\bar{u}_0^7) + \frac{i_4}{8}(1-\bar{u}_0^8) \\
& + \frac{i_5}{9}(1-\bar{u}_0^9) + GG4 \cdot f_{14} + GG5 \cdot f_{24} + GG6 \cdot f_{34} \quad (c)
\end{aligned}$$

$$\begin{aligned}
A_{64} = & \begin{array}{l} -i_0 a_0 \quad : N_s = 1 \\ -i_0 a_1 \quad : N_s = 2 \end{array} \quad : \xi = 0
\end{aligned}$$

$$\begin{aligned}
A_{64} = & [GG4 \cdot f_{11} + GG5 \cdot f_{21} + GG6 \cdot f_{31} + JJ1 \cdot j_{01} \\
& + JJ2 \cdot j_{11} + JJ3 \cdot j_{21} + JJ4 \cdot j_{31} + JJ5 \cdot j_{41} \\
& + JJ6 \cdot j_{51} + (j_0 b_0 - i_0 a_0) \bar{u}_0 + (j_0 b_1 + j_1 b_0 - i_0 a_1 \\
& - i_1 a_0) \bar{u}_0^2 + (j_0 b_2 + j_1 b_1 + j_2 b_0 - i_0 a_2 - i_1 a_1 - i_2 a_0) \bar{u}_0^3 \\
& + (j_1 b_2 + j_2 b_1 + j_3 b_0 - i_1 a_2 - i_2 a_1 - i_3 a_0) \bar{u}_0^4 \\
& + (j_2 b_2 + j_3 b_1 + j_4 b_0 - i_2 a_2 - i_3 a_1 - i_4 a_0) \bar{u}_0^5 \\
& + (j_3 b_2 + j_4 b_1 + j_5 b_0 - i_3 a_2 - i_4 a_1 - i_5 a_0) \bar{u}_0^6 \\
& + (j_4 b_2 + j_5 b_1 - i_4 a_2 - i_5 a_1) \bar{u}_0^7 + (j_5 b_2 - i_5 a_2) \bar{u}_0^8] \frac{1}{\bar{u}_0^{N_s}} \quad (d)
\end{aligned}$$

$$\begin{aligned}
A_{65} = & \begin{array}{l} JJ1 \cdot j_{05} + JJ2 \cdot j_{15} + JJ3 \cdot j_{25} + JJ4 \cdot j_{35} \\ \frac{6}{6} \quad \quad \quad \frac{6}{6} \quad \quad \quad \frac{6}{6} \quad \quad \quad \frac{6}{6} \\ JJ5 \cdot j_{45} + JJ6 \cdot j_{55} + II1 \cdot i_{05} + II2 \cdot i_{15} \\ \frac{6}{6} \quad \quad \quad \frac{6}{6} \quad \quad \quad \frac{6}{6} \quad \quad \quad \frac{6}{6} \\ II3 \cdot i_{25} + II4 \cdot i_{35} + II5 \cdot i_{45} + II6 \cdot i_{55} \\ \frac{6}{6} \quad \quad \quad \frac{6}{6} \quad \quad \quad \frac{6}{6} \quad \quad \quad \frac{6}{6} \end{array} \quad (e)
\end{aligned}$$

(4.2.10)

where

$$\begin{aligned}
 h_1 &= \lambda c_0 + 1; \quad h_2 = \lambda c_1 + (1 - \lambda)c_0 \\
 h_3 &= \lambda(1 - c_1 - c_0) + (1 - \lambda)c_1; \quad h_4 = (1 - \lambda)(1 - c_1 - c_0)
 \end{aligned}
 \tag{4.2.11}$$

$$\begin{aligned}
 i_0 &= h_1 g_1; \quad i_1 = h_1 g_2 + h_2 g_1; \quad i_2 = h_1 g_3 + h_2 g_2 + h_3 g_1 \\
 i_3 &= h_2 g_3 + h_3 g_2 + h_4 g_1; \quad i_4 = h_3 g_3 + h_4 g_2; \quad i_5 = h_4 g_3
 \end{aligned}
 \tag{4.2.12}$$

$$\begin{aligned}
 h_{15} &= \lambda; \quad h_{16} = 0; \quad h_{25} = 1 - \lambda; \quad h_{26} = \lambda; \quad h_{35} = -\lambda \\
 h_{36} &= 1 - 2\lambda; \quad h_{45} = -(1 - \lambda); \quad h_{46} = h_{45} \\
 i_{05} &= h_{15} g_1 + g_{15} h_1; \quad i_{06} = h_{16} g_1 + g_{16} h_1 \\
 i_{15} &= \frac{h_{15} g_2}{6} + \frac{h_{25} g_1}{6} + \frac{h_1 g_{25}}{6} + \frac{h_2 g_{15}}{6} \\
 i_{25} &= \frac{h_{15} g_3}{6} + \frac{h_{25} g_2}{6} + \frac{h_{35} g_1}{6} + \frac{h_1 g_{35}}{6} + \frac{h_2 g_{25}}{6} + \frac{h_3 g_{15}}{6} \\
 i_{35} &= \frac{h_{25} g_3}{6} + \frac{h_{35} g_2}{6} + \frac{h_{45} g_1}{6} + \frac{h_2 g_{35}}{6} + \frac{h_3 g_{25}}{6} + \frac{h_4 g_{15}}{6} \\
 i_{45} &= \frac{h_{35} g_3}{6} + \frac{h_{45} g_2}{6} + \frac{h_3 g_{35}}{6} + \frac{h_4 g_{25}}{6} \\
 i_{55} &= \frac{h_{45} g_3}{6} + \frac{h_4 g_{35}}{6}
 \end{aligned}
 \tag{4.2.13}$$

$$\begin{aligned}
 h_5 &= 2\lambda; \quad h_6 = d_1 \lambda + (1 - \lambda); \quad h_7 = d_2 \lambda + d_1 (1 - \lambda) \\
 h_8 &= d_2 (1 - \lambda)
 \end{aligned}
 \tag{4.2.14}$$

$$\begin{aligned}
h_{61} &= f_{51}\lambda; h_{65} = f_{55}\lambda; h_{66} = f_{66}\lambda; h_{71} = f_{61}\lambda + f_{51}(1 - \lambda) \\
h_{75} &= f_{65}\lambda + f_{55}(1 - \lambda); h_{76} = f_{66}\lambda + f_{56}(1 - \lambda); h_{81} = f_{61}(1 - \lambda) \\
h_{85} &= f_{65}(1 - \lambda); h_{86} = f_{66}(1 - \lambda)
\end{aligned} \tag{4.2.15}$$

$$\begin{aligned}
j_0 &= h_5g_4; j_1 = h_5g_5 + h_6g_4; j_2 = h_5g_6 + h_6g_5 + h_7g_4 \\
j_3 &= h_6g_6 + h_7g_5 + h_8g_4; j_4 = h_7g_6 + h_8g_5; j_5 = h_8g_6 \\
j_5 &= h_8g_6
\end{aligned} \tag{4.2.16}$$

$$j_{01} = g_{41}; j_{11} = h_{61}g_4 + h_5g_{51} + h_6g_{41}$$

$$\begin{array}{cccccc}
5 & 5 & 5 & 5 & 5 & 5 \\
6 & 6 & 6 & 6 & 6 & 6
\end{array}$$

$$j_{21} = h_{61}g_5 + h_{71}g_4 + h_5g_{61} + h_6g_{51} + h_1g_{41}$$

$$\begin{array}{cccccc}
5 & 5 & 5 & 5 & 5 & 5 \\
6 & 6 & 6 & 6 & 6 & 6
\end{array}$$

$$j_{31} = h_{61}g_6 + h_{71}g_5 + h_{81}g_4 + h_6g_{61} + h_7g_{51} + h_8g_{41}$$

$$\begin{array}{ccccccc}
5 & 5 & 5 & 5 & 5 & 5 & 5 \\
6 & 6 & 6 & 6 & 6 & 6 & 6
\end{array}$$

$$j_{41} = h_{71}g_6 + h_{81}g_5 + h_7g_{61} + h_8g_{51}$$

$$\begin{array}{cccc}
5 & 5 & 5 & 5 \\
6 & 6 & 6 & 6
\end{array}$$

$$j_{51} = h_{81}g_6 + h_8g_{61}$$

$$\begin{array}{ccc}
5 & 5 & 5 \\
6 & 6 & 6
\end{array} \tag{4.2.17}$$

$$\text{II1} = \frac{a_0}{2}(1 - \bar{u}_0^2) + \frac{a_1}{3}(1 - \bar{u}_0^3) + \frac{a_2}{4}(1 - \bar{u}_0^4)$$

$$\text{II2} = \frac{a_0}{3}(1 - \bar{u}_0^3) + \frac{a_1}{4}(1 - \bar{u}_0^4) + \frac{a_2}{5}(1 - \bar{u}_0^5)$$

$$\begin{aligned}
II3 &= \frac{a_0}{4}(1 - \bar{u}_0^4) + \frac{a_1}{5}(1 - \bar{u}_0^5) + \frac{a_2}{6}(1 - \bar{u}_0^6) \\
II4 &= \frac{a_0}{5}(1 - \bar{u}_0^5) + \frac{a_1}{6}(1 - \bar{u}_0^6) + \frac{a_2}{7}(1 - \bar{u}_0^7) \\
II5 &= \frac{a_0}{6}(1 - \bar{u}_0^6) + \frac{a_1}{7}(1 - \bar{u}_0^7) + \frac{a_2}{8}(1 - \bar{u}_0^8) \\
II6 &= \frac{a_0}{7}(1 - \bar{u}_0^7) + \frac{a_1}{8}(1 - \bar{u}_0^8) + \frac{a_2}{9}(1 - \bar{u}_0^9) \quad (4.2.18)
\end{aligned}$$

$$\begin{aligned}
JJ1 &= b_0 \frac{\bar{u}_0^2}{2} + b_1 \frac{\bar{u}_0^3}{3} + b_2 \frac{\bar{u}_0^4}{4} \\
JJ2 &= b_0 \frac{\bar{u}_0^3}{3} + b_1 \frac{\bar{u}_0^4}{4} + b_2 \frac{\bar{u}_0^5}{5} \\
JJ3 &= b_0 \frac{\bar{u}_0^4}{4} + b_1 \frac{\bar{u}_0^5}{5} + b_2 \frac{\bar{u}_0^6}{6} \\
JJ4 &= b_0 \frac{\bar{u}_0^5}{5} + b_1 \frac{\bar{u}_0^6}{6} + b_2 \frac{\bar{u}_0^7}{7} \\
JJ5 &= b_0 \frac{\bar{u}_0^6}{6} + b_1 \frac{\bar{u}_0^7}{7} + b_2 \frac{\bar{u}_0^8}{8} \\
JJ6 &= b_0 \frac{\bar{u}_0^7}{7} + b_1 \frac{\bar{u}_0^8}{8} + b_2 \frac{\bar{u}_0^9}{9} \quad (4.2.19)
\end{aligned}$$

The integrals that make up the C_i are integrated numerically.

4.3 Initial Conditions for the Integration

a_0 , a_1 and a_2 are determined by a least squares polynomial fit to data representing the initial velocity profile. Initially u_0 is zero. c_0 is set equal to $\frac{H_w}{H_2}$ while c_1 is determined

by requiring the stagnation enthalpy approximation, eqn. (4.1.6a) and the actual initial value of \bar{H} at $\bar{u} = 0.5$ to coincide.

The system of ordinary first order differential equations, (4.2.1), are integrated starting from these initial conditions, by following a step by step process downstream.

When the initial velocity profile is a parabola-type (i.e. $N_s = 2$), there is the additional difficulty that the $j = 1$ and $k = 1$ integral relations are inadmissible at $x = 0$, owing to the singularity of the integrals on the right hand side. This problem is overcome by setting $c_1 = 0$, introducing the "j=4" integral relation and reducing the number of independent variables to five for the first integration step.

4.4 Determination of Velocity-Defect Thickness

$$\left(\frac{\Delta^*}{L}\right) = \int_0^{\bar{u}_0} \bar{u} \bar{T}^{\ell} \zeta^{\ell} d\bar{u} + \int_{\bar{u}_0}^1 (1 - \bar{u}) \bar{T}^{\ell} \zeta^{\ell} d\bar{u} \quad (4.4.1)$$

where

$$\bar{T} = (1 + m)\bar{H} - m\bar{u}^2 \quad (4.4.2)$$

Carrying out the integration leads to the following expression for $\left(\frac{\Delta^*}{L}\right)$.

$$\begin{aligned} \frac{\Delta^*}{L} = & t_0 \bar{u}_0 + t_1 \frac{\bar{u}_0^2}{2} + \frac{t_2}{3} \bar{u}_0^3 + \frac{t_3}{4} \bar{u}_0^4 + \frac{t_4}{5} \bar{u}_0^5 \\ & + \frac{t_5}{6} \bar{u}_0^6 + t_6 (1 - \bar{u}_0) + \frac{t_7}{2} (1 - \bar{u}_0^2) \\ & + \frac{t_8}{3} (1 - \bar{u}_0^3) + \frac{t_9}{4} (1 - \bar{u}_0^4) + \frac{t_{10}}{5} (1 - \bar{u}_0^5) + \frac{t_{11}}{6} (1 - \bar{u}_0^6) \end{aligned} \quad (4.4.3)$$

$$\begin{aligned}
t_0 &= k_0 b_0; \quad t_1 = k_0 b_1 + k_1 b_0; \quad t_2 = k_0 b_2 + k_1 b_1 + k_2 b_0 \\
t_3 &= k_1 b_2 + k_2 b_1 + k_3 b_0; \quad t_4 = k_2 b_2 + k_3 b_1; \quad t_5 = k_3 b_2 \\
t_6 &= k_4 a_0; \quad t_7 = k_4 a_1 + k_5 a_0; \quad t_8 = k_4 a_2 + k_5 a_1 + k_6 a_0 \\
t_9 &= k_5 a_2 + k_6 a_1 + k_7 a_0; \quad t_{10} = k_6 a_2 + k_7 a_1; \quad t_{11} = k_7 a_2
\end{aligned}
\tag{4.4.4}$$

$$\begin{aligned}
k_0 &= (1 + m)\lambda; \quad k_1 = (1 + m)(1 - \lambda + \lambda d_1) \\
k_2 &= (1 + m) [\lambda d_2 + d_1(1 - \lambda)] - m; \quad k_3 = (1 + m)(1 - \lambda)d_2 \\
k_4 &= (1 + m)\lambda c_0; \quad k_5 = (1 + m) [\lambda c_1 + (1 - \lambda)c_0] \\
k_6 &= (1 + m) [\lambda(1 - c_1 - c_0) + (1 - \lambda)c_1] \\
k_7 &= (1 + m)(1 - \lambda)(1 - c_1 - c_0)
\end{aligned}
\tag{4.4.5}$$

4.5 Determination of Location of Dividing Streamline

This is achieved by the integration of eqn. (2.5.28), which, it will be recalled, is written

$$\frac{dy_0}{d\xi} + \frac{1}{(1 - \bar{\rho}_0 \bar{u}_0)} \frac{d\delta_1}{d\xi} = 0
\tag{4.5.1}$$

Now

$$\begin{aligned}
\frac{\delta_1}{L} &= \int_{\bar{u}_0}^1 (\bar{T} - \bar{u}) \zeta(\xi, \bar{u}) d\bar{u} \\
&= \ell_0(1 - \bar{u}_0) + \frac{\ell_1}{2}(1 - \bar{u}_0^2) + \frac{\ell_2}{3}(1 - \bar{u}_0^3) + \frac{\ell_3}{4}(1 - \bar{u}_0^4) \\
&\quad + \frac{\ell_4}{5}(1 - \bar{u}_0^5)
\end{aligned}
\tag{4.5.2}$$

where $\ell_0 = (1 + m)(g_1 + 1)a_0$

$$\ell_1 = (1 + m)(g_1 + 1)a_1 + [(1 + m)g_2 + m] a_0$$

$$\ell_2 = (1 + m)(g_1 + 1)a_2 + [(1 + m)g_2 + m] a_1 + (1 + m)g_3 a_0$$

$$\ell_3 = [(1 + m)g_2 + m] a_2 + (1 + m)g_3 a_1$$

$$\ell_4 = (1 + m)g_3 a_2 \tag{4.5.3}$$

Differentiation of eqn. (4.5.2) leads to the following form for eqn. (4.5.1)

$$\begin{aligned} \frac{dy_0}{d\xi} = & - \frac{1}{(1 - \bar{\rho}_0 \bar{u}_0)} \left\{ [(1 - \bar{u}_0) \ell_{02} + \frac{1}{2}(1 - \bar{u}_0^2) \ell_{12} + \frac{1}{3}(1 - \bar{u}_0^3) \ell_{22}] \right. \\ & \cdot \frac{da_0}{d\xi} + \left[\frac{1}{2}(1 - \bar{u}_0^2) \ell_{13} + \frac{1}{3}(1 - \bar{u}_0^3) \ell_{23} + \frac{1}{4}(1 - \bar{u}_0^4) \ell_{33} \right] \frac{da_1}{d\xi} \\ & + \left[\frac{1}{3}(1 - \bar{u}_0^3) \ell_{24} + \frac{1}{4}(1 - \bar{u}_0^4) \ell_{34} + \frac{1}{5}(1 - \bar{u}_0^5) \ell_{44} \right] \frac{da_2}{d\xi} \\ & + \left[- \ell_0 - \ell_1 \bar{u}_0 - \ell_2 \bar{u}_0^2 - \ell_3 \bar{u}_0^3 - \ell_4 \bar{u}_0^4 \right] \frac{1}{\bar{u}_0 N_s} \cdot \bar{u}_0 N_s \frac{d\bar{u}_0}{d\xi} \\ & + [(1 - \bar{u}_0) \ell_{05} + \frac{1}{2}(1 - \bar{u}_0^2) \ell_{15} + \frac{1}{3}(1 - \bar{u}_0^3) \ell_{25} + \frac{1}{4}(1 - \bar{u}_0^4) \ell_{35} \\ & + \frac{1}{5}(1 - \bar{u}_0^5) \ell_{45}] \frac{dc_0}{d\xi} \\ & + [(1 - \bar{u}_0) \ell_{06} + \frac{1}{2}(1 - \bar{u}_0^2) \ell_{16} + \frac{1}{3}(1 - \bar{u}_0^3) \ell_{26} + \frac{1}{4}(1 - \bar{u}_0^4) \ell_{36} \\ & + \frac{1}{5}(1 - \bar{u}_0^5) \ell_{46}] \frac{dc_1}{d\xi} \left. \right\} \tag{4.5.4} \end{aligned}$$

$$\begin{aligned}
l_{02} &= (1+m)(g_1+1); \quad l_{05} = (1+m)a_0g_{15}; \quad l_{06} = 0; \quad l_{12} = (1+m)g_2 + m \\
l_{13} &= (1+m)(g_1+1); \quad l_{15} = (1+m)a_1g_{15} + a_0(1+m)g_{25}; \quad l_{22} = (1+m)g_3 \\
l_{23} &= (1+m)g_2 + m; \quad l_{24} = (1+m)(g_1+1); \quad l_{25} = (1+m)a_2g_{15} \\
&\quad + (1+m)a_1g_{25} + (1+m)a_0g_{35} \\
l_{32} &= 0; \quad l_{33} = (1+m)g_3; \quad l_{34} = (1+m)g_2 + m; \quad l_{35} = a_2(1+m)g_{25} \\
&\quad + a_1(1+m)g_{35} \\
l_{42} = l_{43} &= 0; \quad l_{44} = (1+m)g_3; \quad l_{45} = (1+m)a_2g_{35} \quad (4.5.5)
\end{aligned}$$

There is some difficulty in starting the integration of this differential equation because the right hand side becomes infinite at $\xi = 0$. There are a number of ways of dealing with this problem. However the simplest, which only involves a small error, is to approximate $1 - \bar{\rho}_0 \bar{u}_0$ by 1 in equation (4.5.1), and to set $\bar{y}_0(\xi) = \delta_1(0) - \delta_1(\xi)$ at the first step, from thereon eqn. (4.5.4) may be integrated by a step by step process.

4.6 Calculation of Velocity Profile

Lower part:

$$\bar{y} = \bar{y}_0 - \int_{\bar{u}}^{\bar{u}_0} \bar{T}^{\xi} d\bar{u} \quad : \quad \bar{u} \leq \bar{u}_0 \quad (4.6.1)$$

$$= \bar{y}_0 - [t_0 \cdot JY0 + t_1 \cdot JY1 + t_2 \cdot JY2 + t_3 \cdot JY3 + t_4 \cdot JY4 + t_5 \cdot JY5] \quad (4.6.2)$$

where

$$JYk = \int_{\bar{u}}^{\bar{u}_0} \bar{u}^k \frac{d\bar{u}}{\bar{u}} \quad : \quad k = 0,1,2, \dots \quad (4.6.3)$$

$$JY0 = \log \left(\frac{\bar{u}_0}{\bar{u}} \right); \quad JY1 = (\bar{u}_0 - \bar{u}); \quad JY2 = \frac{1}{2}(\bar{u}_0^2 - \bar{u}^2)$$

$$JY3 = \frac{1}{3}(\bar{u}_0^3 - \bar{u}^3); \quad JY4 = \frac{1}{4}(\bar{u}_0^4 - \bar{u}^4); \quad JY5 = \frac{1}{5}(\bar{u}_0^5 - \bar{u}^5) \quad (4.6.3)$$

Upper part:

$$\bar{y} = \bar{y}_0 + \int_{\bar{u}_0}^{\bar{u}} \bar{T}^u \zeta^u d\bar{u} \quad : \quad \bar{u} \geq \bar{u}_0 \quad (4.6.4)$$

$$= \bar{y}_0 + t_6 \cdot IY0 + t_7 \cdot IY1 + t_8 \cdot IY2 + t_9 \cdot IY3 + t_{10} \cdot IY4 + t_{11} \cdot IY5 \quad (4.6.5)$$

where

$$IYk = \int_{\bar{u}_0}^{\bar{u}} \frac{\bar{u}^k d\bar{u}}{(1-\bar{u})} \quad : \quad k = 0,1,2, \dots \quad (4.6.6)$$

$$IY0 = \log \left[\frac{(1-\bar{u}_0)}{(1-\bar{u})} \right] \quad (a); \quad IY1 = \bar{u}_0 - \bar{u} + IY0 \quad (b)$$

$$IY2 = \frac{1}{2} [(1-\bar{u}_0)^2 - (1-\bar{u})^2] + \bar{u}_0 - \bar{u} + IY1 \quad (c)$$

$$\begin{aligned}
IY3 = & [-\bar{u}^3 + 3 \{-(1-\bar{u}) + (1-\bar{u})^2 - \frac{1}{3}(1-\bar{u})^3\}] \log(1-\bar{u}) \\
& + [\bar{u}_0^3 + 3 \{(1-\bar{u}_0) - (1-\bar{u}_0)^2 + \frac{1}{3}(1-\bar{u}_0)^3\}] \log(1-\bar{u}_0) \\
& + 3 [(1-\bar{u}) - (1-\bar{u}_0) - \frac{1}{2}(1-\bar{u})^2 + \frac{1}{2}(1-\bar{u}_0)^2 + \frac{1}{9}(1-\bar{u})^3 \\
& - \frac{1}{9}(1-\bar{u}_0)^3] \quad (d)
\end{aligned}$$

$$\begin{aligned}
IY4 = & [-\bar{u}^4 + 4 \{-(1-\bar{u}) + \frac{3}{2}(1-\bar{u})^2 - (1-\bar{u})^3 + \frac{1}{4}(1-\bar{u})^4\}] \log(1-\bar{u}) \\
& - [-\bar{u}_0^4 + 4 \{-(1-\bar{u}_0) + \frac{3}{2}(1-\bar{u}_0)^2 - (1-\bar{u}_0)^3 + \frac{1}{4}(1-\bar{u}_0)^4\}] \log(1-\bar{u}_0) \\
& + 4 [(1-\bar{u}) - (1-\bar{u}_0) - \frac{3}{4}(1-\bar{u})^2 + \frac{3}{4}(1-\bar{u}_0)^2 + \frac{1}{3}(1-\bar{u})^3 \\
& - \frac{1}{3}(1-\bar{u}_0)^3 - \frac{1}{16}(1-\bar{u})^4 + \frac{1}{16}(1-\bar{u}_0)^4] \quad (e)
\end{aligned}$$

$$\begin{aligned}
IY5 = & [-\bar{u}^5 + 5 \{-(1-\bar{u}) + 2(1-\bar{u})^2 - 3(1-\bar{u})^3 + (1-\bar{u})^4 - \frac{1}{5}(1-\bar{u})^5\}] \log(1-\bar{u}) \\
& - [-\bar{u}_0^5 + 5 \{-(1-\bar{u}_0) + 2(1-\bar{u}_0)^2 - 3(1-\bar{u}_0)^3 + (1-\bar{u}_0)^4 \\
& - \frac{1}{5}(1-\bar{u}_0)^5\}] \log(1-\bar{u}_0) \\
& + 5 [(1-\bar{u}) - (1-\bar{u}_0) - (1-\bar{u})^2 + (1-\bar{u}_0)^2 + \frac{2}{3}(1-\bar{u})^3 \\
& - \frac{2}{3}(1-\bar{u}_0)^3 - \frac{1}{4}(1-\bar{u})^4 + \frac{1}{4}(1-\bar{u}_0)^4 + \frac{1}{25}(1-\bar{u})^5 - \frac{1}{25}(1-\bar{u}_0)^5] \quad (f)
\end{aligned}$$

(4.6.7)

4.7 Calculation of Temperature Profile

Lower part:

$$\bar{T}^l = k_0 + k_1 \bar{u} + k_2 \bar{u}^2 + k_3 \bar{u}^3 \quad : \quad \bar{u} < \bar{u}_0 \quad (a)$$

Upper part:

$$\bar{T}^u = k_4 + k_5 \bar{u} + k_6 \bar{u}^2 + k_7 \bar{u}^3 \quad : \quad \bar{u} > \bar{u}_0 \quad (b)$$

(4.7.1)

4.8 Calculation of Properties on Dividing Streamline

Velocity gradient:

$$\frac{\partial \bar{u}}{\partial \eta}(\xi, \bar{u}_0) = \frac{1}{\zeta(\xi, \bar{u}_0)} = \frac{(1 - \bar{u}_0)}{a_0(\xi) + a_1(\xi)\bar{u}_0 + a_2(\xi)\bar{u}_0^2} \quad (4.8.1)$$

Temperature gradient:

$$\frac{\partial \bar{T}}{\partial \eta}(\xi, \bar{u}_0) = [k_1 + 2k_2 \bar{u}_0 + 3k_3 \bar{u}_0^2] \frac{\partial u}{\partial \eta}(\xi, \bar{u}_0) \quad (4.8.2)$$

Nusselt number:

$$Nu_0 = + q_0 \frac{x}{k_1 (\bar{T}_1 - \bar{T}_2)} = - k_0 \frac{\partial \bar{T}_0}{\partial \eta} \frac{1}{\bar{T}_0} \frac{\xi}{(1 - \lambda_T)} \quad (4.8.3)$$

where $\lambda_T = \frac{\bar{T}_2}{\bar{T}_1} = (1 + m)\lambda$ and $\frac{\partial \bar{T}_0}{\partial \eta} \frac{1}{\bar{T}_0} = \frac{\partial \bar{T}_0}{\partial \bar{y}}$

In the laminar case Brown and Donoughe⁵⁸ are followed i.e., it is assumed

$$\bar{k}_0 = \frac{\bar{\mu}_0 \bar{C}_p}{\bar{\sigma}_0} = (\bar{T}_0)^{0.85} \quad (4.8.4)$$

and in the turbulent case it is assumed that $\bar{k} = 1$.

Shear stress coefficient:

$$C_{f0} = \frac{\xi^{\frac{1}{2}}}{\delta_0^{**} u_1 / \nu_1} \frac{\bar{\mu}}{\bar{T}} \frac{\partial \bar{u}}{\partial \eta} \quad (4.8.5)$$

4.9 Calculation of Position of Virtual Origin

Take the position of the virtual origin to be $(-x_V, y_V)$. Suppose x_A and x_B to be two different values of x that are sufficiently great for the shear layer to be considered as having reached asymptotic conditions for all practical purposes. This being so it can be written that

$$\frac{y_V - y_{0A}}{(x_A + x_V)^{\nu/2}} = \frac{y_V - y_{0B}}{(x_B + x_V)^{\nu/2}} \quad (4.9.1)$$

$$\frac{y_{0.95A} - y_V}{(x_A + x_V)^{\nu/2}} = \frac{y_{0.95B} - y_V}{(x_B + x_V)^{\nu/2}} \quad (4.9.2)$$

1 : laminar

where $\nu =$

2 : turbulent

and $y_{0.95}$ = value of y at which $\bar{u} = 0.95$.

The above two equations give the required expressions for x_V and y_V .

$$x_V = \frac{x_B [y_{0.95A} - y_{0A}]^{3-\nu} - x_A [y_{0.95B} - y_{0B}]^{3-\nu}}{[y_{0.95B} - y_{0B}]^{3-\nu} - [y_{0.95A} - y_{0A}]^{3-\nu}} \quad (4.9.3)$$

$$y_v = \frac{\frac{y_{0A}}{(x_A + x_v)^{v/2}} - \frac{y_{0B}}{(x_B + x_v)^{v/2}}}{\frac{1}{(x_A + x_v)^{v/2}} - \frac{1}{(x_B + x_v)^{v/2}}} \quad (4.9.4)$$

5. DISCUSSION

5.1. Preliminary Remarks

Before entering into a detailed discussion of the results, it will be helpful to examine the basic physical processes involved in the development of free shear layers.

If, as is assumed here, the free shear layer develops from an attached boundary layer; then, the shear force, which was responsible for the body drag, begins to drive the quiescent air as the shear layer leaves the body, causing fluid to be entrained into the mixing layer from below. Concomitant with this process, the velocity along the dividing streamline rises from its value of zero at separation until it reaches its asymptotic level far downstream.

Perhaps the process described above can best be understood in terms of a vorticity transfer. Since vorticity cannot be created in the interior of a fluid, the vorticity flux through a cross-section of the free shear layer remains constant. Owing to the boundary-layer approximation, the vorticity at a point in the shear layer is given by

$$\omega = \frac{\partial u}{\partial y}$$

Thus, the total vorticity below a particular streamline at a specific station x is given by

$$\int_{-\infty}^{y(x)} \omega dy = \int_{-\infty}^{y(x)} \frac{\partial u}{\partial y} dy = u(x)$$

This shows that $\bar{u}_0(x)$ is a measure of the ratio of the total amount of vorticity below the dividing streamline to the total vorticity flowing through a cross-section of the shear layer.

The development of the free shear layer can be explained by observing that vorticity will be diffused across the dividing streamline in order to balance the torque about the origin arising from the change in the rate of convection of angular momentum which occurs during the passage downstream. Eventually, sufficient vorticity is transferred into the lower region for the change in convection rates above and below the dividing streamline to counter-balance one another. When this condition is reached, the velocity along the dividing streamline becomes constant.

The effect of such factors as compressibility and heat transfer on this basic process will be discussed in the ensuing sections.

5.2. Discussion of Results for Laminar Case

5.2.1 A Comparison of Various Approximations for the Coefficient of Viscosity

Plots of \bar{u}_0 versus $\frac{v_1 x}{u_1 \delta_0^{**2}}$ are shown in Fig. 5.1 corre-

sponding to three different expressions for the coefficient of viscosity, viz.

- (i) $\bar{\mu} = \bar{T}$: $\omega = 1.0$
- (ii) $\bar{\mu} = \bar{T}^{0.75}$: $\omega = 0.75$
- (iii) $\bar{\mu} = \frac{T_1 + 198.6}{\bar{T} + 198.6} \left(\frac{\bar{T}}{T_1}\right)^{3/2}$: Sutherland's law

The calculations were performed for the case of $M_1 = 3.0$ with a Blasius profile in (ξ, η) coordinates as an initial condition. The free stream stagnation temperature, T_{O_1} , was set at 500°R . Here, and in subsequent computations, T_1 was assumed to correspond to an isentropic expansion from $M = 0$ to M_1 , i.e.

$$T_1 = T_{O_1} / \left(1 + \frac{\gamma - 1}{2} M_1^2\right)$$

As might be expected, approximation (i) leads to rather poor results. However, the second approximation is shown to compare quite favorably with Sutherland's law.

Also, shown in Figure 5.1 are some points calculated from Denison and Baum's²³ results. The conversion factor between their distance coordinate, s^* , and $\frac{v_1^x}{u_1 \delta_o^{**2}}$ is $\frac{1}{0.04863}$. A comparison between the curve for $\omega = 1.0$ and these points gives a good indication of the accuracy of the results herein presented. The small discrepancy occurring at the early stages of development could be more apparent than real, owing to the small size of the figure in reference 27

and the necessity of transforming from semi-log coordinates to natural ones and back again. Another indication of the accuracy of the results is given by the fact that the exact asymptotic value for \bar{u}_0 , namely 0.587 is attained in the $\omega = 1$ case.

5.2.2 The Effect of Compressibility

One would surmise that since the effect of compressibility is to intensify the diffusion process then the development of a free shear layer would be more rapid the higher the Mach number. Examination of Figures 5.2 a-e show this to be, in fact, the case.

At first sight it might seem odd that, as Figure 5.2a shows, the asymptotic value for \bar{u}_0 is not significantly increased at higher Mach numbers. It would seem that, as the gas in the lower part of the shear layer becomes more rarified, the relative angular momentum flux of the upper portion would increase considerably requiring a greater proportion of vorticity to be transferred to the lower stream. However, this condition also produces a much increased displacement effect leading to a substantially larger displacement of the dividing streamline downward, as shown in Figure 5.2d. This tends to negate the effect of the rise in angular momentum flux.

Figure 5.2c shows plots of the development of the shear stress coefficient for various values of the Mach number.

Note that the asymptotic level of $(xRe_{\delta_o^{**}})^{1/2} C_{fo}$ at first decreases with M_1 , but somewhere between $M_1 = 3.0$ and 4.0 , this trend is reversed. This is in contradiction to Mills²¹ results which show a monotonic decrease with M_1 . This apparent anomaly is the result of using Sutherland's law. Initially, the decrease in slope of the velocity at the dividing streamline as M_1 rises is not quite compensated for by the greater value of the coefficient of viscosity. Ultimately, though, as indicated by Figure 5.3b, the drop in T_1 as M_1 is increased leading to a higher growth rate for μ , which eventually dominates the effect of the diminishing $\frac{\partial u}{\partial y}$.

It is also important to note that the velocity profile data, which is not shown here, indicates that in general the locus of the points of maximum shear stress and the dividing streamline only coincide when asymptotic conditions have been attained.

The initially positive displacement of the dividing streamline shown in Figure 5.2d occurs because of a decrease in displacement thickness immediately after separation. The surprisingly large asymptotic values of $\frac{y_o}{(\delta_o^{**x})^{1/2}}$ are consistent with those reported by Mills²¹.

The effect of compressibility on the heat transfer properties is illustrated in Figure 5.2e. The local Nusselt number at the dividing streamline is defined as

$$Nu_o = \frac{+q_o x}{k_1 (T_1 - T_2)} = - \frac{k_o}{k_1} \frac{\partial T}{\partial y} \Big|_o \frac{x}{T_1 - T_2}$$

Thus, heat transfer is positive when passing from the quiescent region to the main stream, in which case, $T_1 < T_2$ and $Nu_0 < 0$.

As might be expected, the greater temperatures, associated with the higher Mach numbers, are responsible for increased conduction rates leading to a more rapid attainment of asymptotic conditions. Notwithstanding this fact, the final level for the heat transfer coefficient steadily declines with an increase in Mach number. This is a direct consequence of viscous heating which reaches a maximum at the dividing streamline, bringing about a decrease in the effective temperature difference between the outer stream and the dividing streamline. Viscous dissipation is also responsible for displacing the locus of the points of maximum heat transfer considerably below the dividing streamline.

TABLE I

VARIATION OF THE POSITION OF THE
VIRTUAL ORIGIN WITH MACH NUMBER

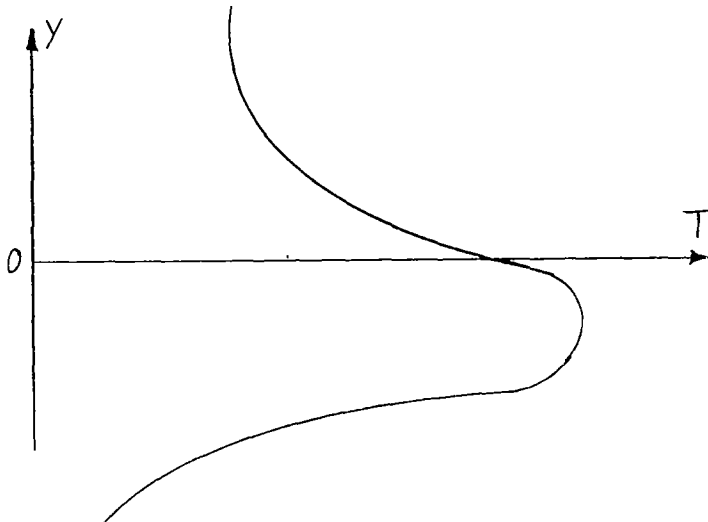
M_1	$\frac{x_v}{u_1 \delta_o^{**2}}$	$\frac{y_v}{\delta_o^{**}}$
0.0	14.85	5.57
1.0	13.37	5.75
2.0	9.98	5.96
3.0	7.01	6.02
4.0	4.90	6.00
5.0	3.44	5.93
10.0	1.13	5.46

5.2.3 The Effect of Change in Free Stream Stagnation Temperature

This is illustrated in Figs. 5.3a and b. The results being quite predictable on the basis of the foregoing discussion.

5.2.4 The Effect of Change in the Total Enthalpy Ratio, λ .

Since an increase in H_2/H_1 leads to higher temperatures, at the dividing streamline, it is predictable that the rate of diffusion will rise, implying a more rapid growth to asymptotic conditions, as H_2/H_1 becomes larger. Figs. 5.4 confirm this prognostication. Once again the effects of viscous dissipation are responsible for the rather eccentric results corresponding to values of λ below one in Figures 5.4b and e. The curves in these figures are a testament to the fact that temperature profiles corresponding to a cold quiescent region have the following general shape.



The peak in the temperature profile occurs because of the viscous heating. In the early stages of development, the locus of the points of maximum shear stress, where the effects of viscous dissipation are greatest, lies at a considerable distance above the dividing streamline, consequently the peak in the temperature profile is also located above y_0 . Hence, the initially negative Nusselt numbers for $\lambda = 0.0$ and 0.25 in Figure 5.4e are explained. However, as the development progresses, the point of maximum shear stress moves toward the dividing streamline, until the slope of the temperature profile becomes negative at y_0 . These results are at the very least in qualitative agreement with those of Mills²¹.

It is also interesting to note that Fig. 5.4e seems to imply that the asymptotic level of $Nu_0 (u_1 x / \nu_1)^{1/2}$ tends to a value of approximately -0.135 , independently of λ for $\lambda > 0.75$. In addition, it could be remarked that Figure 5.4e shows that an estimate of heat transfer across the dividing streamline based on asymptotic conditions would probably be in serious error unless $\frac{\nu_1 x}{u_1 \delta_0^{**2}}$ exceeded 1000, or more.

TABLE II
VARIATION OF THE POSITION OF THE
VIRTUAL ORIGIN WITH TOTAL ENTHALPY RATIO

$$M_1 = 3.0$$

λ	$\frac{x_v^{v1}}{u_1 \delta_o^{**2}}$	$\frac{y_v}{\delta_o^{**}}$
0.0	-18.00	-9.04
0.25	6.45	4.64
0.50	18.48	6.96
0.75	14.65	6.89
1.00	7.01	6.02
1.30	-1.50	4.21
1.50	-6.73	3.12
2.0	-13.65	0.95
5.0	-8.14	0.64

The position coordinates for the virtual origin recorded in Table II display a strong dependency on λ . The negative values of x_v corresponding to $\lambda = 0.0$ and $\lambda \geq 1.3$ are convincing evidence of the general invalidity of the type of virtual origin approximation discussed in Section 1.3.

5.2.5. The Effect of a Discontinuity in the Total Enthalpy Ratio at the Origin

This is illustrated in Figures 5.5. The results are quite predictable, although the magnitude of the effect is perhaps rather surprising.

5.2.6. The Influence of the Initial Velocity Profile

The growth of the dividing streamline velocity profiles corresponding to three different values of the Falkner-Skan⁵⁹ parameter, β , is shown in Fig. 5.6. The data was taken from the calculations of Evans⁶⁰, the profiles being assumed invariant with Mach number when cast in (ξ, η) coordinates.

The influence of the initial velocity profile is not very pronounced at $M_1 = 3.0$. However, the effect may be expected to be intensified at lower Mach numbers.

The results obtained can be explained by observing that initially the driving shear force is greater for larger β . Alternatively, it may be said that the rate of transfer of vorticity - $v \frac{\partial^2 u}{\partial y^2}$ is higher the larger β is. However, the results in Fig. 5.6 also show that the $\beta = -0.18$ case reaches asymptotic conditions slightly earlier than the $\beta = 1.0$ case. Possibly this is because the rate of convection of angular momentum is greater for initial profiles near separation.

5.3 Discussion of Results for the Turbulent Case

Owing the tentative nature of the hypotheses advanced in Chapter 3, concerning the eddy viscosity model, a detailed study of the turbulent case was not undertaken at this time.

The theoretical prediction of the growth of the velocity along the dividing streamline, for two initial velocity profiles with $M_1 = 3.0$ and $Pr \approx 0.5$, is shown in Fig. 5.7. One of these profiles was reported by Reda and Page⁶¹; it was determined from data taken after the initial expansion at the trailing edge of a rearward-facing step, consequently, it should be typical of the initial conditions required for a free shear layer developing behind a rearward facing step or base. The other is a parabolic profile, which is not of much practical interest, but does represent the sole power-law profile that can be treated exactly, when using only three velocity-profile parameters, viz. a_0 , a_1 , and a_2 .

The virtual origin for the Reda-Page profile was determined to be at

$$\frac{x_v}{\delta_0^{**}} = 39.75$$

$$\frac{y_v}{\delta_0^{**}} = 7.37$$

Although the development of a free shear layer is highly dependent on the choice of constant and functional form for the eddy viscosity, it can be seen that the transforma-

tion

$$\chi = 0.016 \int_0^{\xi} \Delta^*(\bar{x}) d\bar{x}$$

reduces eqns. (2.4.7 and 8) to a form independent of constant and $\Delta^*(\bar{x})$. Therefore, the inference is made that the asymptotic value of \bar{u}_0 is unaffected by the choice of constant and functional form for $\Delta^*(\bar{x})$. In particular, it follows that the incompressible value of $\bar{u}_0(\infty)$ for the turbulent case is identical with its laminar counterpart. Fig. 5.7, which was taken in part from Jacques and Gailly²², shows a comparison of the prediction of $\bar{u}_0(\infty)$ following various theories, including the one presented here.

TABLE III
THE ASYMPTOTIC VALUE OF \bar{u}_0 AS A
FUNCTION OF M_1

Pr = 0.5

$\bar{u}_0(\infty)$	M_1
0.587	0
0.598	1
0.624	2
0.646	3
0.662	4

6. CONCLUSIONS

1. The method of numerical integration presented in Chapter 2 could easily be modified for application to more involved problems, e.g. the case of $u_2 \neq 0$, confined mixing etc. It would be particularly advantageous where treatment of discontinuities, such as embedded shock waves, is required.
2. The calculated results indicate that both compressibility and stagnation enthalpy ratio have a great influence on the development of free shear layers.
3. The development is also strongly affected by a temperature discontinuity at the origin.
4. The level of free stream total temperature only has a slight effect on the free shear layer properties.
5. The influence of the initial velocity profile is only of importance during the initial stages of development.
6. The position of the virtual origin was found to be downstream of the real one, for some values of H_2/H_1 . Therefore, it is inferred that this type of an approximation is not generally valid.
7. Calculations for the heat transfer across the dividing streamline, based on asymptotic conditions, are unlikely to be accurate unless $\frac{v_1 x}{u_1 \delta_0^{**2}}$ exceeds 1000 or more.

REFERENCES

1. Chapman, D. R., "An Analysis of Base Pressure at Supersonic Velocities and Comparison with Experiment," NACA T.N. 2137, 1950.
2. Chapman, D. R., Kuehn, D. M., and Larson, H. K., "Investigation of Separated Flows in Supersonic and Subsonic Streams with Emphasis on the Effect of Transition," NACA T.N. 3869, March 1957.
3. Korst, H. H., "Comments on the Effect of Boundary Layer on Sonic Flow Through An Abrupt Cross-Sectional Area Change," J. Ae. Sci., Vol. 21, p. 568, 1954.
4. Korst, H. H., Page, R. H., and Childs, M. E., "A Theory for Base Pressure in Transonic and Supersonic Flow," University of Illinois, M.E. TN 392-2, March 1955.
5. Korst, H. H., "A Theory for Base Pressures in Transonic and Supersonic Flow," J. Appl. Mech., Vol. 23, p. 593, 1956.
6. Carpenter, P. W., and Tabakoff, W., "Survey and Evaluation of Supersonic Base Flow Theories," NASA C.R. 97129 (N68-36011), July 1968.
7. Goldstein, S., "Concerning Some Solutions of the Boundary Layer Equations in Hydrodynamics," Proc. Camb. Phil. Soc. 26, pp. 1-30, 1930.
8. Görtler, H., "Berechnung von Aufgaben der freien Turbulenz auf Grund eines neuen Näherungsansatzes," Z.A.M.M. Bd. 22 Nr. 5, Okt. 1942.
9. Reichardt, H., "Über eine neue Theorie der freien Turbulenz," Z.A.M.M. Bd. 21, Nr. 5, Okt. 1941.
10. Prandtl, L., "Bemerkungen zur Theorie der freien Turbulenz," Z.A.M.M. Bd. 22, Nr. 5, Okt. 1942.
11. Clauser, F. H., "The Turbulent Boundary Layer," Advances in Applied Mechanics, Vol. 4, Academic Press, pp. 1-51, 1956.
12. Dorodnitsyn, A. A., "Solution of Mathematical and Logical Problems on High-Speed Digital Computers," Proc. Conf. Develop. Soviet Math. Machines Devices, Part 1, pp. 44 - 52 VINITI, Moscow 1956.

13. Dorodynitsyn, A. A., "General Method of Integral Relations and Its Application to Boundary Layer Theory," *Advances in Aeronautical Sciences*, Vol. 3, Pergamon Press, New York, 1962.
14. Belotserkovskii, O. M., and Chushkin, P. I., "The Numerical Solution of Problems in Gas Dynamics," Basic Developments in Fluid Dynamics, (Holt, M.; Ed.) Vol. 1, Academic Press, New York, 1965.
15. Tollmien, W., "Berechnung turbulenter Ausbreitungsvorgunge," *Z.A.M.M.*, Vol. 6, pp. 1-12, 1926.
16. Keulegan, G. H., "Laminar Flow at the Interface of Two Liquids," *J. of Research, National Bureau of Standards*, Vol. 32, p. 303, June 1944.
17. Lock, R. C., "The Velocity Distribution in the Laminar Boundary Layer Between Parallel Streams," *Qu. J. Mech.* 4, pp. 42-63, 1951.
18. Lessen, M., "On the Stability of the Free Laminar Boundary Layer Between Parallel Streams," NACA TN 1929, August 1949.
19. Chapman, D. R., "Laminar Mixing of a Compressible Fluid," NACA Rep. 958, 1950, (replaces NACA TN 1800).
20. Crane, L. J., "The Laminar and Turbulent Mixing of Jets of Compressible Fluid," *J. Fld. Mech.*, Vol. 3, Part 1, October 1957.
21. Mills, R. D., "Numerical and Experimental Investigation of the Shear Layer Between Two Parallel Streams," *J.F.M.* Vol. 33, Part 3, pp. 591-616, 1968.
22. Jacques, R., and Gailly, A., "Melange supersonique turbulent et application aux problemes de recollement," AGARD Conf. Proc. No. 4, May 1966.
23. Denison, M. R., and Baum, E., "Compressible Free Shear Layer with Finite Initial Thickness," *A.I.A.A. J.*, Vol. 1, pp. 342-349, 1963.
24. Baum, E., "Initial Development of the Laminar Separated Shear Layer," *A.I.A.A. J.*, Vol. 2, pp. 128-131, January 1964.
25. Kobota, T., and Dewey, C. F., "Momentum Integral Methods for the Laminar Free Shear Layer," *A.I.A.A. J.*, Volume 2, pp. 625-629, April 1964.

26. Pai, S. I., "Two-Dimensional Jet Mixing of a Compressible Fluid," J. Ae. Sci., Vol. 16, No. 8, Aug. 1949.
27. Chapman, A. J., and Korst, H. H., "Free Jet Boundary with Consideration of the Initial Boundary Layer," Proc. of Second Cong. of Applied Mech., ASME, 1954.
28. Korst, H. H., Page, R. H., and Childs, M. E., "Compressible Two-Dimensional Jet Mixing at Constant Pressure," University of Illinois, ME TN392-1, April 1954.
29. Page, R. H., and Korst, H. H., "Nonisoenergetic Turbulent Compressible Jet Mixing with Consideration of Its Influence on the Base Pressure Problem," Proc. Fourth Midwestern Conf. on Fluid Mech., Purdue University, September 1955.
30. Korst, H. H., and Chow, W. L., "Non-isoenergetic Turbulent ($Pr_t = 1$) Jet Mixing Between Two Compressible Streams at Constant Pressure," NASA CR-419, April 1966.
31. Kirk, F. N., "An Approximate Theory of Base Pressure in Two-Dimensional Flow at Supersonic Speeds," R.A.E. T.N. Aero. 2377, 1954.
32. Nash, J. F., "An Analysis of Two-Dimensional Turbulent Base Flow, Including the Effect of the Approaching Boundary Layer," A.R.C. R&M, No. 3344, July 1962.
33. Hill, W. G., "Initial Development of Compressible Turbulent Free Shear Layer," Ph.D. Thesis, Rutgers-The State University, May 1966.
34. Hill, W. G., and Page, R. H., "Initial Development of Turbulent Compressible Free Shear Layers," J. of Basic Eng., Trans. ASME, March 1969.
35. Carriere, P., and Sirieix, M., "Facteurs d'influence du recollement d'un ecoulement supersonique," Proc. of Tenth Int. Congr. of Appl. Mech., Stresa, 1960.
36. Golik, R. J., "On the Dissipative Mechanisms Within Separated Flow Regions," Ph.D. Thesis, University of Illinois, 1962.
37. Carpenter, P. W., "A Numerical Study of the Development of a Compressible Free Shear Layer from Arbitrary Initial Conditions," Ph.D. Dissertation, Dept. of Aerospace Engineering, University of Cincinnati, July 1970.
38. Baum, E., "An Interaction Model of a Supersonic Laminar Boundary Layer on Sharp and Rounded Backward Facing Steps," A.I.A.A. J., Vol. 6, No. 3, March 1968.

39. Weinbaum, S., "Rapid Expansion of a Supersonic Boundary Layer and Its Application," A.I.A.A. J., Vol. 4, No. 2, February 1966.
40. Hama, F. R., "Experimental Investigations of Wedge-Base Pressure and Lip Shock," NASA CR-81031, December 1966.
41. Ting, L., "On the Mixing of Two Parallel Streams," J. Math. and Phys., Vol. 38, No. 3, October 1959.
42. Back, L. H., "Conservation Equations of a Viscous Heat-Conducting Fluid in Curvilinear Orthogonal Coordinates," NASA T.R. 32-1332, 1968.
43. Ackeret, J., Z. Flugtech. Motorluftschiff, pp. 72-74, 1925, (Trans. in NACA TM 317).
44. Lighthill, M. J., "Supersonic Flow Past Bodies of Revolution," A.R.C., R&M, No. 2003, 1945.
45. Munk, M. M., NACA Rep. No. 142, 1924.
46. Glauert, H., A.R.C., R&M, No. 910, 1924.
47. Kaplun, S., "Low Reynolds Number Flow Past a Circular Cylinder," J. Math. Mech. 6, pp. 595-603, 1957.
48. Rotta, J. C., "Turbulent Boundary Layers in Incompressible Flow," Progress in Aero. Sci. Vol. 2, Pergamon Press, New York, 1962.
49. Lamb, J. P., "The Development of Free Turbulent Shear Layers," AEDC-TR-65-184, 1965.
50. Lamb, J. P., "An Approximate Theory for Developing Turbulent Free Shear Layers," J. Basic Eng., Trans. ASME, September 1967.
51. Lamb, J. P., and Bass, R. L., "Some Correlations of Theory and Experiment for Developing Turbulent Free Shear Layers," J. Basic Eng., Trans. ASME, December 1968.
52. Nash, J. F., "The Effect of an Initial Boundary Layer on the Development of a Turbulent Free Shear Layer," A.R.C. C.P. No. 682, June 1962.
53. Morkovin, M. V., "Effects of Compressibility of Turbulent Flows," International Symposium on the Mechanics of Turbulence, Paris, pp. 367-380, 1962.

54. Bradshaw, P., "The Insensitivity of Turbulent Flow to Changes in Reynolds Number and Mach Number," NPL Aero. Note 1957, May 1967.
55. Mellor, G. L., and Gibson, D. M., "Equilibrium Turbulent Boundary Layers," J.F.M., Vol. 24, pp. 225-253, 1966.
56. Herring, H. J., and Mellor, G. L., "A Method of Calculating Compressible Turbulent Boundary Layers," NASA CR-1144, 1968.
57. Maise, G., and McDonald, H., "Mixing Length and Kinematic Eddy Viscosity in a Compressible Boundary Layer," A.I.A.A. J., Vol. 6, No. 1, January 1968.
58. Brown, W. B., and Donoughe, P. L., "Tables of Exact Laminar-Boundary-Layer Solutions When the Wall is Porous and Fluid Properties are Variable," NACA TN-2479, September 1951.
59. Falkner, V. M., and Skan, S. W., "Some Approximate Solutions of the Boundary-Layer Equations," A.R.C., R&M, 1314, 1930.
60. Evans, H. L., "Laminar Boundary-Layer Theory," Addison-Wesley, 1968.
61. Reda, D. C., and Page, R. H., "Supersonic Turbulent Flow Reattachment Downstream of a Two-Dimensional Backstep," Department of Mechanical and Aerospace Engineering, Rutgers-The State University, Rep. No. (RU-TR 125-MAE-F), May (1969), {Also AFOSR Scientific Report AFOSR 69-1592TR}.
62. Abramovich, G. N., "The Theory of a Free Jet of a Compressible Gas," Central Aero-Hydrodynamic Inst., Rep. No. 377, 1939, (Trans. in NACA TM 1058).
63. Brink, D. F., "Jet Mixing Under the Influence of a Pressure Gradient," Ph.D Thesis, University of Illinois, Urbana-Champaign, 1970.

FIG. 5.1 COMPARISON OF VARIOUS APPROXIMATIONS FOR THE COEFFICIENT OF VISCOSITY

$M_1 = 3.0$; $T_{o_1} = 500^\circ R$; $\lambda = 1.0$; $\lambda_w = 1.0$; $\beta = 0.0$

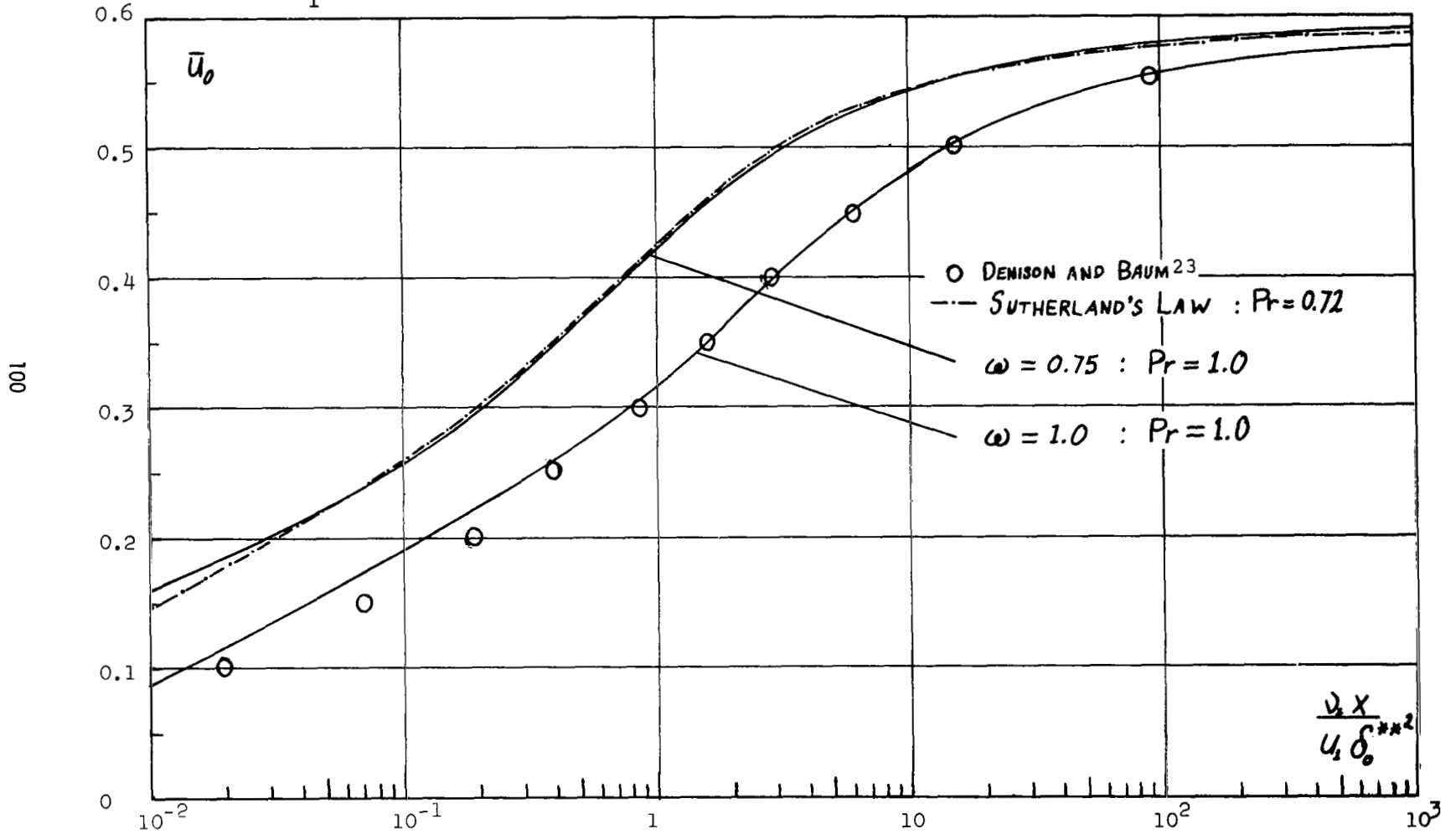


FIG. 5.2a VARIATION OF DIVIDING STREAMLINE VELOCITY DEVELOPMENT WITH MACH NUMBER

$Pr = 0.72$; $T_{o1} = 500^\circ R$; $\lambda = 1.0$; $\lambda_w = 1.0$; $\beta = 0.0$

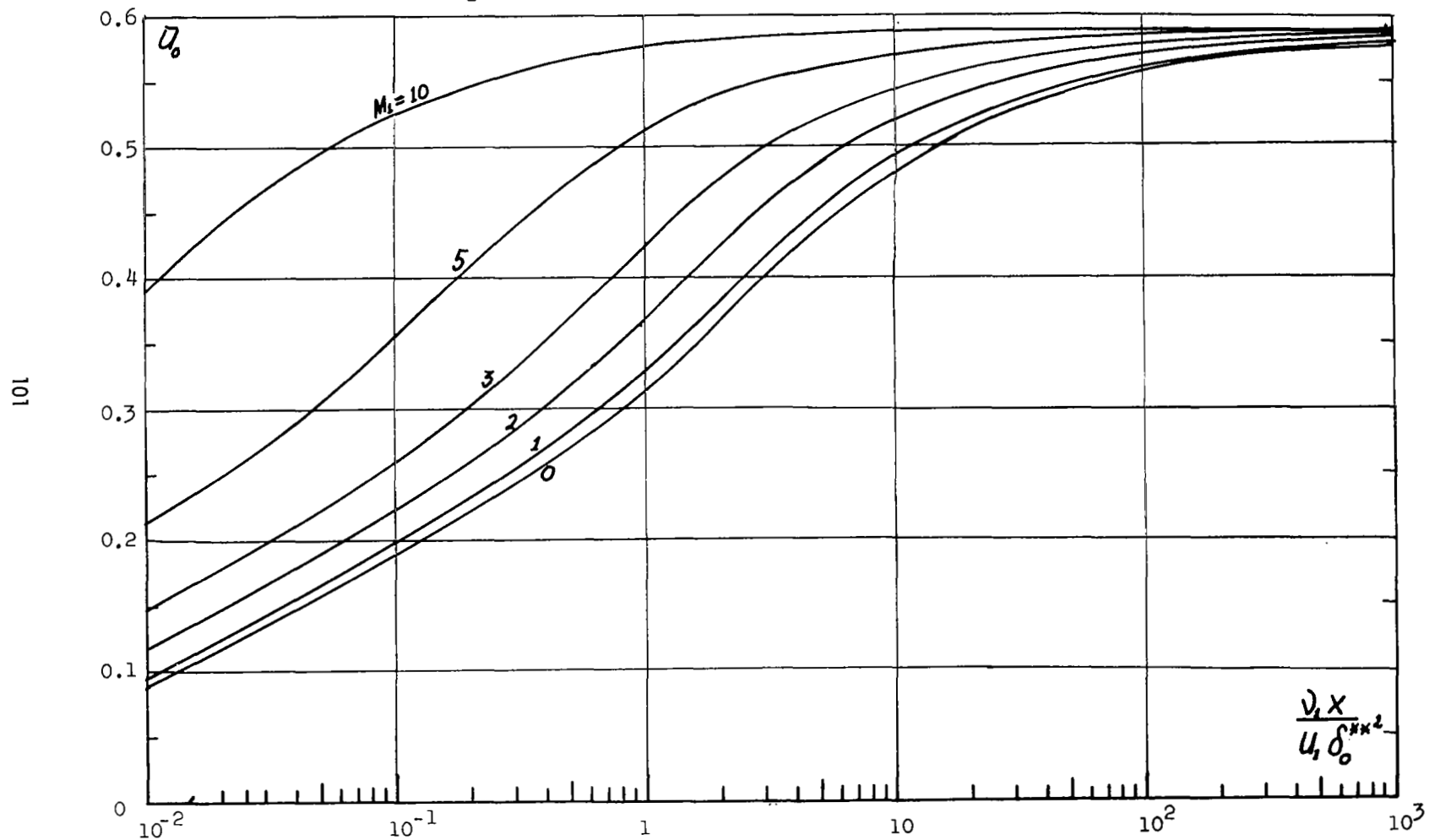


FIG. 5.2b VARIATION OF DIVIDING STREAMLINE TEMPERATURE DEVELOPMENT WITH MACH NUMBER

$Pr = 0.72$; $T_{O_1} = 500^\circ R$; $\lambda = 1.0$; $\lambda_w = 1.0$; $\beta = 0.0$

102

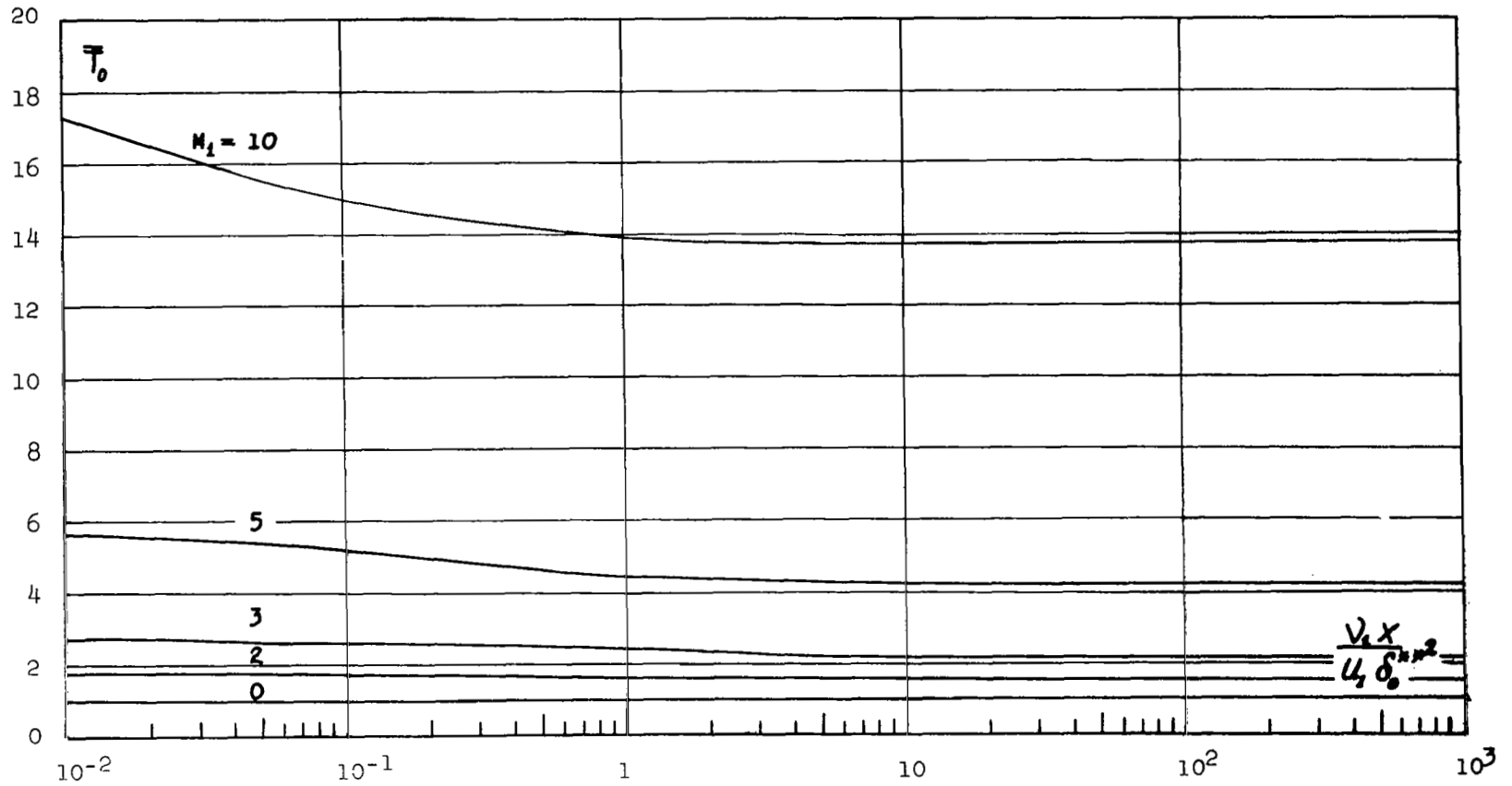


FIG. 5.2c VARIATION OF SHEAR STRESS COEFFICIENT DEVELOPMENT WITH MACH NUMBER

$Pr = 0.72$; $T_{o1} = 500^\circ R$; $\lambda = 1.0$; $\lambda_w = 1.0$; $\beta = 0.0$

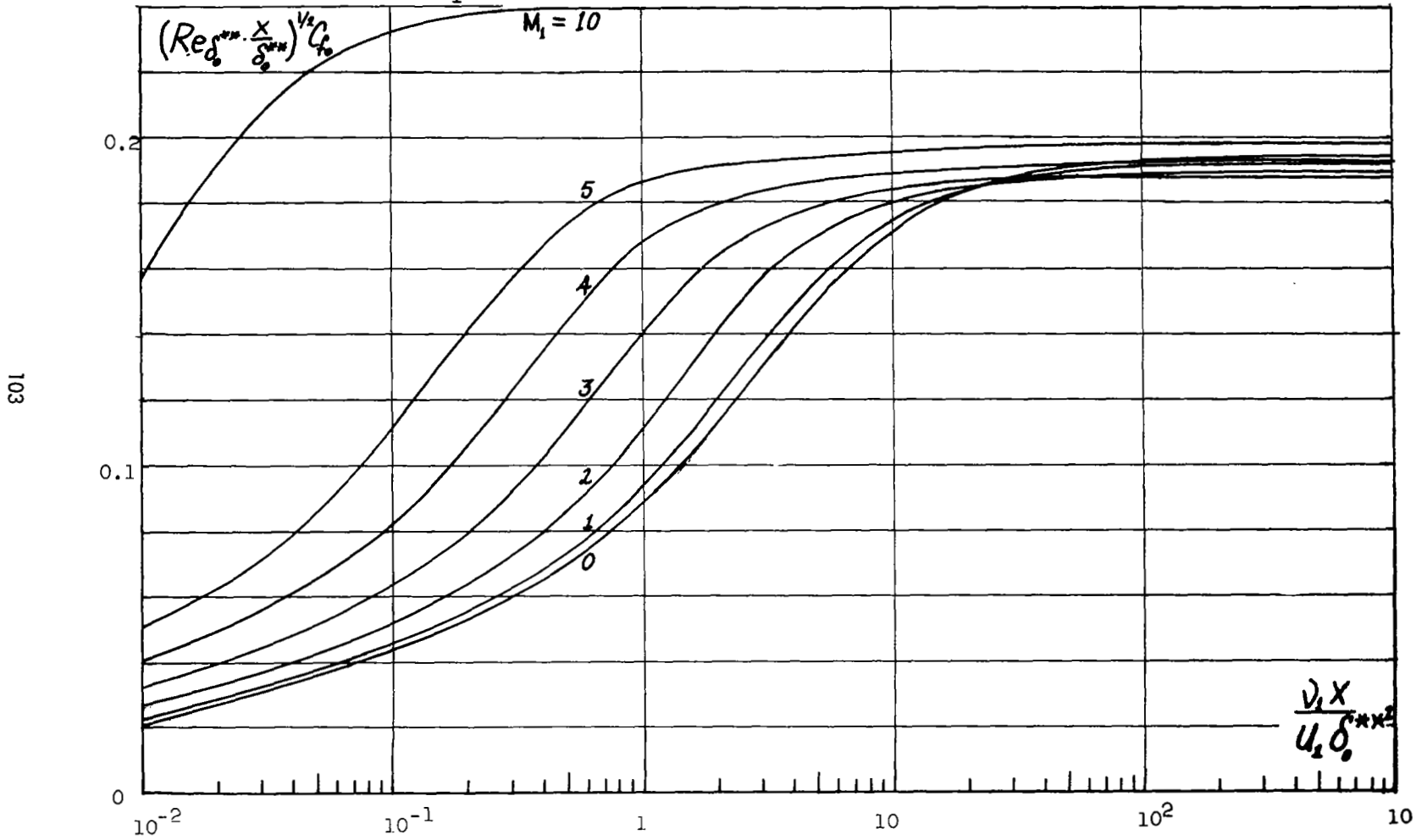


FIG. 5.2d VARIATION OF THE DEVELOPMENT OF DIVIDING STREAMLINE LOCATION WITH MACH NUMBER
 (Larger scale corresponds to case of $M_1 = 10$)

$Pr = 0.72$; $T_{o1} = 500^\circ R$; $\lambda = 1.0$; $\lambda_w = 1.0$; $\beta = 0.0$

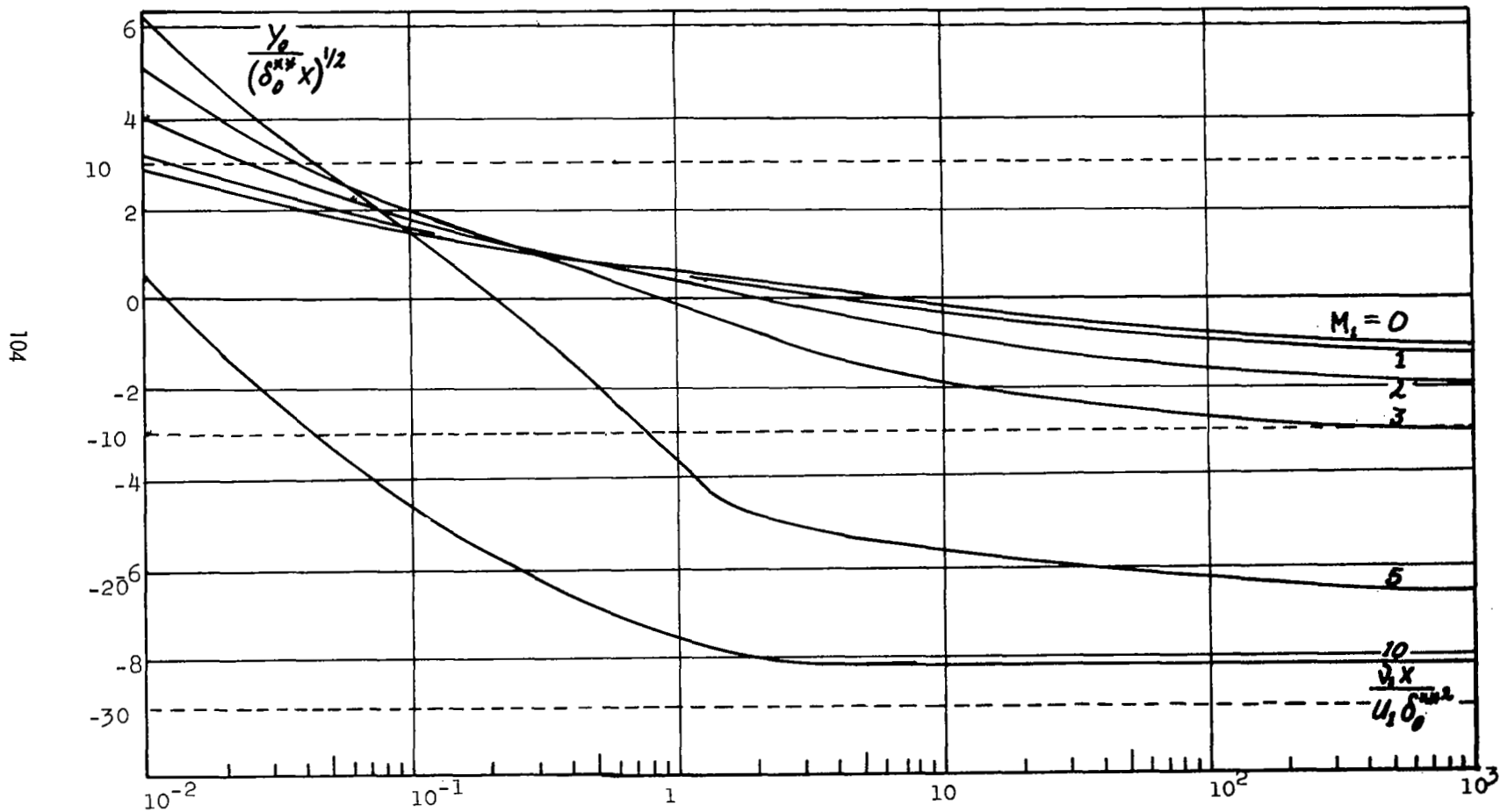


FIG. 5.2e VARIATION OF LOCAL NUSSELT NUMBER DEVELOPMENT WITH MACH NUMBER

$Pr = 0.72; T_{o1} = 500^\circ R; \lambda = 1.0; \lambda_w = 1.0; \beta = 0.0$

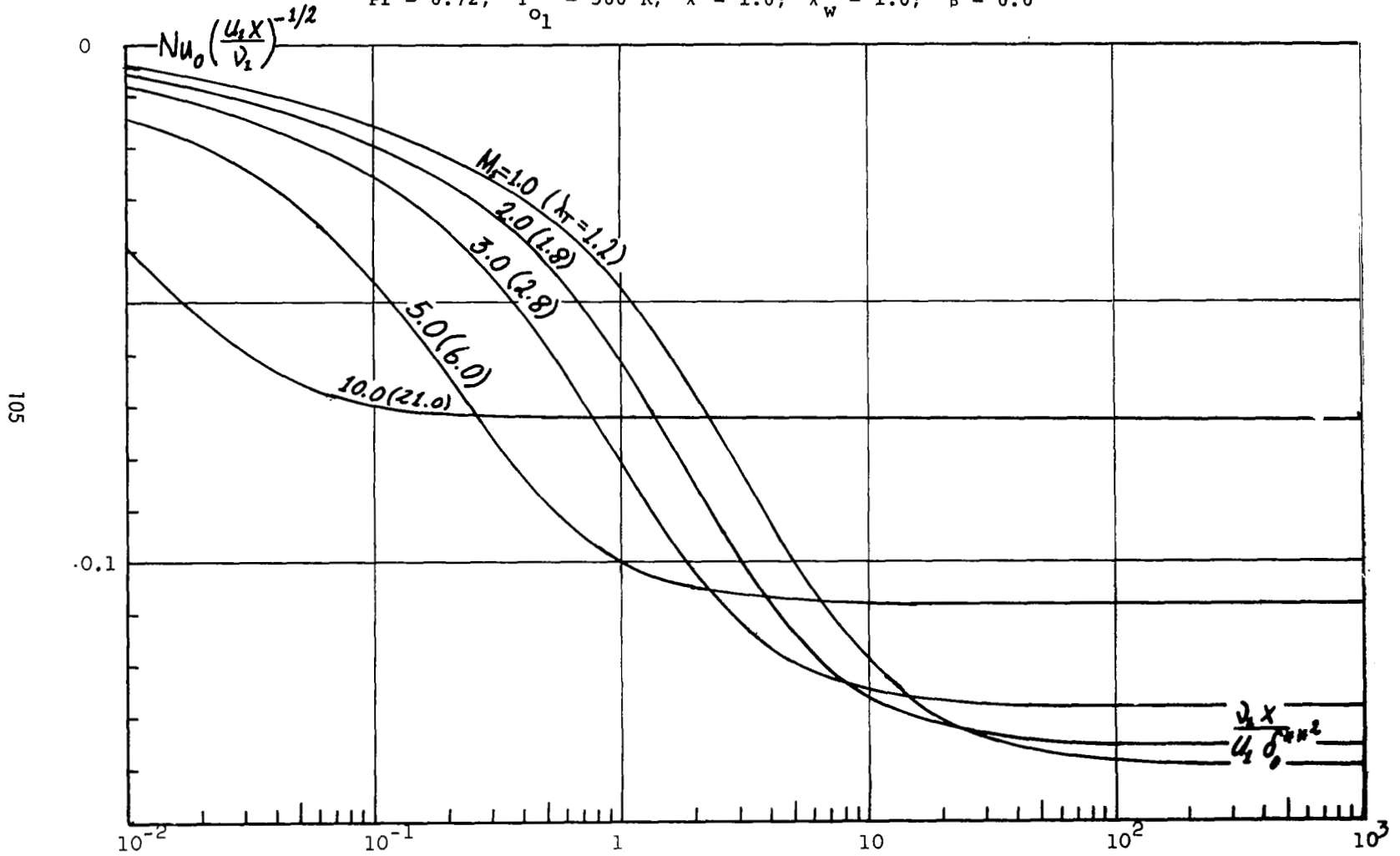


FIG. 5.3a VARIATION OF DIVIDING STREAMLINE VELOCITY DEVELOPMENT WITH FREE STREAM STAGNATION TEMPERATURE

$M_1 = 3.0; Pr = 0.72; \lambda = 1.0; \lambda_w = 1.0; \beta = 0.0$

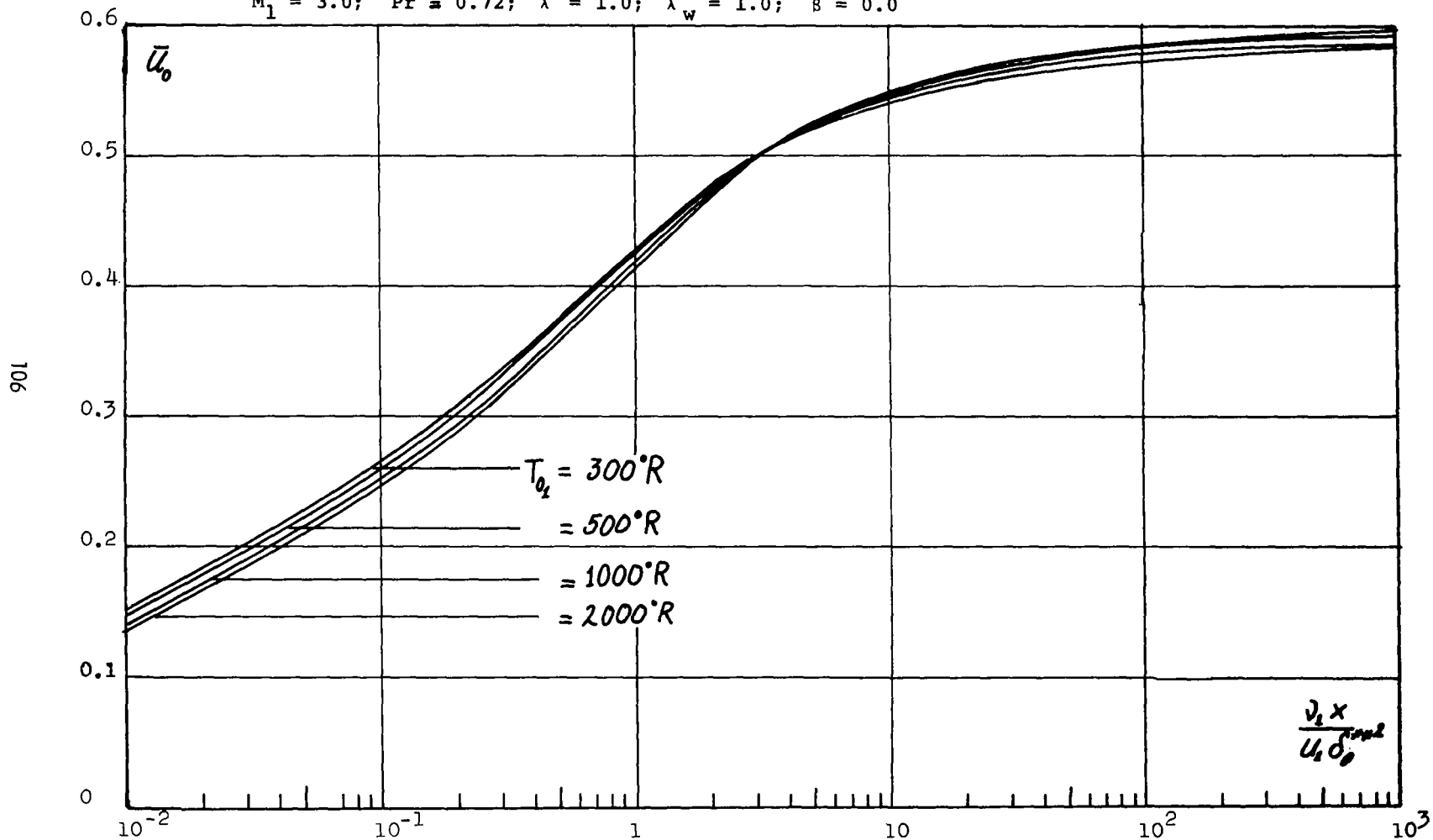


FIG. 5.3b VARIATION OF SHEAR STRESS COEFFICIENT DEVELOPMENT WITH FREE STREAM STAGNATION TEMPERATURE

$M_1 = 3.0$; $Pr = 0.72$; $\lambda = 1.0$; $\lambda_w = 1.0$; $\beta = 0.0$

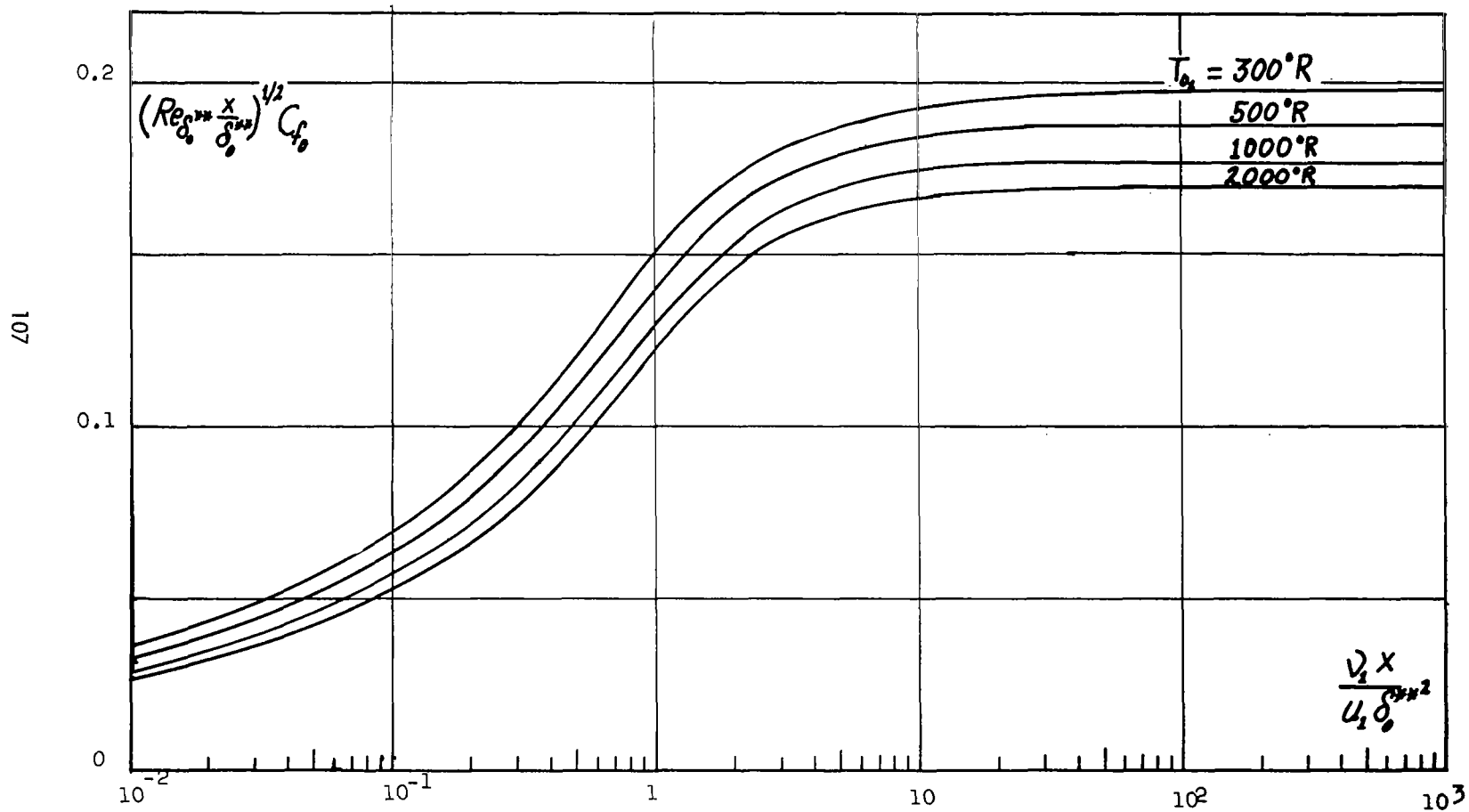


FIG. 5.4a VARIATION OF DIVIDING STREAMLINE VELOCITY DEVELOPMENT WITH TOTAL ENTHALPY RATIO
 $M_1 = 3.0$; $Pr = 0.72$; $T_{o1} = 500^\circ R$; $\beta = 0.0$

108

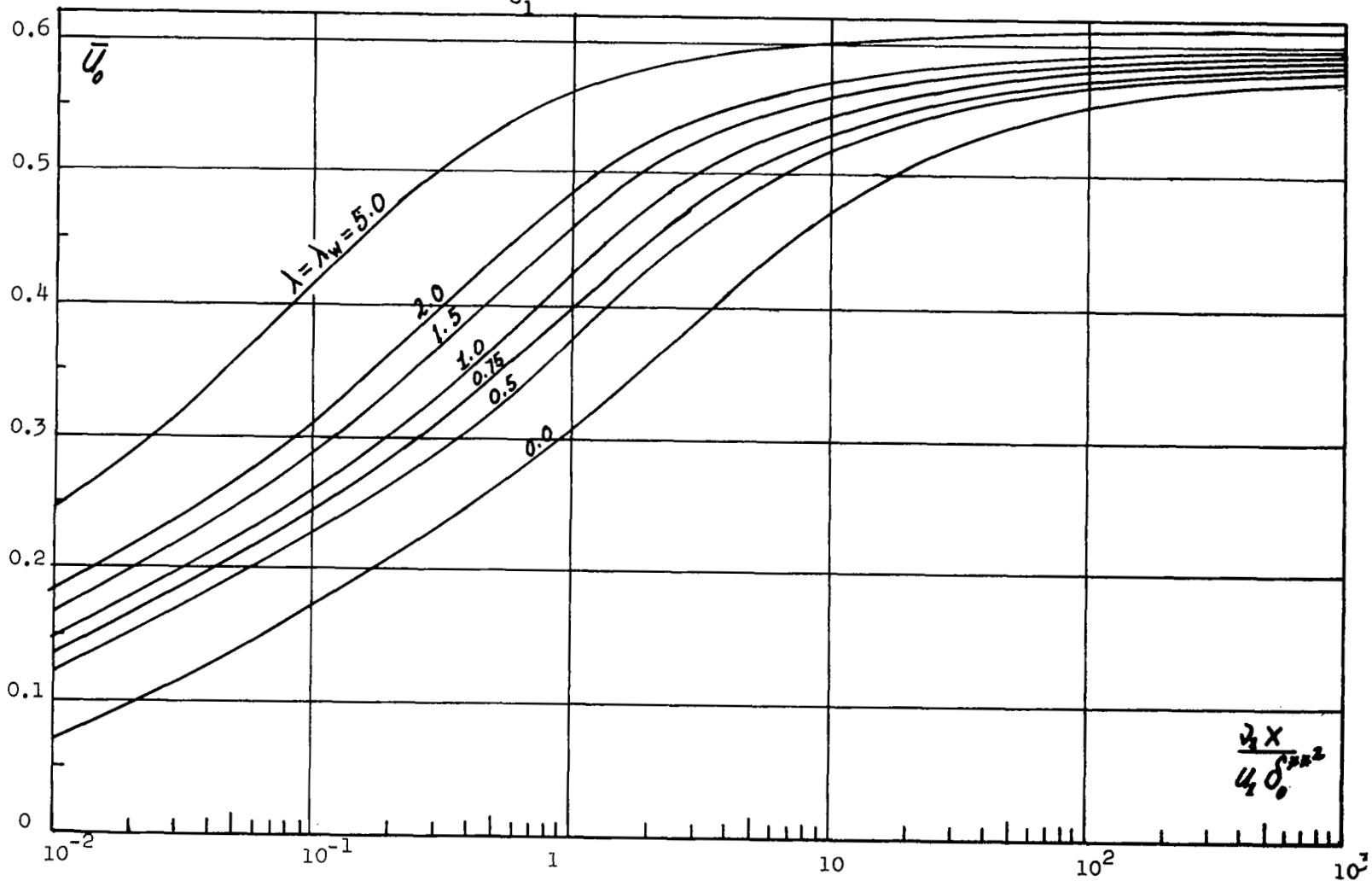


FIG. 5.4b VARIATION OF DIVIDING STREAMLINE TEMPERATURE DEVELOPMENT WITH TOTAL ENTHALPY RATIO

$M_1 = 3.0$; $Pr = 0.72$; $T_{o1} = 500^\circ R$; $\beta = 0.0$

109

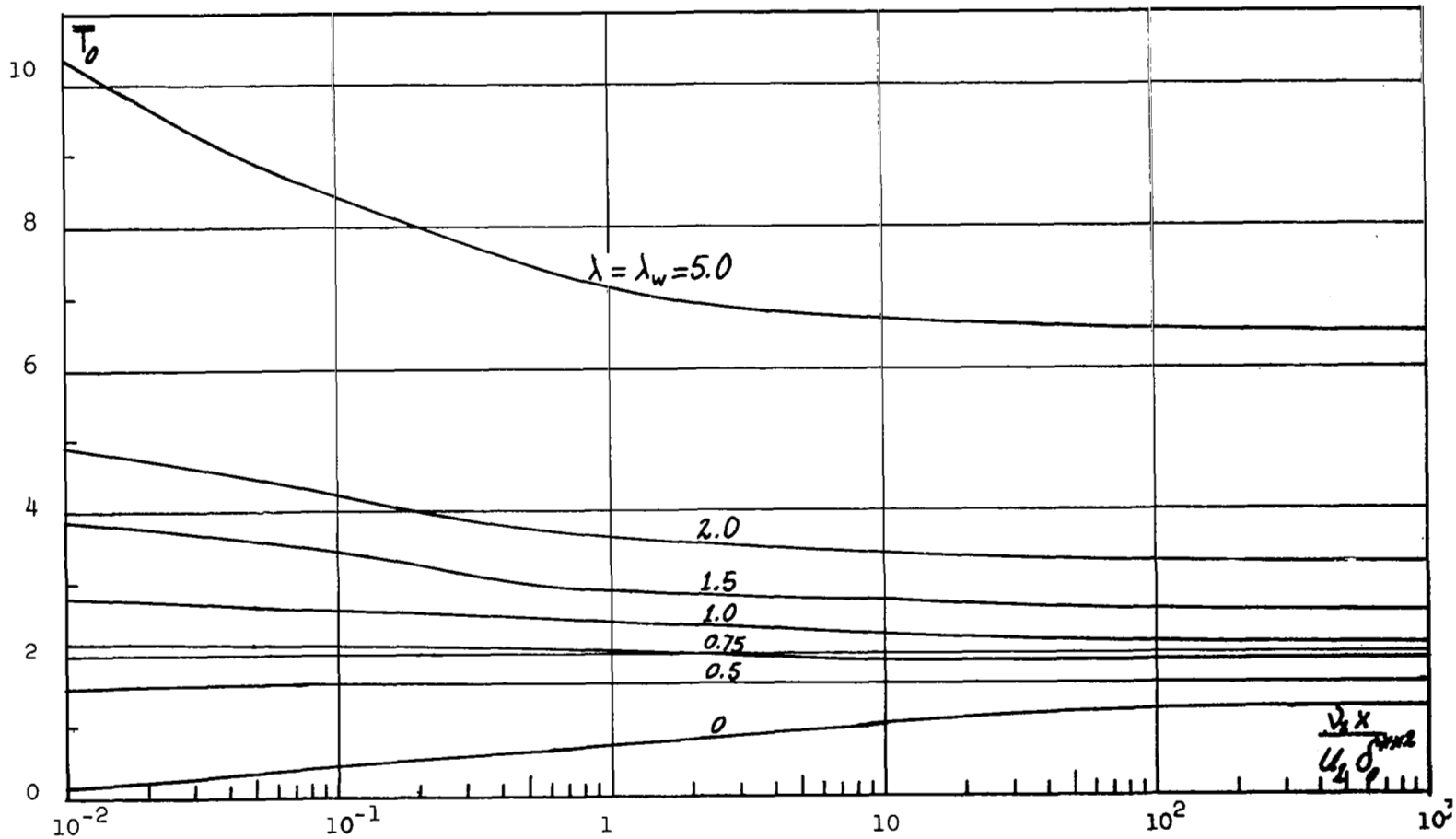


FIG. 5.4c VARIATION OF SHEAR STRESS COEFFICIENT DEVELOPMENT WITH TOTAL ENTHALPY RATIO

$M_1 = 3.0$; $Pr = 0.72$; $T_{o1} = 500^\circ R$; $\beta = 0.0$

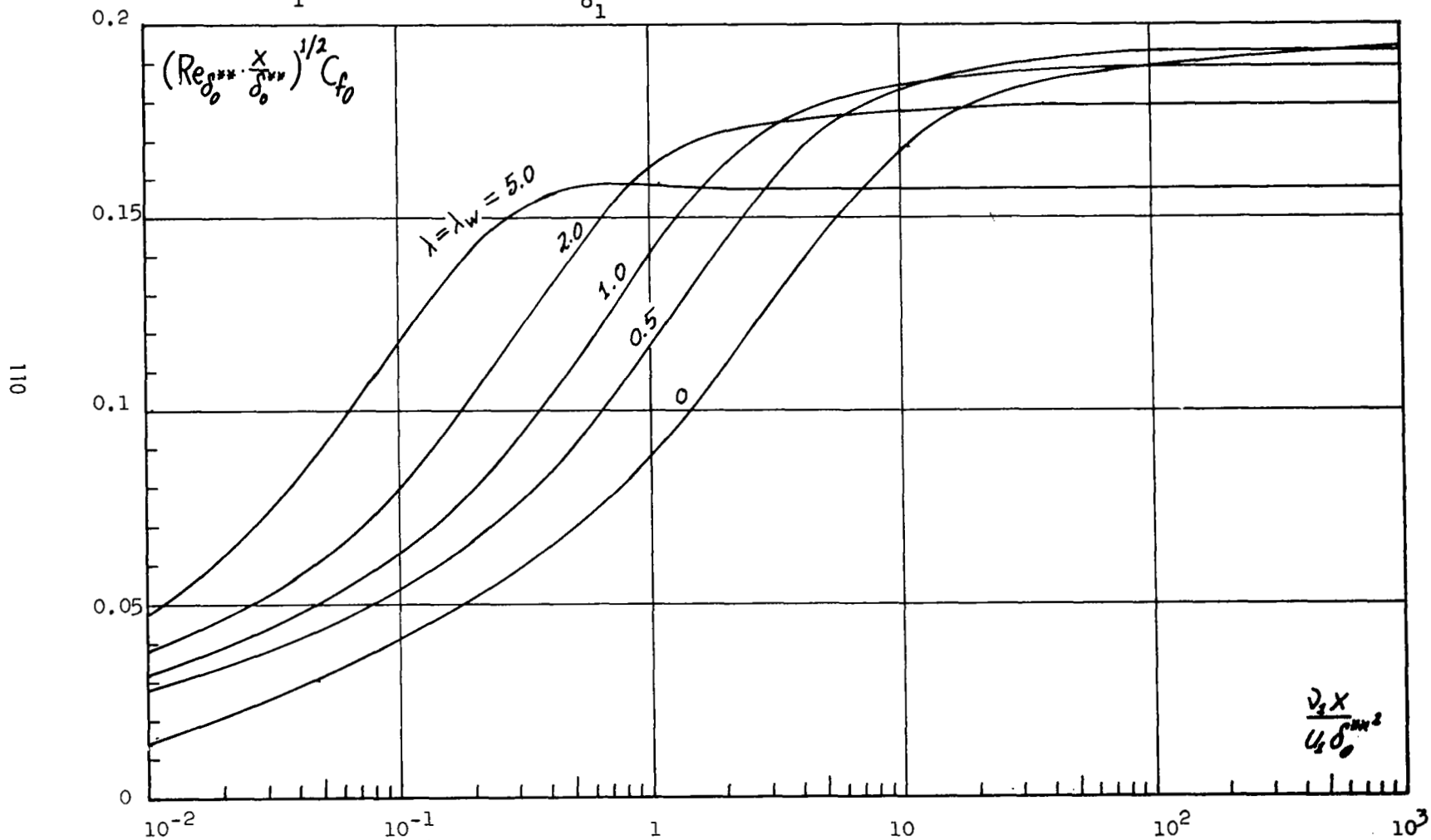


FIG. 5.4d VARIATION OF THE DEVELOPMENT OF DIVIDING STREAMLINE LOCATION WITH TOTAL ENTHALPY RATIO
 $M_1 = 3.0$; $Pr = 0.72$; $T_{o1} = 500^\circ R$; $\beta = 0.0$

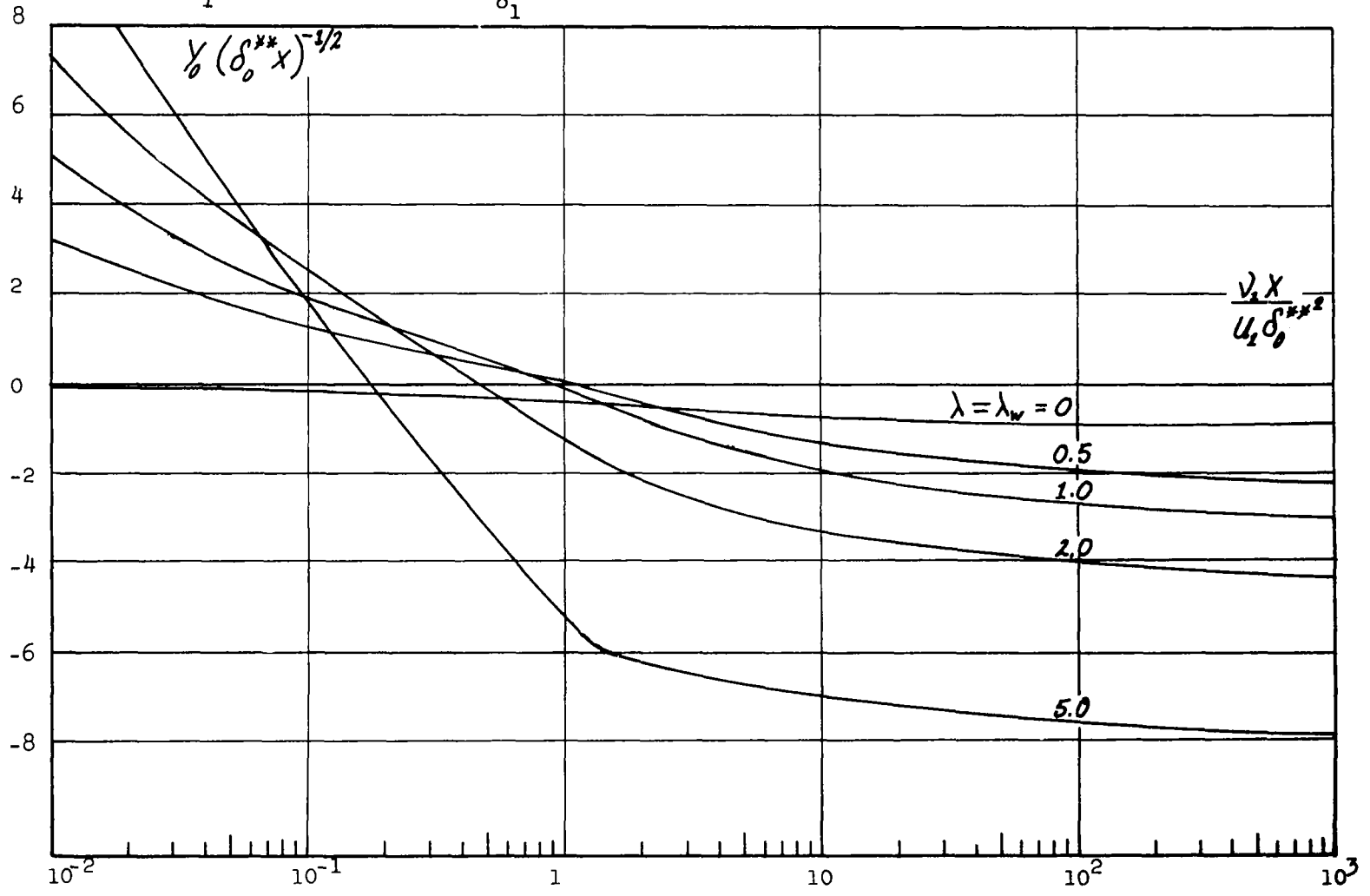


FIG. 5.4e VARIATION OF LOCAL NUSSELT NUMBER DEVELOPMENT ALONG THE DIVIDING STREAMLINE WITH TOTAL ENTHALPY RATIO

$M_1 = 3.0$; $Pr = 0.72$; $T_{O_1} = 500^\circ R$; $\beta = 0.0$

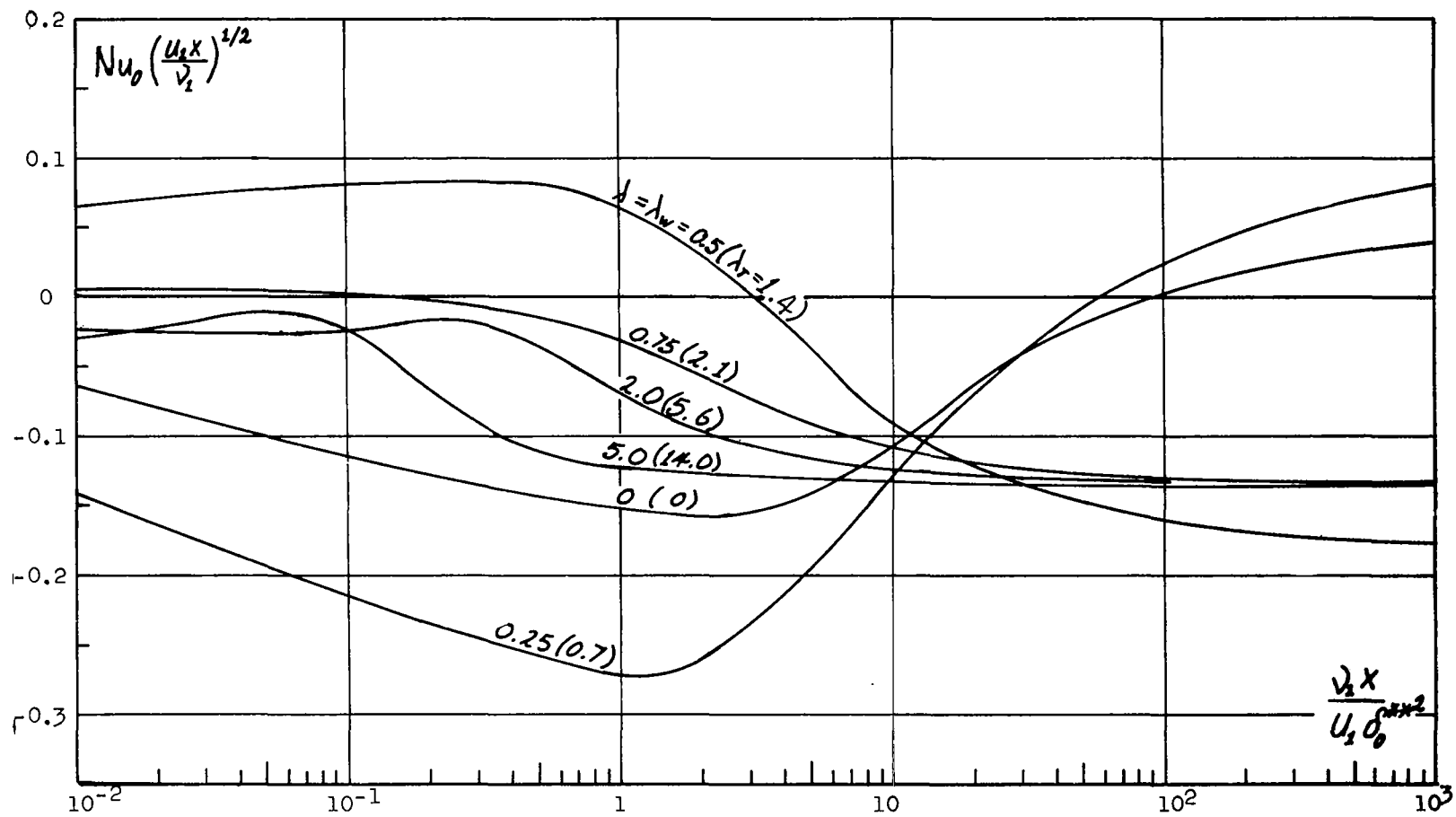


FIG. 5.5a EFFECT OF A DISCONTINUITY IN TOTAL ENTHALPY RATIO AT ORIGIN ON THE DEVELOPMENT OF DIVIDING STREAMLINE VELOCITY

$M_1 = 3.0$; $Pr = 0.72$; $T_{O_1} = 500^\circ R$; $\lambda = 2.0$; $\beta = 0.0$

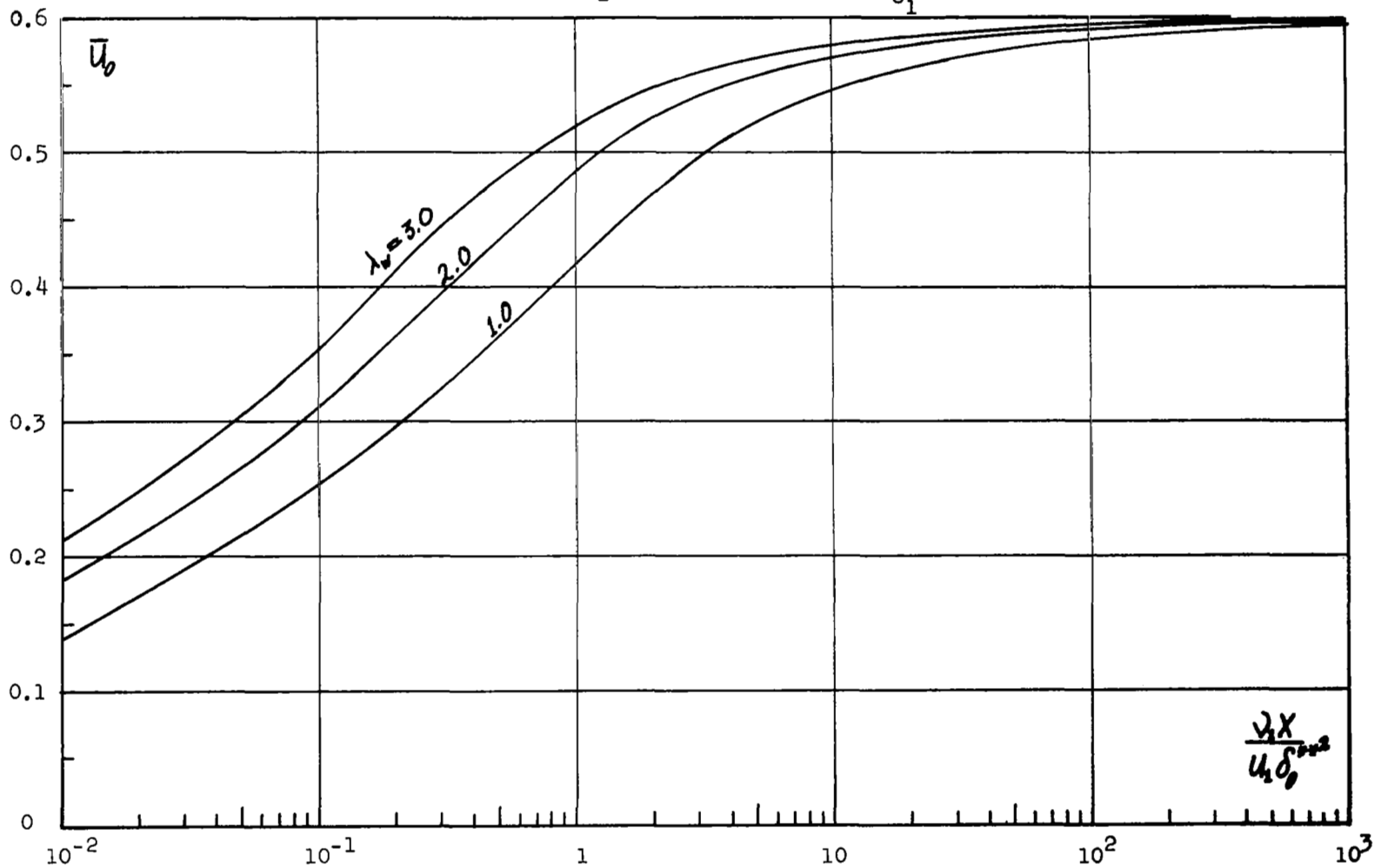


FIG. 5.5b EFFECT OF A DISCONTINUITY IN TOTAL ENTHALPY RATIO AT THE ORIGIN ON THE DEVELOPMENT OF DIVIDING STREAMLINE TEMPERATURE

$M_1 = 3.0$; $Pr = 0.72$; $T_{o1} = 500^\circ R$; $\lambda = 2.0$; $\beta = 0.0$

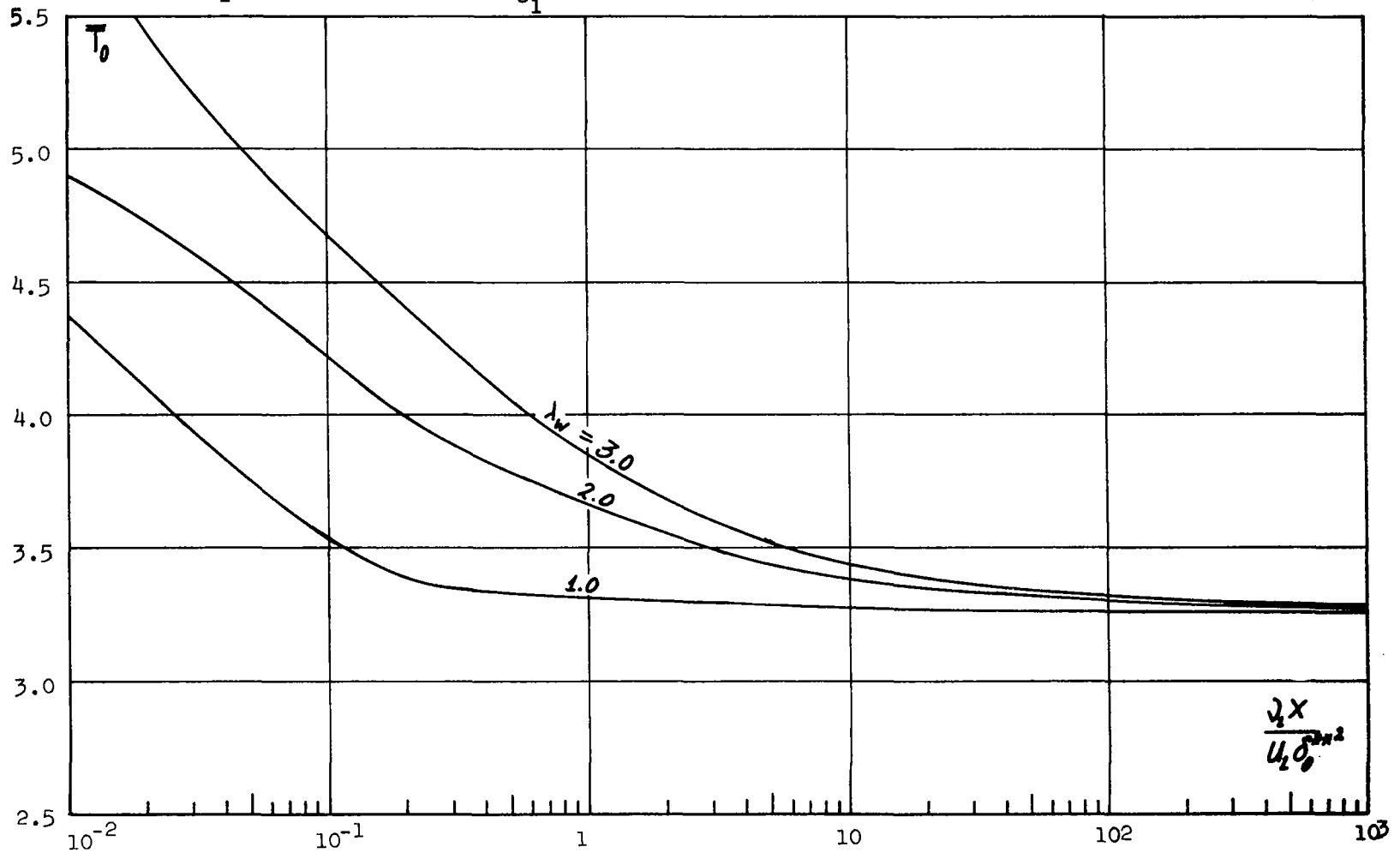


FIG. 5.5c EFFECT OF A DISCONTINUITY IN TOTAL ENTHALPY RATIO AT THE ORIGIN ON THE DEVELOPMENT OF SHEAR STRESS COEFFICIENT

$M_1 = 3.0$; $Pr = 0.72$; $T_{o1} = 500^\circ R$; $\lambda = 2.0$; $\beta = 0.0$

115

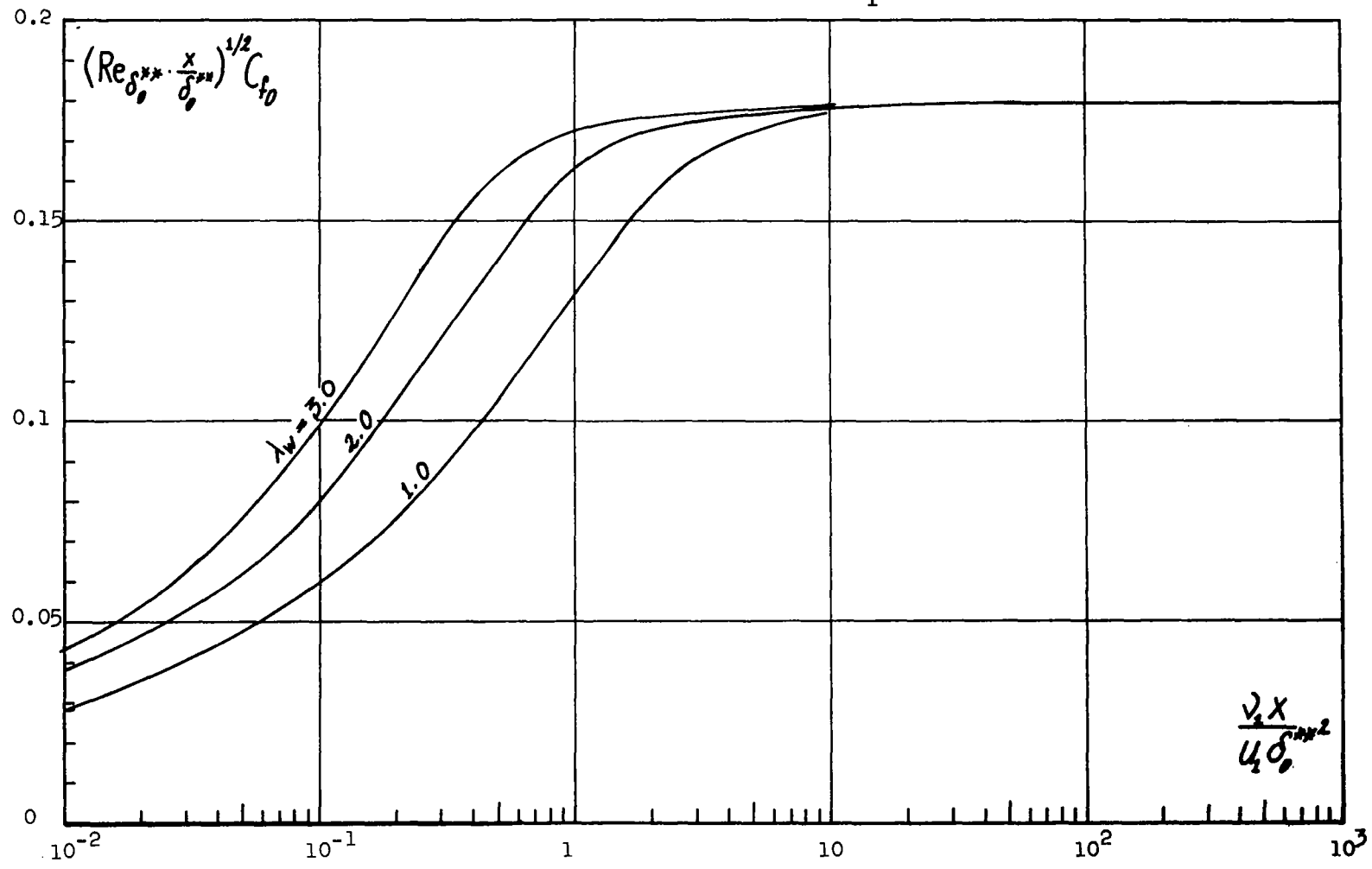


FIG. 5.5d EFFECT OF A DISCONTINUITY IN TOTAL ENTHALPY RATIO AT ORIGIN ON THE DEVELOPMENT OF DIVIDING STREAMLINE LOCATION $M_1 = 3.0$; $Pr = 0.72$; $T_{o_1} = 500^\circ R$; $\lambda = 2.0$; $\beta = 0.0$

116

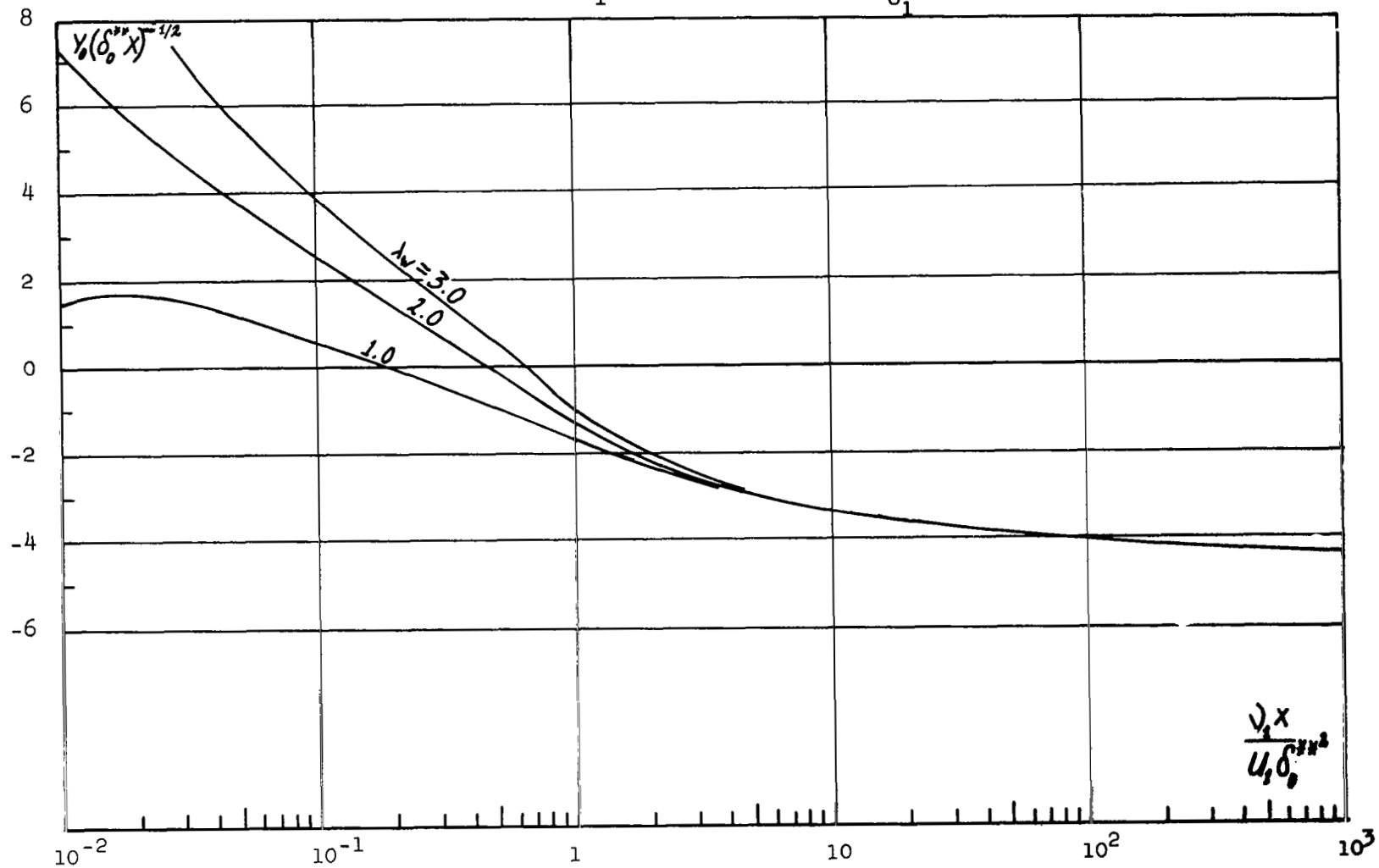


FIG. 5.5e EFFECT OF A DISCONTINUITY IN TOTAL ENTHALPY RATIO AT ORIGIN ON THE DEVELOPMENT OF LOCAL NUSSELT NUMBER

$M_1 = 3.0$; $Pr = 0.72$; $T_{O_1} = 500^\circ R$; $\lambda = 2.0$; $\beta = 0.0$

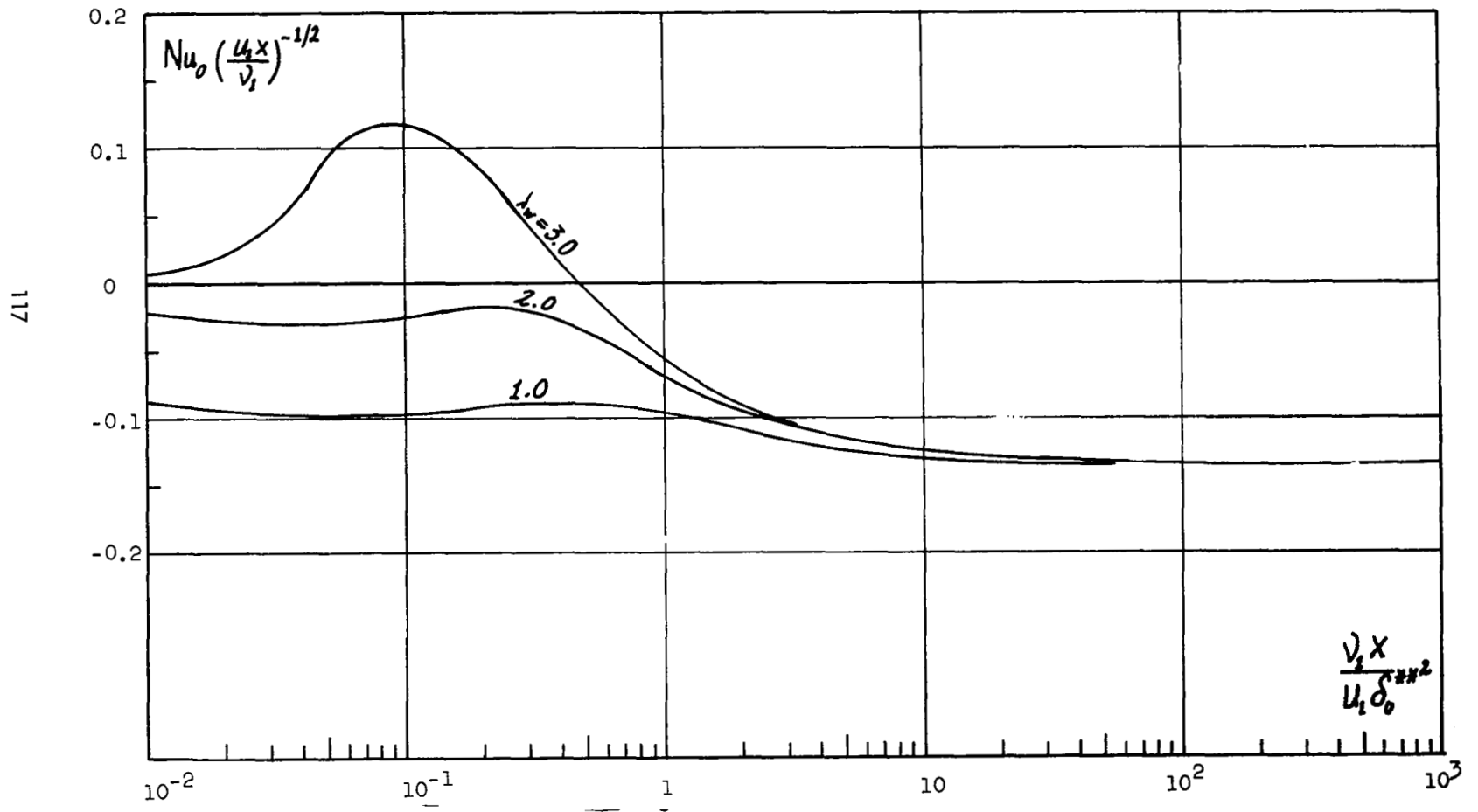


FIG. 5.6 THE INFLUENCE OF THE INITIAL VELOCITY PROFILE ON THE DEVELOPMENT OF DIVIDING
 STREAMLINE VELOCITY

$M_1 = 3.0$; $Pr = 0.72$; $T_{O_1} = 500^\circ R$; $\lambda = 1.0$; $\lambda_w = 1.0$

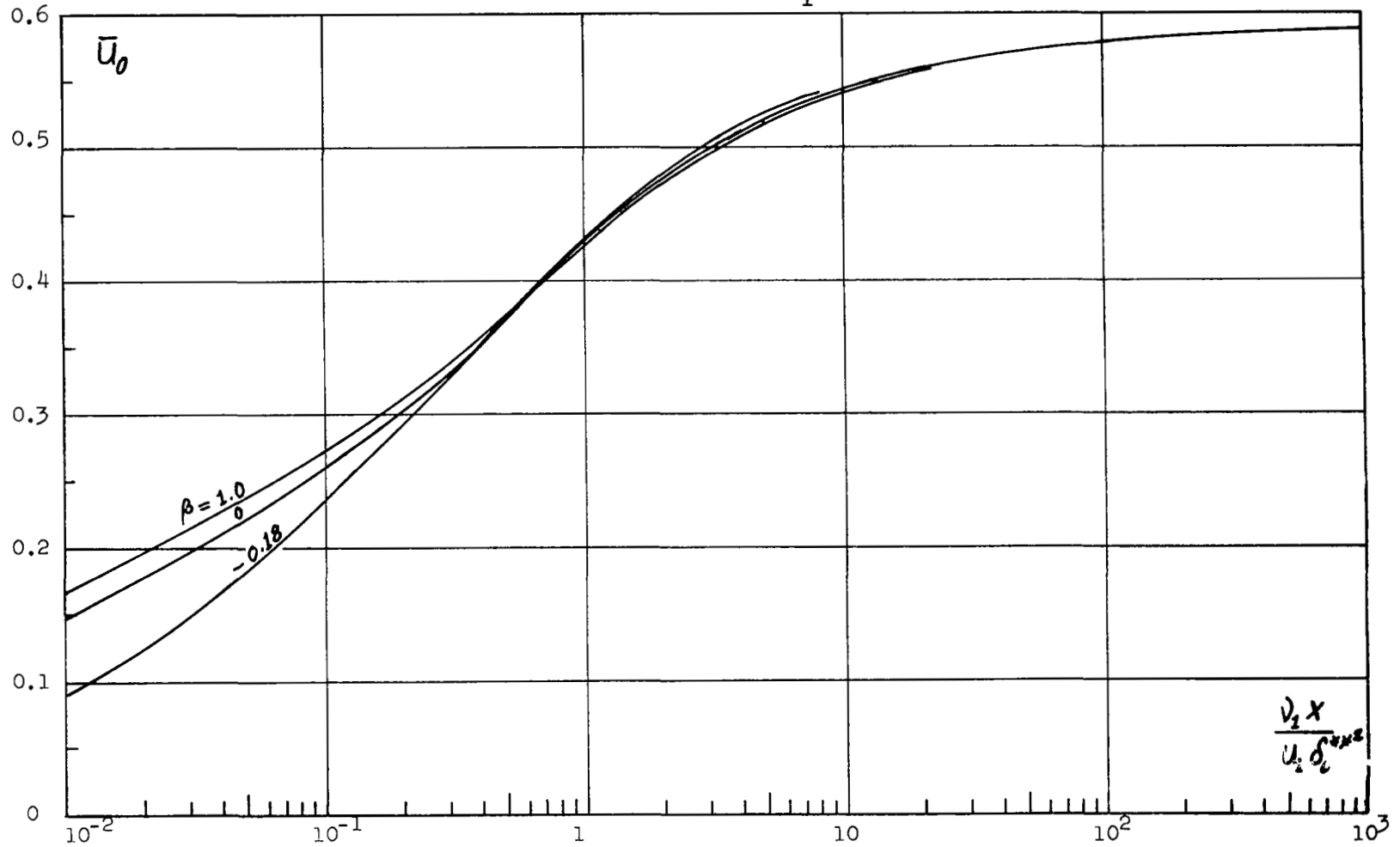
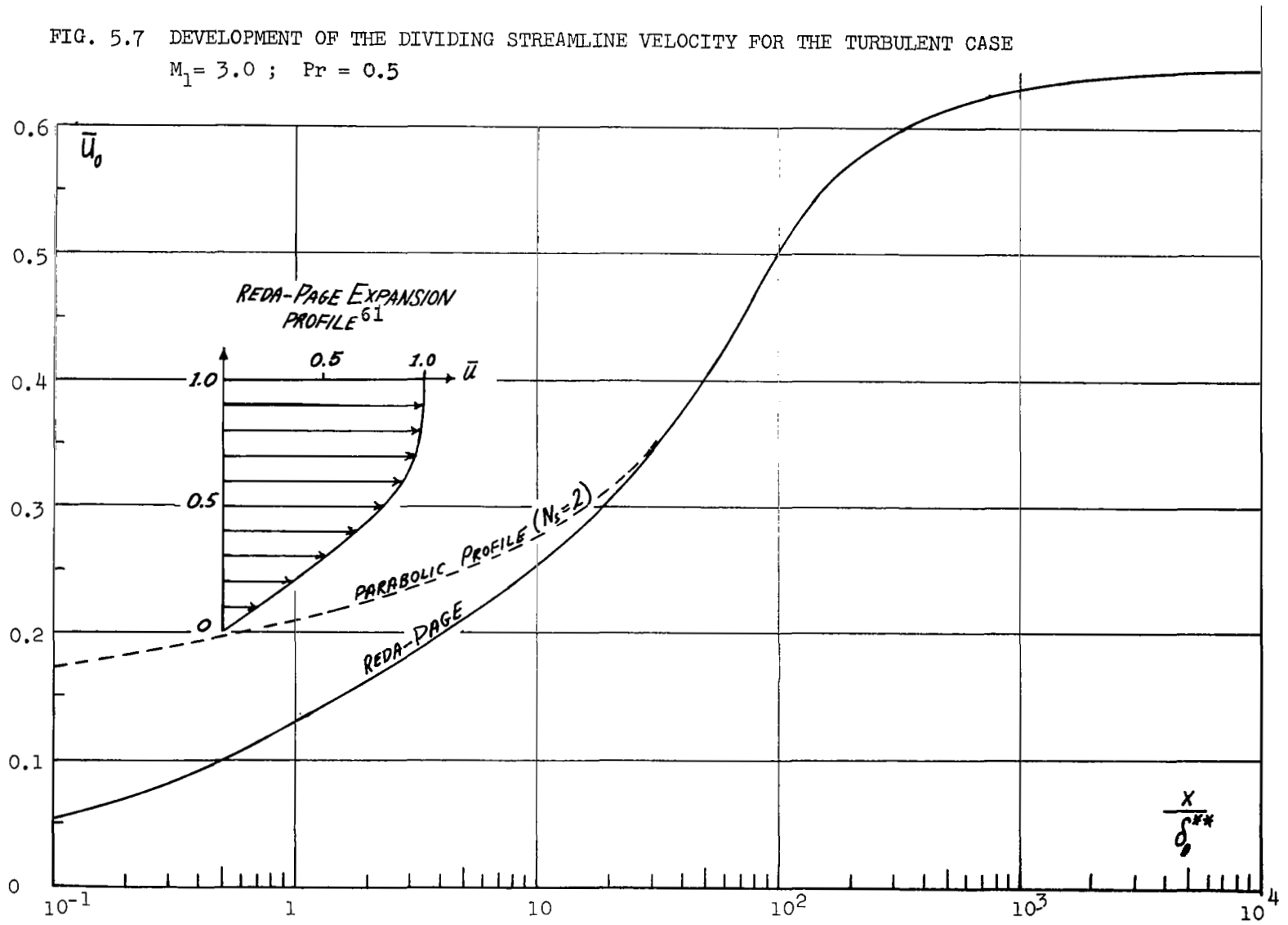


FIG. 5.7 DEVELOPMENT OF THE DIVIDING STREAMLINE VELOCITY FOR THE TURBULENT CASE

$M_1 = 3.0$; $Pr = 0.5$

119



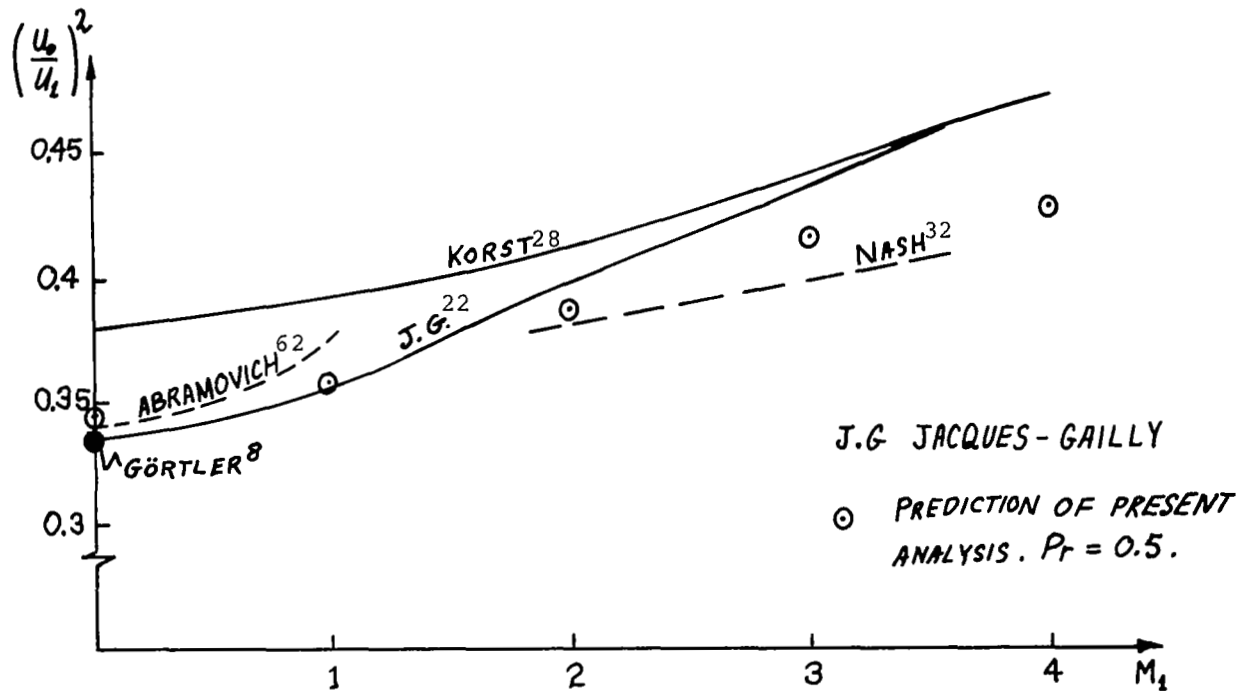


FIG. 5.8 COMPARISON OF VARIOUS THEORETICAL PREDICTIONS FOR THE VARIATION OF THE ASYMPTOTIC VALUE OF DIVIDING STREAMLINE VELOCITY WITH MACH NUMBER